Aus der Medizinischen Universitätsklinik und Poliklinik Tübingen

Abteilung Innere Medizin II

(Schwerpunkt: Hämatologie, Onkologie, Klinische Immunologie, Rheumatologie)

# Mechanism of Leukaemogenesis Downstream of *CSF3R-, RUNX1-* Mutations and Trisomy 21

**Inaugural-Dissertation**
**zur Erlangung des Doktorgrades**
**der Medizin**

**der Medizinischen Fakultät**
**der Eberhard Karls Universität**
**zu Tübingen**

**vorgelegt von**

**Stein, Frederic**

**2021**

Dekan: Professor Dr. B. Pichler

1. Berichterstatter: Professorin Dr. J. Skokowa, Ph.D
2. Berichterstatter: Professor Dr. P. J. Lang

Tag der Disputation: 22.09.2021

Vielen Dank an alle.

Kerstin.

Dieter.

# Contents

# List of Figures

# List of Tables

# Abbreviations

**Table 1: Abbreviations**

| Abbreviation | Meaning |
|---|---|
| AA, aa | amino acid |
| A | alanine; adenosine |
| AD | activation domain; autosomal dominant |
| AGO | argonaute protein |
| Akt | serine/threonine-specific protein kinase |
| AML | acute myeloid leukemia |
| AMKL | acute megakaryoblastic leukemia |
| ANC | absolute neutrophil count |
| APC | antigen-presenting cells |
| AR | autosomal recessive |
| BEN | benign ethnic neutropenia |
| BS | Barth syndrome |
| C | cytosine |
| Cas9 | CRISPR-associated protein 9 |
| CD | cluster of differentiation |
| CFU | colony-forming unit |
| CFU-G | colony-forming unit granulocytes |
| ChIP | chromatin immunoprecipitation |
| Chr | chromosome |
| CLP | common lymphoid progenitor |
| CML | chronic myeloid leukemia |
| CMML | chronic myelomonocytic leukemia |

Continued on next page

**Table 1: Abbreviations – continued from previous page**

| Abbreviation | Meaning |
|---|---|
| CMP | common myeloid progenitor |
| CN | (severe) congenital neutropenia |
| CR | complete remission |
| CRISPR | clustered regularly interspaced short palindromic repeats |
| CSF | colony stimulating factor |
| Ct | C-terminal truncating mutation or C-terminal truncated |
| Ct | cycle threshold |
| CyN | cyclic neutropenia |
| D | aspartatic acid |
| diff | differentiated iPSCs clone |
| DNA | deoxyribonucleic acid |
| DS | Down Syndrome |
| DSMZ | Leibniz Institute DSMZ- Deutsche Sammlung von Mikroorganismen und Zellkulturen |
| dPCR | digital PCR |
| EHT | endothelial-to-haematopoietic transition |
| EoBMaP | eosinophil-basophil-mastcell progenitor |
| EPO | erythropoietin |
| ER | endoplasmic reticulum |
| ERK | extracellular signal regulated kinase |
| FA | Fanconi anemia |
| FAB | French-American-British classification systems for hematological disease |
| FACS | Fluorescence-activated cell sorting |
| FCS | fetal calf serum |
| FPD/AML | familial platelet disorder with propensity to AML |
| Fs | frameshift mutation / mutated |
| G | glycine; guanosine |

Continued on next page

**Table 1: Abbreviations – continued from previous page**

| Abbreviation | Meaning |
|---|---|
| G-CSF | granulocyte CSF |
| G-CSFR | receptor of G-CSF |
| gDNA | genomic DNA |
| GF | hepatocyte growth factor |
| GM-CSF | granulocyte monocyte CSF |
| GTP | Guanosine-5'-triphosphate |
| GMP | granulocyte-monocyte progenitor |
| HCC | hepatocellular carcinoma |
| HCV | hepatitis c virus |
| hiPSC | inducible pluripotent stem cell |
| hsa | homo sapiens (prefix) |
| HSC | hematopoietic stem cell |
| HSC-Tx | hematopoietic stem cell transplantation |
| HSPCS | hematopoietic stem and progenitor cells |
| IBMFS | inherited bone marrow failure syndromes |
| ID | inhibitory domain |
| JAK | Janus kinases |
| L | leucine |
| LMPP | lympho-myeloid multi-potential progenitor |
| LT-HSC | long term repopulating HSC |
| MACS | magnetic-activated cell sorting |
| MAPK | mitogen-activated protein kinase |
| MDS | myelodysplastic syndrome |
| MEP | megakaryocyte erythroid progenitor |
| miR | microRNA |
| miRNA | microRNA |
| MPD | myeloproliferative disease |
| MPO | myeloperoxidase |

Continued on next page

**Table 1: Abbreviations – continued from previous page**

| Abbreviation | Meaning |
|---|---|
| MPPs | multi potent progenitor cells |
| mRNA | messenger RNA |
| Ms | missense mutated |
| MT | mutated or mutant |
| N | asparagine |
| NE | neutrophil elastase |
| NETs | neutrophil extracellular traps |
| NG | neutrophil granulocyte |
| NGS | next-generation sequencing |
| NLS | nuclear localization signal |
| NMD | nonsense-mediated mRNA decay |
| NMTS | nuclear matrix targeting signal |
| NK | natural killer cells |
| Nt | N-terminal truncating mutation ; N-terminal truncated |
| nt | nucleotide |
| OS | overall survival |
| PCR | polymerase chain reaction |
| PI3K | Phosphoinositide 3-kinases |
| Pol | polymerase (enzyme) |
| PV | Polycythemia vera |
| qPCR | quantitative PCR |
| R | arginine |
| (mi) RISC | (micro) RNA-induced silencing complex |
| RHD | runt homology domain |
| RNA | ribonucleic acid |
| ROS | reactive oxygen species |
| RT | room temperature, reverse-transcription |
| SCF | stem cell factor |

Continued on next page

**Table 1: Abbreviations – continued from previous page**

| Abbreviation | Meaning |
|---|---|
| SDS | Shwachmann-Diamond syndrome |
| snoRNA | smal nucleolar RNA |
| SNP | single nucleotide polymorphism |
| STAT | signal transducer and activator of transcription proteins |
| ST-HSC | short term repopulating HSC |
| TAD | trans-activation domain |
| TAM | transient abnormal myelopoiesis |
| TF | transcription factor |
| TPO | thrombopoietin |
| U | uracil |
| UPR | unfolded protein response |
| UTR | untranslated region |
| v | viral |
| WHO | World Health Organization |
| WT | wild type |
| Y | tyrosine |

# 1 Introduction

## 1.1 Hematopoiesis

Hematopoiesis, the production and differentiation of mature blood cells, e.g. erythrocytes, platelets and leukocytes, is a complex multistep process. Its orchestration is highly versatile and relies on intracellular and extracellular stimuli, which are to some degree mediated by the stem cell niche, the microenvironment surrounding the hematopoietic cells [Crane et al., 2017]. Those stimuli cover the range from transcription factors (TF) and their target sites (C/EBP$\alpha$, PU.1, etc.), over hematopoietic cytokines and their receptors (G-CSF, stem cell factor (SCF), erythropoietin (EPO), thrombopoietin (TPO), etc.) to epigenetic regulatory elements regulating each step until mature cells are derived [Álvarez-Errico et al., 2015; Drissen et al., 2016; Metcalf, 2008; Ostuni et al., 2016; Rosenbauer and Tenen, 2007]. The role of TFs is described in section 1.1.3.

In general, hematopoiesis can be divided into several pathways, myelopoiesis, erythropoiesis, thrombopoiesis and lymphopoiesis. Since granulocytes and granulocytic disorders are the subjects of this study, the focus will be on myelopoiesis, the production and maturation of myeloid cells, i.e. granulocytes and monocytes.

The model of differentiation of hematopoietic pluripotent stem cells, first suggested by Jacobson and Marks, demonstrated in practice by Till and McCulloch, confirmed by Bradley and Metcalf, reviewed by Tsai and Orkin and Orkin et al., is the commonly accepted basis for most of the existing in vitro models of hematopoiesis [Bradley and Metcalf, 1966; Jacobson and Marks, 1949; Orkin et al., 2015; Till and McCulloch, 1961; Tsai and Orkin, 1997].

Mature blood cells are derived from undifferentiated hematopoietic stem cells (HSC) over intermediate differentiation states. Two capacities characterize a stem cell, the capacity of self-renewal and the ability to differentiate into different mature blood cells [Doulatov et al., 2012]. HSCs reside on the apex of a hierarchical tree and are divided into two groups: long-term reconstituting stem cells (LT-HSCs) which have a high self-renewal potential, and short-term reconstituting stem cells (ST-HSCs). ST-HSCs are prone to give rise to more committed progenitor cells, called multipotent progenitors (MPPs) [Orkin and Zon, 2008]. MPPs inherit a reduced capacity of self-renewal and differentiate into more committed cells, called common lymphoid or myeloid progenitor cells (CLP and CMP) [Orkin and Zon, 2008]. CLP and CMP further differentiate into more specialized cells (CFUs = colony forming units) and mark the earliest bifurcation between myeloid and lymphoid branches. Of note, there is another entity of HSC, the lympho-myeloid multipotential progenitor (LMPPs) which inherits the potential of differentiating into both granulocyte-monocyte progenitors (GMPs) and CLPs *in vitro* [Karamitros et al., 2018]. Further differentiation of common progenitors results via highly restricted progenitors (GMPs, MEPs = megacaryocyte-erythrocyte progenitors, CLPs, etc.) in terminally differentiated, mature blood cells, such as erythrocytes, representing the vast majority of blood cells, granulocytes, monocytes, thrombocytes and lymphocytes [Orkin and Zon, 2008].

### 1.1.1 Myelopoiesis with focus on granulocytic differentiation

In humans, myelopoiesis mainly occurs in the bone marrow and it takes about two weeks from HSC to mature neutrophils [Ostuni et al., 2016].

Starting with common myeloid progenitors (CMPs), the myeloid lineage con-

sists of all cells rising from MPPs but those committed to the lymphoid lineage (except for the above mentioned LMPPs). MPPs give rise to CMPs which then differentiate stochastically into megakaryocyte-erythroid progenitor cells (MEPs), granulocyte-monocyte progenitor cells (GMPs), eosinophil and basophil/mast-cell progenitors (EoBMaP) [Doulatov et al., 2012; Orkin and Zon, 2008; Orkin et al., 2015]. Myeloid cell fate decision requires specific myeloid, transcription factors such as PU.1, C/EBP$\alpha$, C/EBP$\varepsilon$, and epigenetic modifies, e.g. histone modifiers [Blumenthal et al., 2017]. In GMPs, it is their timed expression ratio, which regulates whether the differentiation is guided towards a granulocytic (granulocyte colony-forming units; CFU-G) or monocytic (monocyte colony-forming units; CFU-M) fate [Blumenthal et al., 2017]. Of note, in contrast to GMP which inherit monocytic and granulocytic potential, CFU-G and CFU-M are unilineage-restricted [Sieff et al., 2015], thus CFU-Gs give rise to myeloblasts which differentiate into mature segmented neutrophils via pro-myelocyte, myelocyte, meta- and band-myelocyte state [Lawrence et al., 2018; Sieff et al., 2015]. Whereas CFU-Ms differentiate into mature monocytes. In early phases of granulocytic differentiation, some TFs serve as pioneering TFs, meaning previously unaccessible chromatin is made accessible by them for further, lineage-specific TFs [Ostuni et al., 2016]. In myeloid progenitor cells, PU.1 is described to act as priming TF, making chromatin accessible for C/EBP$\alpha$ [Ohlsson et al., 2016]. At steady-state granulopoiesis, differentiation into granulocytes is driven by high-levels of C/EBP$\alpha$ and relatively lower levels of PU.1 [Álvarez-Errico et al., 2015; Friedman, 2007; Ohlsson et al., 2016; Ostuni et al., 2016]. C/EBP$\varepsilon$, another member of the C/EBP family, regulates the transition from promyelocyte to myelocyte state and interacts with GFI-1 and LEF-1, both crucial for granulocytic lineage commitment [Ostuni et al., 2016]. In addition to the TFs mentioned above, growth factors (GFs), or cytokines, are needed for normal granulopoiesis and lineage commitment. For example, Granulocyte colony-stimulating factor (G-CSF) can induce both proliferation and maturation of myeloid progenitors at CFU-GM level [Sieff et al., 2015; Skokowa et al., 2006; Touw et al., 2013]. In 2006, Skokowa et al. showed that G-CSF induces expression of LEF-1 transcription factor which activates C/EBP$\alpha$ [Skokowa et al.,

2006].

**Figure 1.1** provides comprehensive information about the maturation of neutrophils and **figure 1.2** shows a scheme of the hierarchical model of hematopoiesis.

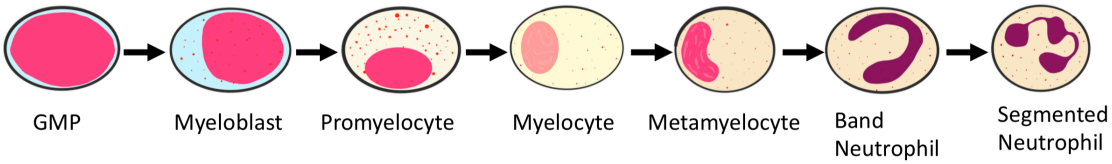


**Figure 1.1: Granulocytic maturation**
GMPs give rise to myeloblasts which differentiate via several intermediate states to mature segmented neutrophils.
*Adapted from Skokowa et al. [2017]: Severe congenital neutropenias. Nature Reviews Disease Primers 3:17032.*

#### 1.1.1.1 Neutrophils and function

Neutrophil granulocytes (neutrophils) are major players in the innate immune response and make up approx. 60% of the peripheral blood leukocyte fraction (4.000 - 12.000/ul) in healthy individuals [Herold, 2016; Rosales, 2018]. Neutrophils are cells of the first-line immune defence. These are the first to respond to (bacterial) infections and are further recruited by the resulting chemokines, so neutrophils are essential for both the innate and acquired immune response and survival [Dinauer et al., 2015]. As research on neutrophils is ongoing, their further functions are discovered [Rosales, 2018]. Currently, neutrophils are not only seen as phagocytes, ingesting and digesting pathogens, but also as essential mediators between primary innate immunological response and secondary adaptive response [Dinauer et al., 2015]. This crosslink between the myeloid and lymphoid system does not only rely on antigen-presenting cells like monocytes and antigen-presenting dendritic cells (APC), but also on defensines produced and released by neutrophils as well as antigen-presentation by activated neutrophils [Dinauer et al., 2015]. The granulocytic pathogen containment capacity comprises phagocytosis, the ingestion, and digestion of, e.g. bacteria and the ability of neutrophils to release neutrophil extracellular traps (NETs) [Brinkmann and Zychlinsky, 2012;

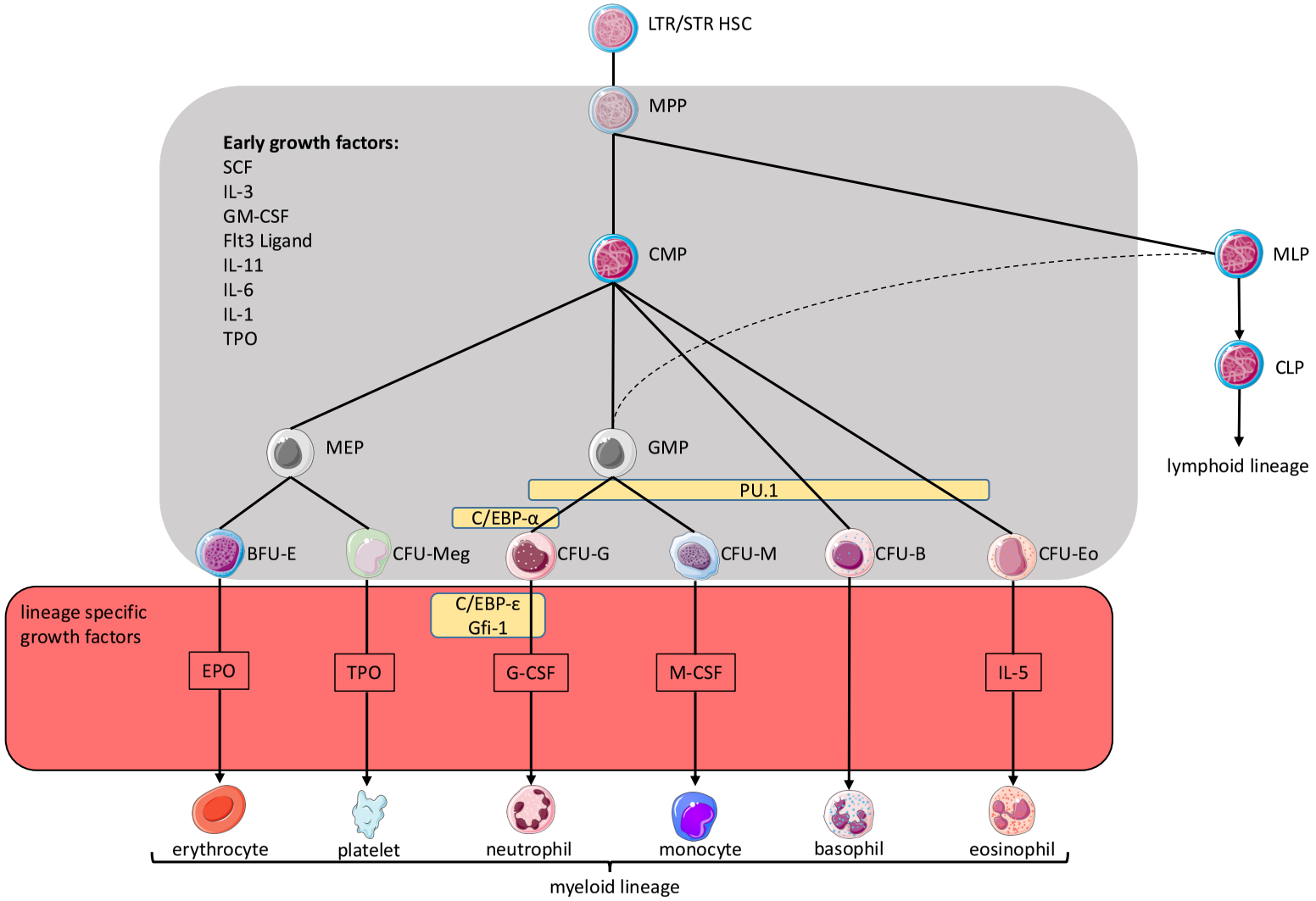
LTR/STR HSC
MPP
Early growth factors:
SCF
IL-3
GM-CSF
Flt3 Ligand
IL-11
IL-6
IL-1
TPO
CMP
MLP
CLP
lymphoid lineage
MEP
GMP
PU.1
C/EBP-α
BFU-E
CFU-Meg
CFU-G
CFU-M
CFU-B
CFU-Eo
lineage specific
growth factors
C/EBP-ε
Gfi-1
EPO
TPO
G-CSF
M-CSF
IL-5
erythrocyte
platelet
neutrophil
monocyte
basophil
eosinophil
myeloid lineage

Dinauer et al., 2015]. NETs consist, among others, of chromatin, lysosomal enzymes, as e.g., neutrophil elastase (NE), and myeloperoxidase (MPO). Together they build up a 3D net-like structure aiming to bind pathogens and neutralize them at the site of infection, thus neutrophils prohibit further spreading of infection [Brinkmann and Zychlinsky, 2012; Dinauer et al., 2015].

### 1.1.2 New model of hematopoiesis

Currently, the model of hematopoietic differentiation, at least for hematopoiesis in adults, is challenged and about to be redesigned. Several articles have been published, where a model was reported not compatible with the current, above described paradigm of hierarchical hematopoiesis [Drissen et al., 2016; Notta et al., 2016; Paul et al., 2015; Velten et al., 2017]. It was reported, that all lineages emerge directly from multi-potent HSCs which were described by Velten et al. as a 'cellular continuum of low-primed undifferentiated HSPCs (CLOUD-HSPCs)' [Velten et al., 2017]. This continuum of HSPCs includes cells phenotypically resembling MPPs, MLPs and LMPPs [Velten et al., 2017]. In this new model, these cells do not represent a single, stable entity, but represent a transient state of differentiation and are already functionally uni-potent [Velten et al., 2017]. Supporting this theory of early fate decision, Notta et al. observed and reported the differentiation of uni-potent erythroid-megakaryocytic progenitors directly from the

**Figure 1.2 *(preceding page)*: Scheme of the standard model of hematopoiesis with focus on myelopoiesis**
Long-term and short-term repopulating hematopoietic stem-cells (LT-/ST-HSC) give rise to more committed multi-potent progenitor-cells (MPP). Those MPPs do not have the potential of self-renewal but differentiate to either committed myeloid progenitors (CMP) or multipotent lymphoid progenitors (MLP). MLPs form the basis of the lymphoid lineage (not ultimately shown), and CMPs differentiate into divers myeloid lineages. Differentiation is guided by the presence (or absence) of specific growth factors, transcription factors and other mechanisms of hematopoietic differentiation. Granulocyte-monocyte progenitors (GMP) are the common progenitors of the more mature colony-forming units (CFU) of neutrophils and monocytes. Differentiation into both lineages is supported by the presence of a granulocyte-monocyte colony stimulating factor (GM-CSF), whereas differentiation from CFU-G into mature granulocytes requires the presence of granulocyte-colony stimulating factor (G-CSF).
*Adapted and modified from Sieff et al. [2015] 'Nathan & Oski's - Hematology and Oncology of Infancy and Childhood.' Chapter 1 'Anatomy and Physiology of Hematopoiesis'. Elsevier/Saunders. 8$^{th}$ Edition. p.3-51.e21.*

HSPC-compartment [Notta et al., 2016]. Similarly, neutrophils and lymphocytes, together with monocytes, emerged from this compartment without the presence of CMPs or other intermediate cells [Notta et al., 2016]. Furthermore, Karamitros et al. observed, that LMPPs had the potential to differentiate into both GMPs and CLPs but mostly differentiated in an unilinear manner *in vitro* [Karamitros et al., 2018]. The performed *in vivo* experiments showed, that multilineage-potential of single cells was possibly smaller than proposed previously, suggesting that pluripotency of individual cells was more likely a result of the assays used, which do not reflect *in vivo* cell fate potential, rather than the unbiased fate of the cells themselves [Karamitros et al., 2018]. In conclusion, it seems that fate decision happens on HSC level, and hematopoietic differentiation is not a tree-like model, but it resembles a more continuous model like a 'Waddington's landscape', where differentiation begins early and the differences between the different cell lines become more significant the further the cells are differentiated (**figure 1.3**) [Velten et al., 2017].

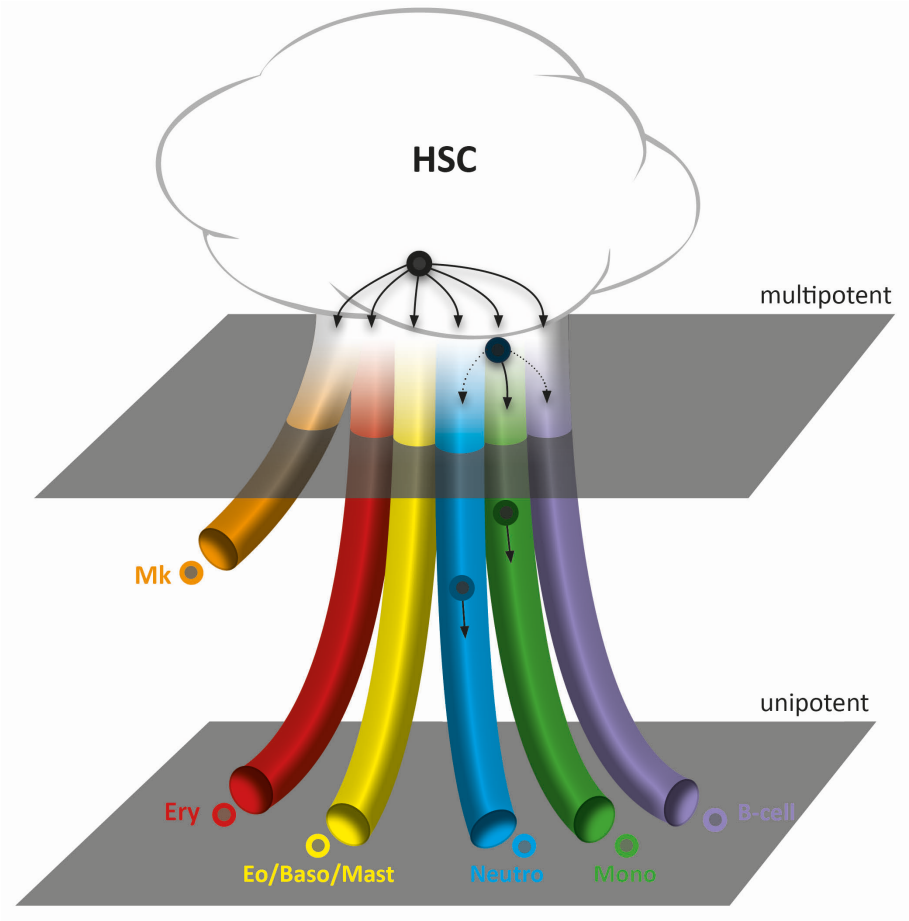


**Figure 1.3: Early lineage restriction in hematopoiesis**
A cellular continuum of HSCs undergoes early lineage restriction and gives rise to uni-lineage primed progenitor cells which differentiate into mature blood cells. Differences in cell entities increase while differentiation continues.
*Adapted, modified and merged from Velten et al. [2017] 'Human hematopoietic stem cell lineage commitment is a continuous process'. (Nature Cell Biology. 19:4. p271-281.) and Notta et al. [2016] 'Distinct routes of lineage development reshape the human blood hierarchy across ontogeny'. (Science. 351:6269. p.aab2116-aab2116-9)*

### 1.1.3 Transcription factors in hematopoiesis

Transcription factors comprise a group of proteins with the ability to bind to specific DNA regions and regulating accession and transcription of DNA [Friedman, 2007; Maston et al., 2006]. They function in a tightly controlled mode of action and can induce their effect alone or as part of a complex with other proteins and either work as inducers or suppressors [Maston et al., 2006]; by this TFs enable priming of a distinct phenotype or provoke a specific cellular response [Friedman, 2007].

#### 1.1.3.1 ETS family of transcription factors

In humans, ETS (E26 transformation-specific) family of transcription factors comprises 28 genes all related to each other by the presence of ETS domain in their protein structure [Ciau-Uitz et al., 2013; Sizemore et al., 2017]. Most prominent in hematopoiesis and myeloid differentiation is *Spi.1* which encodes PU.1 protein [Rosenbauer and Tenen, 2007].

##### 1.1.3.1.1 PU.1 (*Spi.1*) transcription factor

PU.1 regulates hematopoietic differentiation at several levels in the maturation hierarchy. PU.1 reduces HSC self-renewal capacity and induces maturation into CMPs and CLPs [Rosenbauer and Tenen, 2007]. CMPs can be divided into two groups based on PU.1 expression: CMPs expressing PU.1 can differentiate into all myeloid cells, whereas CMPs deficient of PU.1 can only differentiate into MEPs [Rosenbauer and Tenen, 2007]. Differentiation of CMPs into granulocytes or monocytes is determined by PU.1 expression levels [Rosenbauer and Tenen, 2007]. High levels of PU.1 favor a monocytic phenotype, whereas cells with low levels of PU.1 differentiate into granulocytic precursors [Rosenbauer and Tenen, 2007]. The regulation of myeloid fate is a complex process and, in addition to PU.1, is balanced by C/EBP$\alpha$.

#### 1.1.3.2 *C/EBP* (CCAAT/enhancer binding proteins): *C/EBPα, C/EBPβ, C/EBPε* and *GFI.1*

Activation of C/EBP*α* is required for differentiation from CMP to GMP and is induced by LEF-1 [Friedman, 2007; Sieff et al., 2015; Skokowa et al., 2006]. Although it is expressed throughout differentiation from HSC to mature granulocytes, after GMP stage, C/EBP*α* is no longer required for neutrophil maturation [Rosenbauer and Tenen, 2007]. LEF-1 is down-regulated by hyperactivated STAT5 via enhanced ubiquitination and degradation. In CN, STAT5 is continuously activated and possibly responsible for a block of myeloid differentiation [Gupta et al., 2014; Skokowa et al., 2006]. Furthermore, LEF-1 induces C/EBP*α* in the nucleus by binding to C/EBP*α* promoter region. LEF-1 translocation in the nucleus requires HCLS1 and HAX1, whilst HCLS1 is activated by G-CSFR signaling [Skokowa et al., 2012]. G-CSF can overcome the neutropenic phenotype in CN through the induction of emergency granulopoiesis via C/EBP*β*. C/EBP*β* induces the differentiation of neutrophils via G-CSFR signaling independent of the G-CSF - LEF-1 - C/EBP*α* signaling pathway [Skokowa et al., 2012] (see 1.1.5.2 for further information about CN). The final step from GMP to mature neutrophils is orchestrated by C/EBP*ε*, and GFI1 (growth factor independent 1 transcription-repres-sor protein). The absence of one or both transcription factors leads to a lack of neutrophils [Person et al., 2003; Rosenbauer and Tenen, 2007]. Of note C/EBP*α*, and GFI1 are crucial for maintenance of adult HSCs [Wang et al., 2017].

#### 1.1.3.3 RUNX family of transcription factors

The RUNX (Runt related transcription factor) transcription factor family is highly conserved between species and is involved in regulatory processes of diverse tissues [Tahirov and Bushweller, 2017; Yzaguirre et al., 2017a]. Human RUNX family of transcription factors consists of three structurally highly identical members: RUNX1, RUNX2 and RUNX3 [Van Wijnen et al., 2004; Yzaguirre et al., 2017a]. Their name originated from the conserved runt homology domain (RHD) which resembles the runt transcription factor found in Drosophila [Tahirov and

Bushweller, 2017; Van Wijnen et al., 2004]. At first it was postulated that RUNX3 is required for normal neuronal development, RUNX2 for normal osteogenesis and RUNX1 is crucial for embryonal hematopoiesis and involved in myeloid differentiation [Bonifer et al., 2017]. In the meantime, it is known that functions of RUNX proteins overlap and RUNX proteins can compensate the absence of other family members, hence genotype-phenotype correlation is not always given [Bonifer et al., 2017; de Bruijn and Dzierzak, 2017]. This thesis covers topics in the field of hematology and oncology, so for reasons of importance and simplicity the focus will be on RUNX1. Synonyms of RUNX1 are CBF-$\alpha$, PEPB2a and AML1.

#### 1.1.3.3.1 RUNX1 structure and isotypes

Currently 11 splice variants of RUNX1 - located on chromosome 21 - are known [Bateman, 2019; Uniprot.org], and the most common expression variants are: a shorter RUNX1a isoform (size: 250 aa), the canonical RUNX1b isoform (UniProtKB: Q01196-1; size: 453 aa; in the following all position designations refer to the canonical isoform) and a longer RUNX1c isoform (size: 480 aa), which has 23 additional amino acid residues at its N-terminal region. RUNX1 includes several functional domains: the RHD (128 aa: aa 50 to 177), the nuclear localization signal (NLS; aa 167 to 183), the transactivation domain (TAD; also referred to as transcription activation domain; 80 aa: aa 291-371) - including an activation (AD), an inhibitory signal domain (ID) and a nuclear matrix targeting signal (NMTS; aa 324 to 354) - and a C-terminal VWRPY sequence (aa 449 to 453) [Bonifer et al., 2017; Lam and Zhang, 2012]. The RHD allows interaction with CBF-$\beta$ (core binding factor beta) and binding to DNA, resulting in a RUNX1-CBF-$\beta$-DNA complex formation. Interaction of CBF-$\beta$ with RUNX1 increases the binding affinity of RUNX1 to DNA and inhibits ubiquitin dependent RUNX1 degradation, thus leading to a prolonged RUNX1 protein half-life. Hence, in the absence of CBF-$\beta$, RUNX1 is not able to properly exert its functions [Blumenthal et al., 2017; Lam and Zhang, 2012; Tahirov and Bushweller, 2017]. The function of RUNX1 as either a transcriptional activator or a repressor is dependent on the respective tissue and the associated cooperating proteins, recruited via the RHD to the RUNX1 bind-

ing sites [Lam and Zhang, 2012]. Interacting proteins of RUNX1 besides CBF-$\beta$ are C/EBP$\alpha$, PU.1, FLI1, GATA1, SMAD3, among others [Lam and Zhang, 2012; Michaud et al., 2003]. Besides the RHD, RUNX1 functions can be regulated via the TAD, e.g. by cooperation with MOZ, which depending on its acetylation state, either enhances or represses RUNX1 induced transcription of target genes [Blumenthal et al., 2017; de Bruijn and Dzierzak, 2017]. The NLS is responsible for wild-type RUNX1 localization in the nucleus, whilst via the VWRPY motif inhibition of RUNX1 via Groucho/TEL can be induced [Bonifer et al., 2017; Hughes and Woollard, 2017; Lam and Zhang, 2012]. For RUNX1, to perform its normal functions, the structural integrity of all domains is required.

#### 1.1.3.3.2 Down-stream targets of RUNX1 and its function in hematopoiesis and myelopoiesis

RUNX1 is crucial for the initiation and maturation of blood progenitor cells and HSCs during primitive and definitive hematopoiesis, this process is termed endothelial hematopoietic transition (EHT) [Yzaguirre et al., 2017b]. RUNX1 null embryos die from heavy bleeding and have reduced numbers of blood cells; the same is observed in the absence of CBF-$\beta$, which underlines the importance of RUNX1 and CBF-$\beta$ in general as well as in this early phase of development [de Bruijn and Dzierzak, 2017; Yzaguirre et al., 2017b]. RUNX1 is required for the transition from hemogenic epithelial cells in the embryonal aorta which subsequently differentiate to primitive blood cells - primitive erythrocytic progenitor, primitive bipotent megakaryocytic-erythrocytic progenitors and primitive macrophages [Yzaguirre et al., 2017b]. Following primitive hematopoiesis, definitive hematopoiesis produces lymphoid precursors, myeloid precursors, erythroid-megakaryocytic precursors and pre-HSCs [Yzaguirre et al., 2017b]. They then migrate to the liver, where they differentiate further, and finally these cells move into the bone marrow, where they remain for a lifetime [Yzaguirre et al., 2017b]. During EHT, RUNX1 functions as early acting TF, which means that RUNX1 binds to condensed chromatin, thus making it accessible for further TFs such as SCL/TAL1 and FLI1 [Bonifer et al., 2017; Yzaguirre et al., 2017b]. Further required in the EHT are GFI-1 and GFI-1b,

which mediated the differentiation from endothelial to blood cells [Yzaguirre et al., 2017b].

In adult hematopoiesis, *RUNX1* is expressed in all blood cells except for the mature erythrocytes, there *RUNX1* is downregulated [de Bruijn and Dzierzak, 2017]. In contrast to CBF-$\beta$, RUNX1 is not crucial for the maintenance of hematopoiesis - indicating that other members of the RUNX family compensate RUNX1 deficiency -, but RUNX1 knockout leads to a decrease of LT-HSCs, platelets and lymphoid cells [de Bruijn and Dzierzak, 2017; Mevel et al., 2019]. Interestingly, *RUNX1* haploinsufficiency, also underlying familial platelet disorder with propensity to AML (FPD/AML; OMIM: 601399), reduces lymphoid numbers and platelet count but increases the replating capacity of HSC which indicates increased self-renewal. Furthermore, RUNX1 is involved in the regulation of differentiation of various hematopoietic cells. Whether RUNX1 activates or represses the expression of its target gene, is depending on its cooperation partners and the cell type in which it is expressed. Exemplary targets of RUNX1 are genomic sites of cytokines and cytokine receptors (e.g. of M-CSF, G-CSFR), genes involved in profound regulatory pathways, such as apoptosis and cell cycle progression, other TFs (*Spi.1* (PU.1), *C/EBPα*) and myeloid markers such as *ELANE* (neutrophil elastase, NE), *MPO* (myeloperoxidase) [Chuang et al., 2013; de Bruijn and Dzierzak, 2017; Friedman, 2007, 2009; Hyde et al., 2017; Michaud et al., 2003]. RUNX1 is especially involved in cell homeostasis and the regulation of differentiation and proliferation; enforced expression of *RUNX1a* has been shown to support proliferation whilst RUNX1b promoted differentiation of hematopoietic cells [Chuang et al., 2013]. In summary, although RUNX1 is not necessary for the maintanance of HSC in adult hematopoiesis, the impaired maturation of megakaryocytes and lymphocytes in particular, as well as the expansion of GMPs as a result of RUNX1 knockout, show that balanced RUNX1 expression is important for normal hematopoiesis. Further roles of the RUNX proteins, besides acting as TF, are currently proposed, e.g., Brujin et al. described RUNX1 as well as RUNX3 proteins to be associated with DNA repair mechanism; thus the future might reveal even more astonishing functions of all RUNX proteins in homeostasis [de Bruijn and Dzierzak, 2017].

### 1.1.4 G-CSF, G-CSF receptor and their physiologic roles in neutrophil homeostasis

Growth factors, or cytokines, are signaling molecules that play an essential role in determining cell fate in hematopoietic cells; members of this group are GM-CSF (granulocyte-macrophage colony-stimulating factor), M-CSF (macrophage CSF) and G-CSF (granulocyte CSF; encoded by *CSF3*) with their corresponding cytokine receptors GM-CSFR etc. [Dwivedi and Greis, 2017; Metcalf, 1985]. G-CSF and G-CSFR (granulocyte colony-stimulating factor receptor, encoded by *CSF3R*) are key drivers of granulocytic differentiation and are important for sufficient neutrophil numbers [Touw et al., 2013]. Maintaining a sufficient neutrophil count via G-CSFR signalling involves two modes: (1) basal steady-state granulopoiesis via LEF1 and C/EBP$\alpha$ and (2) emergency granulopoiesis via NAMPT, NAD+ and Sirt, where Sirt finally induces C/EBP$\beta$ (see 1.1.3 for further information about transcription factors involved in neutrophil maturation) [Skokowa and Welte, 2013].

G-CSFR protein consists of three parts: the extracellular domain, the transmembrane domain and the intracellular cytoplasmatic domain [Touw et al., 2013]. The extracellular immunoglobulin-like domain binds G-CSF which activates the receptor via homodimerization in a 2:2 ratio (2 molecules of G-CSF bind 2 molecules of G-CSFR which form a complex). Mutations which result in a truncated extracellular part of G-CSFR cause severe neutropenia (see 1.1.5.2 for further information) [Ward et al., 1999]. After activation, G-CSFR exerts its functions via its cytoplasmatic domain. In congenital neutropenia, nonsense mutations of the intracellular part of G-CSFR are an early event in malignant progression towards MDS/AML (see 1.1.6 for further information about the role of mutant CSF3R) [Touw, 2015]. The intracellular domain of G-CSFR can be categorized in subdomains responsible for proliferation (membrane proximal part) and differentiation (C-terminal part) [Dong et al., 1993; Ziegler et al., 1993].

G-CSFR downstream signaling involves three distinct pathways: (i) a JAK/STAT pathway, (ii) a PI3K/Akt pathway and (iii) a $p21^{RAS}$/MAPK/ERK pathway [Dwivedi

and Greis, 2017; Touw et al., 2013]. In the JAK/STAT pathway G-CSF stimulates STAT3 and STAT5, STAT3 - activated at the C-terminal part - stimulates basal differentiation of granulocytes whilst STAT5 - activated at the membrane proximal domain - induces proliferation [Dong et al., 1993, 1998; Hermans et al., 1999; Touw et al., 2013]. Normally, STAT3 signaling lasts longer (several hours) than STAT5 signaling (minutes); STAT5 activation induces the elevation of reactive oxygen species (ROS) levels [Hermans et al., 1999; Touw et al., 2013]. The PI3K/Akt pathway requires HAX1, inhibits apoptosis (promotes survival), stimulates proliferation and is assumed to produce ROS as well [Dong and Larner, 2000; Skokowa and Welte, 2013]. The role of the $p21^{RAS}$/MAPK/ERK pathway is only partially understood but also important for proliferation, differentiation and possibly ER stress [Dwivedi and Greis, 2017; Skokowa and Welte, 2013]. G-CSFR signaling is abrogated by receptor internalization and negatively influenced by SOCS3 signaling which is activated by STAT3 [Hunter and Avalos, 2000; Touw et al., 2013].

### 1.1.5 Inherited bone marrow failure syndromes

Inherited bone marrow failure syndromes (IBMFS) are a heterogeneous group of genetic diseases with a deficiency of one or more mature blood cell lineages [Collins and Dokal, 2015; Parikh and Bessler, 2012]. Sometimes these blood cell defects are accompanied by additional extra-haematopoietic manifestations, which may become visible even before the haematopoietic disorders [Parikh and Bessler, 2012]. Examples of IBMFS are: Fanconi anemia (FA), Shwachmann-Diamond syndrome (SDS), familial platelet disorder with propensity to AML (FPD / AML), Barth syndrome (BS) and severe congenital neutropenia (CN) [Berman and Look, 2015; Bione et al., 1996; Song et al., 1999; Wilson et al., 2014]. The extra-haematopoietic manifestations are manifold: symptoms of FA include anaemia, altered skin pigmentation, neurological - i.e. developmental - disorders and bone diseases, etc.; while BS is associated with disorders of the neuronal system, bones, heart and skeletal muscles in addition to neutropenia. [Bione et al., 1996; Taylor et al., 2019; Wilson et al., 2014]. Due to their potential of malignant transformation, IBMFS are considered as pre-leukemic syndromes [Collins and Dokal,

2015; Skokowa et al., 2017]. Nowadays, patients suspected of suffering from IBMFS are screened early for genetic alterations - such as mutations, instabilities, deletions, etc. - and, in consequence, treatment can be initiated before the phenotype becomes symptomatic [Collins and Dokal, 2015; Ghemlas et al., 2015; Skokowa et al., 2017; Taylor et al., 2019]. Mutated genes are among others *RUNX1* for FPD/AML, *SBDS* for Shwachmann-Diamond syndrome, multiple *FANC genes* for FA and several genes for CN (see 1.1.5.2.1) [Boztug et al., 2008; Skokowa et al., 2017; Song et al., 1999; Taylor et al., 2019]. New screening techniques such as next-generation sequencing (NGS) can help to identify disease-causing mutations in previously undiagnosed patients, thereby enabling better patient management and consequently reducing costs [Ghemlas et al., 2015].

#### 1.1.5.1 Familial platelet disorder with propensity to acute myeloid leukemia (FPD/AML)

In 1999, Song et al. identified autosomal dominant mutations in *RUNX1* as the underlying cause of FPD/AML (OMIM: 601399) in six affected families [Song et al., 1999]. In contrast to other IBMFS, which are frequently associated with extra-hematopoietic manifestations, FPD/AML patients only show pathologies in blood cells, with a reduced platelet count accompanied by dysfunctional platelets, which can lead to prolonged bleeding times. As in other IBMFS, FPD/AML patients have a high risk of leukemogenic transformation, which is reported to be 20-50% (average 35%) [Hyde et al., 2017; Osato, 2004; Song et al., 1999]. (Further insights on *RUNX1* mutations are provided in section 1.1.6.1.1.)

#### 1.1.5.2 Cyclic and severe congenital neutropenia

Neutropenia is defined by low absolute neutrophil counts (ANC), usually below 1500/ul, and the increased susceptibility to bacterial infections. There are two types of neutropenia. On the one hand, there are acquired forms, which can be caused by infectious diseases (viral - EBV, CMV; bacterial - mycobacteria, salmonella; etc.), certain drugs, (nutritional) deficiencies or can be developed

spontaneously in the course of life. On the other hand, there are hereditary forms of neutropenia, such as benign ethnic neutropenia (BEN), or with life-threatening disease states, such as severe congenital neutropenia (CN) [Boxer, 2012; Gibson and Berliner, 2014; Herold, 2016; Munshi and Montgomery, 2000]. CN is characterized by an ANC below 500/ul, with or without extra-hematopietic manifestations, due to inherited or sporadic mutations in among others, *ELANE, HAX1, SBDS, G6PC3* and *CSF3R* (**figure 1.4**) [Boztug et al., 2008; Skokowa et al., 2017; Triot et al., 2014; Ward et al., 1999; Welte and Zeidler, 2009]. CN is a rare disease with a prevalence of approximately 2.05 per 1 million people. Official numbers vary between 0.1 and 8.6 cases per 1 million people depending on the country (numbers calculated from [Donadieu et al., 2013] for Canada, the EU, Switzerland, Norway and the US). Patients affected by CN suffer from frequent severe bacterial infections, such as pneumonia, oral ulcers and sepsis. When CN is clinically suspected, the diagnostic approach includes repeated blood counts, bone marrow examination and molecular genetic testings (either starting with the gene known to cause CN in a related patient or *ELANE*) [Skokowa et al., 2017; Welte et al., 2006]. In the bone marrow smears a maturation arrest of granulocytic differentiation at the promyelocyte stage is observed, this is often accompanied by eosinophilia and an increase in the numbers of monocytes [Welte et al., 2006]. Prior to the discovery and clinical application of G-CSF, CN patients had a reduced life expectancy with a mortality rate of more than 80%, even despite antibiotic therapy [Dale, 1998; Kalra et al., 1995; Skokowa et al., 2017; Welte and Dale, 1996]. The application of G-CSF results in markedly increased ANC values that are closer to normal (ANC >1000/ul). This provides sufficient protection against bacterial pathogens [Collins and Dokal, 2015; Skokowa et al., 2017]. Besides infections, CN patients carry the risk of a leukemogenic progression to MDS or AML. Malignant transformation has been reported before G-CSF was available for treatment [Gilman et al., 1970], but with a prolonged lifetime and overall survival more cases of leukemogenic progression were observed [Skokowa et al., 2017]. Through the development and implementation of databanks and registries, such as the 'Severe Chronic Neutropenia International Registry' [SCNIR, 2018], patient data can

be collected and investigated. It has been found that within 15 years approximately 22% of people affected by CN and treated with G-CSF develop MDS/AML [Rosenberg et al., 2006, 2010]. The MDS/AML risk of a CN patient under G-CSF treatment is about 2-3% per year [Rosenberg et al., 2010; Skokowa et al., 2017]. It is remarkable that there are CN patients, who require higher dose of G-CSF to achieve granulocyte counts over 1000/ul and these have a consecutively higher MDS/AML risk, reaching values of 40% in a time period of 15 years [Skokowa et al., 2017]. Despite new advances in targeted gene therapy, made possible by iPSC (inducible pluripotent stem cells) and CRISPR-Cas9 based models, the only curative therapy - especially at the event of overt leukemia , i.e. MDS/AML - is allogeneic transplantation of HSCs (HSC-Tx), which inherits its own adverse effects, such as sepsis upon immunosuppression and relapse or progression to leukemia (Of note, success rate and long-term safety of HSC-Tx has improved over the years.) [Nasri et al., 2019; Pittermann et al., 2017; Skokowa et al., 2017; Zeidler et al., 2000, 2013]. Thus, the time point to propose HSC-Tx to a CN patient should be at the end of therapeutic options and chosen carefully [Skokowa et al., 2017; Zeidler et al., 2000].

Cyclic neutropenia (CyN) is characterized by low ANCs and a periodic change in the number of neutrophils and monocytes - the numbers change cyclically over 21 days (interestingly, the number of monocytes behaves anticyclically to that of neutrophils). CyN is caused by *ELANE* mutations [Skokowa et al., 2017]. Until 2015, patients with CyN were not expected to progress to AML, but Klimiankou et al. described a case where CyN patient developed AML [Klimiankou et al., 2016a]. Therefore, both CN and CyN are considered as preleukemic syndromes, with CN having the higher probability of leukemic progression [Skokowa et al., 2017].

#### 1.1.5.2.1 Mutations and mechanisms underlying CN

As mentioned above, CN can be the result of a broad range of mutations, but in approximately 40% of the cases, CN is caused by autosomal-dominant mutations in the *ELANE* gene, encoding neutrophil-specific elastase (NE) [Makaryan et al., 2015; Skokowa et al., 2017]. Mutations in *ELANE* can also be observed in CyN

[Makaryan et al., 2015; Skokowa et al., 2017]. Neutrophil elastase is a cytotoxic serine protease found in neutrophil granules and important for the intracellular processing of protein substrates and extracellular pathogen defense [Skokowa et al., 2017].

The mechanism underlying CN caused by mutated *ELANE* is a subject of current research and several theories of possible pathomechanisms have been proposed over the years. It was observed that the differentiation of neutrophils stopped at the promyelocyte stage and progenitors became apoptotic [Aprikyan et al., 2003; Köllner et al., 2006; Massullo et al., 2005; Skokowa et al., 2017; Welte et al., 2006]. It is currently assumed that mutations in *ELANE* cause protein misfolding and induce the unfolded protein response (UPR) which leads to apoptosis [Dannenmann et al., 2019; Germeshausen et al., 2013; Horwitz et al., 2007; Nustede et al., 2016; Skokowa et al., 2017; Thusberg and Vihinen, 2006; Weischenfeldt et al., 2005]. Further theories include the mislocalization of mutated NE and disturbed biological functions of the NE mutants; but results among different workgroups were inconsistent and could only partially explain the CN pathogenesis [Bellanné-Chantelot et al., 2004; Germeshausen et al., 2010, 2013; Grenda et al., 2007; Köllner et al., 2006; Makaryan et al., 2015; Massullo et al., 2005; Skokowa et al., 2017]. Recent discoveries in iPSC generated myeloid cells of CN patients suggest a connection between the mislocalization theorem and the endoplasmatic reticulum stress-induced UPR hypothesis [Nayak et al., 2015]. Nayak et al. showed that *ELANE* mutations caused a maturation arrest, led to mislocalization of NE and resulted in reduced levels of C/EBP$\alpha$ [Nayak et al., 2015]. In addition, they showed that either correction of the *ELANE* mutations or the administration of Sivelestat (a drug limiting NE misfolding) and low-dose G-CSF allowed myeloid progenitors to differentiate and to overcome the neutropenic phenotype [Nayak et al., 2015]. They hypothesized that Sivelestat and G-CSF restored NE trafficking, i.e. resolved mislocalization, and resolved misfolding what abrogated ER/UPR stress which allowed normal C/EBP$\alpha$ activity, as observed in healthy myelocytes [Nayak et al., 2015]. Nasri et al. went one step further and showed by CRISPR/Cas9 mediated knockout of mutant *ELANE* - they introduced a pre-

mature stop codon in exon 2 which leads to nonsense-mediated mRNA decay inhibiting mutant ELANE expression - granulocytic differentiation could be induced resulting in functional neutrophils [Nasri et al., 2019]. Interestingly, induction of *ELANE* mutations - previously observed in CN patients - in mice did neither induce a neutropenic phenotype nor resulted in malignant transformation of myeloid cell clones [Grenda et al., 2002].

Another point of great interest in CN is the correlation of genotype and phenotype. There have been reports which showed genotype-phenotype correlation by intensive statistical analysis, e.g. some *ELANE* mutants were exclusive to CyN or correlated with a more severe or benign phenotype. However, a reliable phenotype-genotype prediction can not yet be done [Germeshausen et al., 2013; Makaryan et al., 2015; Skokowa et al., 2017]. Genotype-phenotype prediction was further questioned when Newburger et al. and Boxer et al. reported about a sperm donor (phenotypically healthy) with mosaicism for mutant *ELANE* in his spermatozoa who fathered eight children, seven with a CN and one with a CyN phenotype - all positive for the same *ELANE* mutation (NE p.S97L) [Boxer et al., 2006; Newburger et al., 2010; Skokowa et al., 2017]. For CyN besides individual differences in mutant *ELANE* effects, a statistical/mathematical model has been proposed which, by a negative feedback-loop, explains the cycling of neutrophil amounts observed in patients [Horwitz et al., 2007; Skokowa et al., 2017]. Another pathomechanism proposed by Skokowa and Welte concerns CXCR4 expression in HSPCs, which correlates negatively with the release of hematopoietic cells in the blood. CXCR4 is a substrate cleaved by NE and the authors argue that incorrect processing of CXCR4 by the mutated NE could lead to an increased surface expression of CXCR4 and thus limit the release of neutrophils in blood, as observed in CN patients [Skokowa and Welte, 2013].

In addition to *ELANE* mutations, mutations in *SBDS* and *SLC37A3* are the second, respectively third most frequent cause of CN [Skokowa et al., 2017]. *SBDS* encodes the Schwachman-Bodian-Diamond syndrome protein, and in SBDS patients neutropenia is accompanied by pancreatic and the bone disorders [Dale and Welte, 2011; Skokowa et al., 2017; Spoor et al., 2019]. Mutations in *SLC37A4*, en-

coding G6PT (glucose 6 phosphate transporter), lead to neutropenia associated with metabolic disturbances, whilst mutations in *G6PC3*, a G6PCT dependent protein, lead to pancytopenia [Skokowa et al., 2017; Spoor et al., 2019]. Of note, some patients with mutated *G6PC3* have abnormalities in the urogenital system or congenital heart defects [Boztug et al., 2008].

Another cause of CN are autosomal-recessive mutations in the *HAX1* gene [Klein et al., 2007; Skokowa et al., 2017]. *HAX1* encodes the HCSL1-associated protein X1, and *HAX1* mutations lead to CN in approx. 2-7 % of cases [Klein et al., 2007; Skokowa et al., 2017]. Of note, *HAX1* mutations are a more frequent cause of CN in Europe, presumably due to consanguineous families, and also in the pedigree first described by Kostmann in 1956, *HAX1* mutations were found as cause of CN [Klein et al., 2007; Kostmann, 1956]. In Europe, incidence of homozygous *HAX1* mutations reaches 11%, while in the US no *HAX1* mutation was found in CN patients [Donadieu et al., 2013; Skokowa et al., 2017]. *HAX1* mutations may be associated with extra-hematopoietic manifestations, such as abnormal neurologic presentation. In line, *HAX1* deficient mice died as a consequence of neurologic disabilities [Chao et al., 2008; Germeshausen et al., 2008; Skokowa et al., 2017]. Interestingly, the CN phenotype induced by *HAX1* mutations is highly similar to the one induced by *ELANE* mutations [Skokowa et al., 2006; Zeidler et al., 2009]. HAX1 functions as anti-apoptotic protein and in CN due to homozygous truncating mutations can not longer exert its role, thus affected myelocytes undergo apoptosis [Boztug et al., 2008; Klein et al., 2007; Touw, 2015]. Furthermore, it was observed that HAX1 is involved in reducing ER stress, which is also elevated in mutated (MT-)*ELANE* CN, suggesting similarities in CN pathogenesis for both affected genes [Touw, 2015]. Lentiviral induction of *HAX1* in *HAX1*-mutant hiPSC derived cells induced neutrophil maturation - i.e. overcame the CN phenotype [Morishima et al., 2014]. Mutant *HAX1* as cause of CN was further confirmed by Pittermann et al., who corrected mutant *HAX1* p.W44X by CRISPR/Cas9 to wild type *HAX1* in hiPSC derived myeloid cells [Pittermann et al., 2017].

Besides the UPR theory, Skokowa et al. found that in myeloid cells of CN patients with mutations in either *ELANE* or *HAX1*, levels of LEF1 transcription factor,

lymphoid enhancer-binding factor 1, were reduced [Skokowa et al., 2006, 2009]. They postulated a mechanism in which reduced LEF1 levels resulted in reduced NE, CEBP$\alpha$ levels and increased PU.1 levels which lead to a maturation arrest of promyelocytes and favored a monocytic fate [Skokowa et al., 2009]. Of note, reduced LEF1 levels were not observed in samples obtained from CyN patients [Skokowa et al., 2009]. In addition, mutations in other genes cause CN but are rare, and in some cases the cause is unknown [Skokowa et al., 2017].

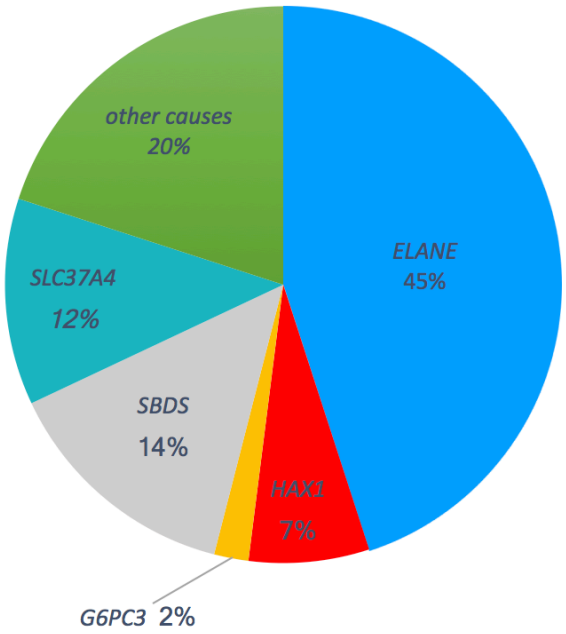


**Figure 1.4: Mutations present in CN**
The genetic causes of CN are highly versatile. In approx. 45% of the cases, CN is caused by mutations within *ELANE*, followed by *SDBS*[§], *SLC37A4*[*], *HAX1* mutations and mutations in the *G6PC3* gene. In the remaining 20% of CN cases, CN is caused by other mutations, not further mentioned here *(WAS*[$]*, CSF3-R, GFI*[£]*, etc.)*.
[†] Glucose-6-Phosphatase Catalytic Subunit 3
[£] Growth Factor Independent 1 Transcriptional Repressor
[§] Ribosome maturation protein SBDS
[*] Solute Carrier Family 37 (Glucose-6-Phosphate Transporter), Member 4
[$] Wiskott - Aldrich - Syndrome
*Adapted from Skokowa et al. [2017]: 'Severe congenital neutropenias'. Nature Reviews Disease Primers 3:17032.*

### 1.1.6 Leukemogenic progression in CN

Leukemogenic progression is a highly versatile multi-step process including genetic or epigenetic mechanisms. On blood cell level, these alterations lead to ei-

ther a pre-leukemic syndrome or leukemia. The mutations, in the process of leukemogenesis, first described by Knudson et al., and referred to as two-hit model of malignant transformation include type-I and type-II mutations [Gilliland et al., 2004; Knudson, 1971].

Type-I mutations, in e.g. *FLT3ITD, bcr-abl, N-ras*, lead to increased proliferation and prolonged survival of the affected cells. On the blood level, type-I mutations can lead to myeloproliferative disorders (MPD) such as increased proliferation and prolonged survival of red blood cells in Polycythemia vera (PV) which is caused by JAK2 mutations [Hyde et al., 2017].

Type-II mutations restrict differentiation, exemplary mutations can be found in *C/EBPα, CSF3R* and *RUNX1* which induce myelodysplastic syndromes (MDS) [Hyde et al., 2017]. Currently, the postulated mechanism of malignant progression is the two-hit model of cooperating type I and II mutations that lead to malignant transformation; however, it must be taken into account that there are other authors which suggest that hematopoietic cells may be more resistant to leukemic transformation and more than ”two hits” may be required to induce a leukemic phenotype [Hyde et al., 2017; Lin et al., 2017; Schnittger et al., 2011].

#### 1.1.6.1 Mechanisms of leukemogenic progression downstream of the CN-assosiated mutations

A frequently observed early event in the leukemogenic transformation of CN patients is the occurrence of myeloid cells clones positive for both a) the inherited mutation underlying the CN phenotype and b) a possibly acquired nonsense mutation in *CSF3R* [Beekman and Touw, 2010; Skokowa and Welte, 2013; Skokowa et al., 2017; Touw et al., 2013; Welte and Zeidler, 2009]. From the early on, nonsense G-CSFR was reported to act dominantly negative over wild type (WT-) G-CSFR in CN patients and mutant G-CSFR seemed to promote proliferation and suppress differentiation [Dong et al., 1994, 1995; Dwivedi and Greis, 2017; Hermans et al., 1999; Qiu et al., 2017; Touw et al., 2013].

It is known that cytoplasmic truncated G-CSFR protein leads to numerous disturbances in the downstream signaling pathway in myeloid cells [Dwivedi and Greis,

2017; Qiu et al., 2017; Touw et al., 2013].

*Mutant CSF3R causes prolonged signaling thus acts dominantly negative over wild type CSF3R.*

It was hypothesized that dominance of nonsense CSF3R over wild type CSF3R is achieved by (i) lower receptor internalization rates [Hermans et al., 1999] and (ii) by avoidance of inhibitory signaling via SOCS3 [Zhuang et al., 2005]. Internalization as well as SOCS3 mediated termination of G-CSFR signaling requires C-terminal domains which are not expressed by nonsense *CSF3R* found in CN. Internalization of G-CSFR disrupts G-CSFR signaling by degradation, thus diminished internalization of nonsense G-CSFR leads to a longer half-life and sustained signaling compared to wild type G-CSFR signaling [Dwivedi and Greis, 2017; Hermans et al., 1999; Touw et al., 2013]. Normally, SOCS3 mediated G-CSFR signaling termination is induced by STAT3 and requires a tyrosine residue not expressed by nonsense G-CSFR.

*JAK2/STAT pathway in nonsense CSF3R clones is altered in favor of proliferation.*

Interestingly, nonsense G-CSFR leads to prolonged STAT5 activity - promoting proliferation - and shortened STAT3 activity - reducing differentiation and reduced SOCS3 activation. This might be due to the fact that the C-terminal region required for activation of STAT3 but not STAT5 is missing. Another explanation was given by Zhang et al. who postulated that STAT3 activation requires internalization while STAT5 activation can occur without internalization [Zhang et al., 2018]. Additionally, the ROS levels are increased by the enhanced STAT5 signaling [Touw et al., 2013].

*Sustained PI3K/Akt pathway signaling in nonsense CSF3R clones suppresses apoptosis and increases ROS production.*

When nonsense G-CSFR is activated, the PI3K/Akt signaling pathway lasts longer, inhibiting apoptosis and further increasing ROS levels [Gits et al., 2006; Touw et al., 2013]. ROS, in concordance with ER stress, results in amplified intracellular stress which might lead to genomic instability and the acquisition of further mutations required for leukemic progression.

*Cooperating effects of nonsense CSF3R and mutant ELANE abrogate UPR and pro-apoptotic signaling.*

A recently published report suggested that nonsense G-CSFR abolished the expression of mutant *ELANE*, thus terminating MT-NE-induced UPR and pro- apoptotic signals [Qiu et al., 2017]. Presumably, in addition to the mechanisms mentioned above, this leads to a switch from production of neutrophils that tend to undergo apoptosis to those that have a proliferative advantage over the other clones that are not positive for nonsense *CSF3R* [Qiu et al., 2017].

#### 1.1.6.1.1 *RUNX1* mutations and their implications in phenotypes other than CN-AML

*RUNX1* point mutations were reported to define early events in malignant transformation in AML and MDS patients with different FAB (French-American-British classification systems for hematological disease) subtypes [Blumenthal et al., 2017; Hyde et al., 2017; Imai et al., 2000; Michaud et al., 2002; Osato et al., 1999]. On average, acquired *RUNX1* mutations can be found in approximately 15% of all AML patients. Additionally, inherited *RUNX1* mutations were found to be the underlying cause of FPD/AML which inherits a high risk - approximately 35% - for leukemogenic progression (see bone marrow failure syndromes) [Haferlach et al., 2016; Osato, 2004; Song et al., 1999; Stengel et al., 2018]. *RUNX1* mutations were especially frequent in FAB M0 subtype, associated with mutagens such as cytotoxic therapy, DNA damage (e.g. caused by radioactivity), older age and confer an unfavorable prognosis [Harada et al., 2003; Hyde et al., 2017; Osato, 2004; Tang et al., 2009].

The observed mutations can be grouped into four categories: (1) N-terminal truncating mutations (Nt), (2) missense mutations (Ms), (3) frameshift mutations resulting in an elongated protein (Fs) and (4) C-terminal truncating mutations (Ct) (**figure 1.5**) [Harada and Harada, 2009; Hyde et al., 2017]. The mechanism that contributes to malignant transformation, is not yet fully understood, but has been broadly elucidated since its first discovery by Ostao et al. in 1999 [Cammenga et al., 2007; Harada and Harada, 2009; Hyde et al., 2017; Osato et al., 1999].

There have been inconsistent reports about the effects of Nt-RUNX1 on its function. On the one hand, it was reported that Nt-RUNX1 lost its ability of DNA- and CBF-$\beta$ -binding, thus presented a loss of function; and on the other hand, Michaud et al. reported for e.g RUNX1p.R174X a dominant negative effect over wild type (WT-) RUNX1 [Hyde et al., 2017; Imai et al., 2000; Michaud et al., 2002; Osato et al., 1999; Song et al., 1999]. However, it is currently assumed that Nt-RUNX1 is degraded by nonsense mediated mRNA decay (NMD), thus is not expressed *in vivo*, which results in haploinsufficiency of *RUNX1*. [Cammenga et al., 2007; Hyde et al., 2017; Maquat, 2004; Weischenfeldt et al., 2005].

Due to the absence of the TAD, elongated Fs-RUNX1 proteins are proposed to have an abrogated protein-protein interactions, thus are also non-functional [Hyde et al., 2017]. In summary, Nt-RUNX1 and Fs-RUNX1 act via haploinsufficiency.

Missense mutations (Ms) alter the aa-residue sequence and cluster mainly in the RHD domain of RUNX1 protein [Metzeler and Bloomfield, 2017]. They were described to interrupt DNA, but not CBF-$\beta$ binding and thus act dominantly negative over WT-RUNX1 [Harada and Harada, 2009; Hyde et al., 2017].

C-terminal truncated RUNX1 proteins do not undergo NMD and are reported to be expressed in $CD34^+$ cells [Schmit et al., 2015]. Although it is still unclear, there are several suggestions that try to explain the leukemogenic potential of Ct-RUNX1: Ct-RUNX1 with absent or impaired TAD might lack important interaction potential with other proteins restricting its trans-activation potential, Ct-RUNX1 might compete with WT-RUNX1 for target genes as well as for CBF-$\beta$ and other coactivator/corepressor proteins and one report proposed that Ct-RUNX1 might repress *Gadd45a* thus interfere with DNA-damage stress response [Bellissimo and Speck, 2017; Harada and Harada, 2009; Hyde et al., 2017; Michaud et al., 2002]. Furthermore, depending on the position of truncation, Ct-RUNX1 resembles the splice-variant RUNX1a, which is also described to inhibit WT-RUNX1 activity. In summary, all proposed effects of Ct-RUNX1 result in a loss of function, which might be accompanied by possibly negative inhibitory effects on WT-RUNX1. Of special interest is, that Ct-RUNX1 and Ms-RUNX1 induce different clinical characteristics. The bone-marrow of patients with Ms-RUNX1 is hypocel-

lular and those of Ct-RUNX1 patients is hypercellular [Harada and Harada, 2009]. Further evidence of the inhibitory potential of some MT-RUNX1 types was derived from FPD/AML patients. Those who were positive for allegedly dominant RUNX1 proteins were more likely to undergo malignant transformation compared to patients in whom the mechanism was explained by *RUNX1* haploinsufficiency [Michaud et al., 2002; Osato, 2004; Song et al., 1999]. Thus, there are some similarities between Ms- and Ct-RUNX1.

Finally, all mutations have in common that they reduce the amount of WT-RUNX1 [Harada and Harada, 2009; Hyde et al., 2017]. In line with a dominant effect of some mutant RUNX1 proteins, Cammenga et al. reported that Ms-RUNX1 mutants resulted in the accumulation of myeloid progenitors at a higher ratio than did RUNX1 deficiency alone [Cammenga et al., 2007]. This implicates that RUNX1 can function simultaneously as tumor suppressor and oncogene. Interestingly, biallelic *RUNX1* mutations are frequently associated to FAB M0 subtype, indicating that absence of RUNX1 causes a more severe leukemic phenotype [Osato, 2004]. In contrast, gain of Chr 21, first reported by Preudhomme et al., is not associated with FAB M0 but accompanied by at least one additional mutant *RUNX1* allele and never by an additional wild type allele [Preudhomme et al., 2000, 2009]. In line with the multiple hit model of malignant transformation, i.e. leukemogenesis, sole *RUNX1* mutations do not induce a malignant phenotype, thus the occurrence of secondary, cooperating events is required [Cammenga et al., 2007; Gilliland et al., 2004; Knudson, 1971]. Downstream of *RUNX1* mutations those cooperating effects include e.g. mutations in *EVI.1, CSF3R, FLT3, KRAS, NRAS, IDH1/2*, monosomy 7, trisomy 13, trisomy 21 [Christiansen et al., 2004; Harada and Harada, 2009; Hyde et al., 2017; Osato, 2004]. On a rare basis, mutations in *C/EBPα* and *NPM1* are found in samples positive for MT-RUNX1 [Harada and Harada, 2009; Hyde et al., 2017; Osato, 2004]. Of special notice is, that *RUNX1* mutations serve as an independent negative predictor for overall survival (OS) and lower rates of complete remission (CR), but not for disease-free survival [Metzeler and Bloomfield, 2017].

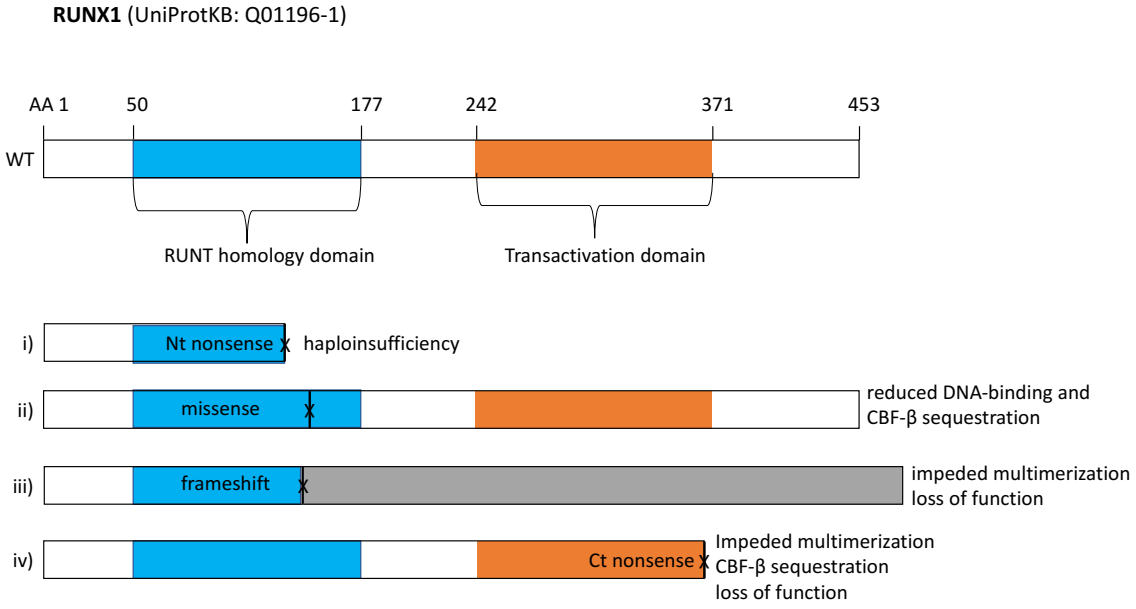


**Figure 1.5: Model of RUNX1 mutations and changes in protein expression**
Different types of RUNX1 mutations found in MDS, CN-AML, FPD/AML, CML and AML patients and their implications for MT-RUNX1 functions. (i) N-terminal (Nt) nonsense mutations result in truncated RUNX1 molecules and due to nonsense-mediated decay lead to RUNX1 haploinsufficiency. (ii) Missense mutations result in impaired DNA binding capacity and confer dominant negative potential. (iii) Frameshift mutations result in an exchange of amino-acids downstream the mutation site, thus impair the protein structure and interrupt RUNX1 multimerization as well as transactivation potential. (iv) Nonsense mutations result in C-terminal (Ct) truncated RUNX1 proteins and lack transactivation potential with retained DNA- and CBF$\beta$-binding potential. They are reported to confer negative dominant potential over WT-RUNX1.
*Adapted from Hyde et al. [2017]'RUNX1 and CBF-$\beta$ mutations and activities of their wild type alleles in AML' Advances in Experimental Medicine and Biology, 2017. vol 962. p.265-282.*

#### 1.1.6.1.2 Role of *RUNX1* mutations in leukemic progression in CN/AML patients

It is particularly striking, that patients harboring clones positive for both the CN-associated mutation and *CSF3R* mutations show no malignant phenotype [Skokowa et al., 2014, 2017]. Hence, further genetic alterations are required for the induction of a leukemic phenotype. In 2014, Skokowa et al. reported that in addition to *CSF3R* mutations, heterozygous mutations in *RUNX1* were a frequent event [Skokowa et al., 2014]. In the cohort investigated, approximately 64% of CN-AML patients were positive for *MT-RUNX1* [Skokowa et al., 2014, 2017]. Furthermore, it was shown that *RUNX1* mutations - distributed across the gene - were

a late event of leukemogenic progression in CN-AML patients and occurred after clones were positive for mutant *CSF3R* (**figure 1.6**) [Skokowa et al., 2014]. The authors proposed a cooperation between MT-G-CSFR and MT-RUNX1 which induced the leukemic phenotype (**figure 1.7**). They suspected that *CSF3R* mutations offered a survival advantage for mutant over wild type clones, in combination with G-CSF administration [Skokowa et al., 2014]. This was further supported by the fact, that in one patient, clones positive for *MT-CSF3R* and *MT-RUNX1* disappeared when G-CSF was discontinued. *In vitro* experiments showed, that $CD34^+$ cells positive for both *RUNX1* and *CSF3R* mutations had reduced differentiation and increased proliferation potential, i.e. presented a leukemic phenotype [Skokowa et al., 2014].

Interestingly, some of the patients were not only positive for *RUNX1* and *CSF3R* mutations but also for mutations related to leukemia such as *SUZ12, EP300, CBL, CREBBP, FLT3-ITD* and some also harbored chromosomal abnormalities such as monosomy 5, monosomy 7, trisomy 21, which were acquired after the occurrence of *RUNX1* mutations [Skokowa et al., 2014]. Of special note is, that *Nras* was found to be mutated in one patient which was negative for both *CSF3R* and *RUNX1* mutations. This was interpreted by the authors as a possible alternative mechanism of leukemogenic progression in CN [Skokowa et al., 2014].

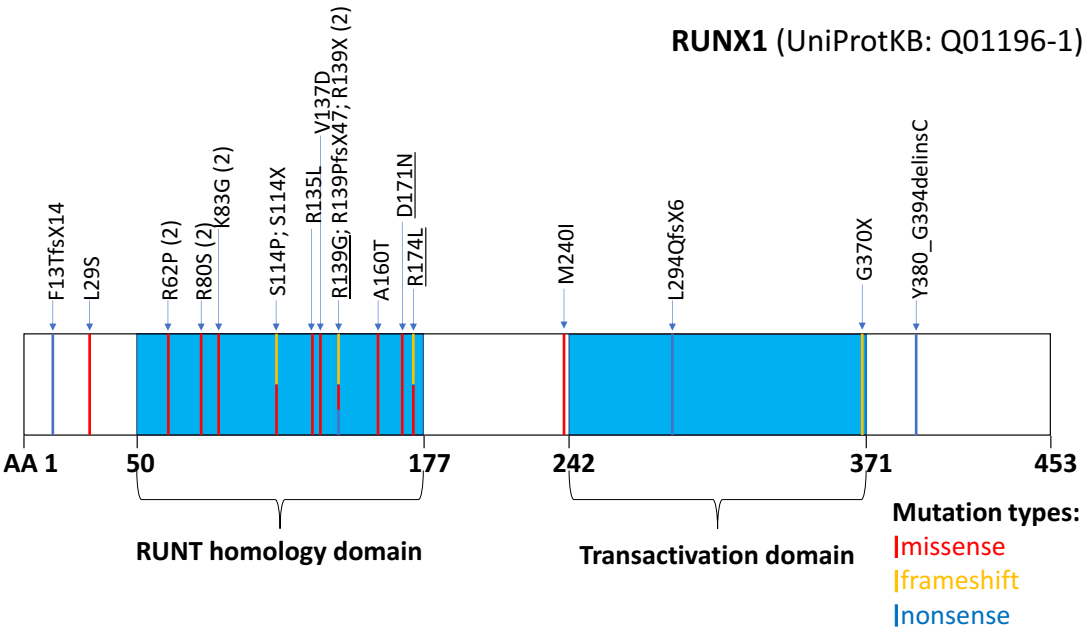


**Figure 1.6: Distribution of *RUNX1* mutations RUNX1 protein identified in CN patient at overt AML**

*RUNX1* mutations were distributed over the whole RUNX1 protein with a cluster in RHD (AA position 50 till 178; first blue box). RHD and TAD (AA 242 - 371) are indicated by blue boxes. Colored vertical lines indicate mutation position (red = missense, yellow = frameshift and blue = nonsense mutation). Letters and numbers indicate AA exchange and AA position respectively. Numbers in brackets indicate multiple patients with the same mutation.

*All info and annotations refer to RUNX1 UniProtKB:Q01196-1 (www.uniprot.org). Adapted from Skokowa et al. [2014] 'Cooperativity of RUNX1 and CSF3R mutations in severe congenital neutropenia: A unique pathway in myeloid leukemogenesis'. Blood, 2014. vol.123. no.13. p.2229-2237.*

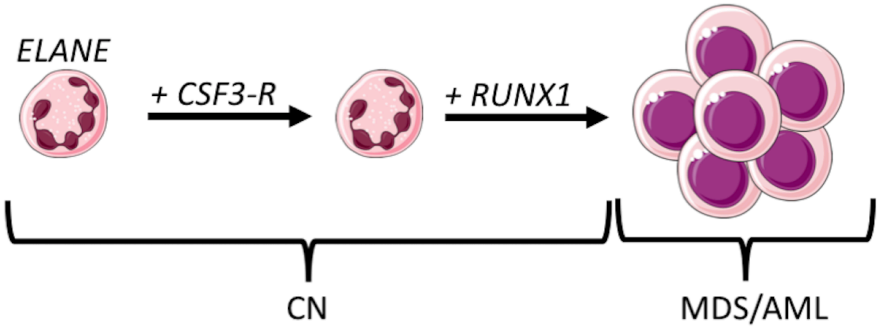


**Figure 1.7: Model of malignant progression in CN**

Somatic *CSF3R* and *RUNX1* mutations follow inherited *ELANE* mutations. A malignant phenotype (MDS/AML) is observed only in cells which inherit *ELANE* and both somatic mutations.

*Adapted from Skokowa et al. [2014] 'Cooperativity of RUNX1 and CSF3R mutations in severe congenital neutropenia: A unique pathway in myeloid leukemogenesis'. Blood, 2014. vol.123. no.13. p.2229-2237.*

## 1.2 Discovery, biogenesis and function of microRNA

### 1.2.1 Discovery of microRNA

MicroRNAs (microRNA, miR) are small approx. 22 nucleotide (nt) long non-coding RNAs, discovered first in the nematode *C. elegans* in the 1990s [Almeida et al., 2011; Lee, 1993; Weiss and Ito, 2018]. Since microRNAs are involved in post-transcriptional regulation of mRNAs (messenger RNA), they are considered as key players in protein regulation, although they are not translated into proteins [Weiss and Ito, 2018].

### 1.2.2 Nomenclature of microRNA

The understanding of microRNA's nomenclature is essential for distinction between different microRNAs (summary in **figure 1.8**, a registry of microRNAs is available at *mirbase.org* [MiRBase, 2018]).

Before 2003, the discovered microRNAs were mostly named either according to the phenotype they induced or genes and organisms in which they were discovered. For example, let-7 microRNA family was named according to its function of controlling steps in larval development in *C. elegans* [Pasquinelli et al., 2000; Weiss and Ito, 2018]. In 2003, when more microRNAs have been discovered, they received numeric names, e.g. *'miR-125'* [Ambros et al., 2003; Griffiths-Jones, 2005; Weiss and Ito, 2018]. It is generally accepted, that microRNAs with homologous sequences from $2^{nd}$ to $8^{th}$ nt (nucleotide) belong to the same family of microRNA and are therefore grouped in microRNAs families [Budak et al., 2016]. MicroRNAs differing in only a few nucleotides (usually 2 nt) are even closer related *(they represent so-called sister microRNAs)*; thus a letter is added to the numeric name, e.g., *'miR-125a'* and *'miR-125b'*. If different genomic regions code for the same microRNA, the microRNA receives a number following the actual name, e.g., *'miR-125b-1'* and *'miR-125b-2'*. MicroRNAs from the same locus consist of two different strands, the 3'-strand and the 5'-strand, the suffix at the end of a microRNA's name gives information about its origin, e.g., *'miR-125b-2-3p'* and

*'miR-125b-2-5p'* [Budak et al., 2016; Ha and Kim, 2014]. Several prefixes exist to indicate the organism in which the microRNA occurs, for example, *hsa*-miR-125b is found in human *(homo sapiens)* [Budak et al., 2016].

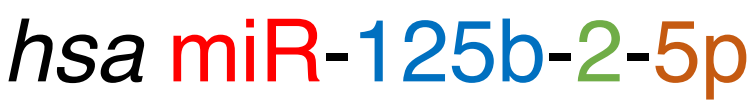


**Figure 1.8: Summary of nomenclature of microRNA**
A letter code is indicating the species, e.g., *'hsa'* for *'homo sapiens'* or *'v'* for *'viral'* ***(black)***. A letter code following the species indicates the grade of processing. The prefix *'pri-'* indicates a microRNA not yet processed by Drosha, whereas a *'pre-'* indicates a microRNA already processed by Drosha but not yet by Dicer. Mature microRNAs do not require a prefix ***(red)***. In most cases a numeral code represents the name and the family of the microRNA. A letter following the numeral code indicates similarity between two microRNAs which only differ in a few nucleotides *(e.g. 'a' for sub-type 'a' and 'b' for sub-type 'b')* ***(blue)***. A number following the microRNA's name indicates that there are several gene loci coding for the exact same microRNA ***(green)***. The suffix *'5p'* or *'3p'* represents the strand the miR is descending ***(brown)***.
*Some microRNAs, discovered before 2003, do not follow this strict nomenclature.*

### 1.2.3 Biogenesis of microRNA

The synthesis of microRNAs follows either a canonical Dicer-dependent pathway or a Dicer-independent ('slicer' and RNA-POL III dependent) pathway [O'Connell et al., 2011]. Of note, the comprehensive description of microRNA biogenesis in the following chapter covers the canonical pathway only and does not apply to the synthesis of all yet known microRNAs (**figure 1.9**). The description of all possibilities of microRNA biogenesis would exceed the capacity of this thesis, thus we refer to further literature on microRNA-biogenesis, e.g. by MacFarlane and Murphy, Weiss and Ito, Krol et al. or Ha and Kim [Ha and Kim, 2014; Krol et al., 2010; MacFarlane and R. Murphy, 2010; Weiss and Ito, 2018].

The microRNA biogenesis starts, similar those of mRNA, with transcription by RNA Polymerase II. The initially produced transcript is termed pri-miRNA and is longer than the final structure (approx. 1kb). Pri-miRNAs already contain the final microRNA sequence which includes the stem- or hairpin-loop. The characteristic loop results from Watson-Crick pairing of complementary nucleotides, which is

later forming the 3' and 5' microRNAs strands. In the nucleus, pri-miRNAs are processed by an enzyme complex, termed the Microprocessor, including Drosha Ribonuclease III [Weiss and Ito, 2018]. As a result of being processed by the Microprocessor complex, pri-miRNAs lose large parts of their sequence and mainly consist of their hairpin-loop, a 3' tail 2 nt longer than the 5' tail and are from this point referred to as pre-miRNAs. Pre-miRNAs are approx. 70 nts long and delivered in the cytoplasm via transporter protein EXP5 in a GDP-dependent manner [Weiss and Ito, 2018]. In the cytoplasm, pre-miRNAs are cleaved at their hairpin-loop by the Dicer enzyme complex, an RNA Polymerase III. It cuts the 5' pre-miRNA strand after 22 nt in 3' direction right below the hairpin-loop and leaves a double-stranded but very short RNA structure. Those RNA strands are mature 5'-miRNA and 3'-miRNA [Ha and Kim, 2014].

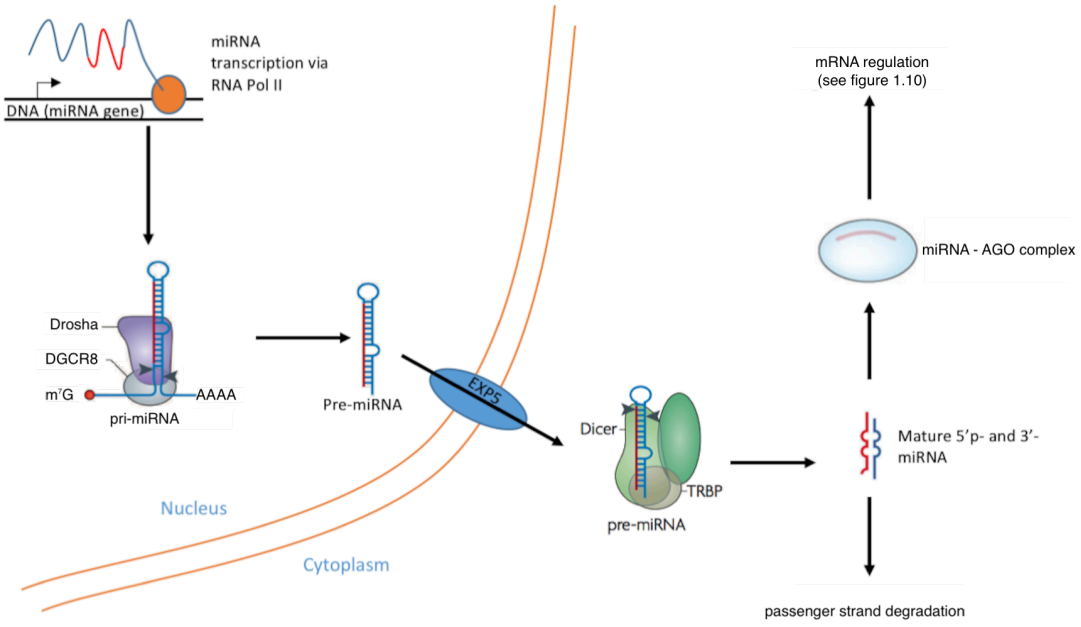


**Figure 1.9: Scheme of microRNA biogenesis**
Pri-microRNA is transcribed by RNA Pol II and afterward processed by Drosha with support from DGCR8. The resulting pre-microRNA is transferred via a GTP dependent mechanism from the nucleus into the cytoplasm by exportin 5 (EXP5). In cytoplasm, pre-microRNA is processed and cleaved by an enzyme complex including Dicer. Afterward, one mature microRNA strand is selected and used for post-transcriptional regulation by AGO protein. The passenger strand is degraded.
*Adapted and merged from Ha and Kim [2014] 'Regulation of microRNA biogenesis'. Nature Reviews Molecular cell biology. 15:8. p.509-534 and Krol et al. [2010] 'The widespread regulation of microRNA biogenesis, function and decay'. Nature Reviews Genetics. 11:9. p.597-610.*

### 1.2.4 Functions of microRNA

Dicer in interplay with human AGO (argonaute) protein selects the strand with the lower binding energy in its 5' end, thus the thermodynamically more unstable, or the strand with an uracil ('U') residue in 1$^{st}$ nucleotide position as the guiding strand [Ha and Kim, 2014; Weiss and Ito, 2018]. The selected microRNA strand is transferred into an AGO protein and later serves as a template for mRNA binding. AGO proteins inherit endonucleolytic activity and mediate the function of small RNAs, e.g. by binding microRNAs and recruitment of other enzymes and factors. This effector complex is termed microRNA induced silencing complex (miRISC) and is responsible for the diverse ways of post-transcriptional repression of mRNA by microRNA [Höck and Meister, 2008; Weiss and Ito, 2018]. The strand that was not selected as guiding strand, is released and quickly degraded by component 3 promotor of RISC (C3PO) [Weiss and Ito, 2018]. In contrast to early publications, both microRNA strands inherit the potential to act as guiding strand and not always the 5'-strand is preferably selected [Ha and Kim, 2014]. After the AGO proteins bound to a microRNA, the complex of microRNA and AGO protein binds to a specific mRNA via Watson-Crick base-pairing and assembles the RISC on the spot. Watson-Crick base pairing occurs between the 2$^{nd}$ and 8$^{th}$ nt of the microRNA and mainly the 3'-untranslated region (UTR) of the target mRNA, but binding of microRNA to 5'-UTR and central parts of mRNA structure has also been described [Almeida et al., 2011; Ha and Kim, 2014; MacFarlane and R. Murphy, 2010; Weiss and Ito, 2018]. AGO proteins and RISC assembly lead to translational repression of the affected mRNA via three canonical pathways (**figure 1.10**):

i) mRNA degradation:
   If the microRNA binds to the mRNA and their sequences match completely, cleavage of the mRNA is immediately initiated by the miRISC, and as a result, mRNA is degraded on the spot [Höck and Meister, 2008; Jonas and Izaurralde, 2015].

ii) Translational inhibition:
   If the microRNA's sequence does not match the mRNA's completely, translational repression can be achieved by inhibition of cap-dependent translational initiation; of note, the exact molecular process remains a subject of

current research [Jonas and Izaurralde, 2015]. It is assumed, that translational repression accounts for 6-26% of microRNAs repression capacity [Jonas and Izaurralde, 2015].

iii) Deadenylation and subsequent decapping and degradation:
After the microRNA has bound to the mRNA, a poly-enzyme complex initiates deadenylation of the poly-A tail. Subsequently, decapping is performed by another enzyme-complex and leaves an mRNA ready for degradation by 5' to 3' exonuclease enzyme XRN1 [Jonas and Izaurralde, 2015].
Of note, it is currently proposed, that there is a close link between the pathways 'ii)' and 'iii)'. Since untranslated mRNA is inevitably degraded, it is hard to distinguish between the effect of translational inhibition and the effects of deadenylation, decapping and degradation in terms of mRNA silencing by microRNA [Jonas and Izaurralde, 2015].

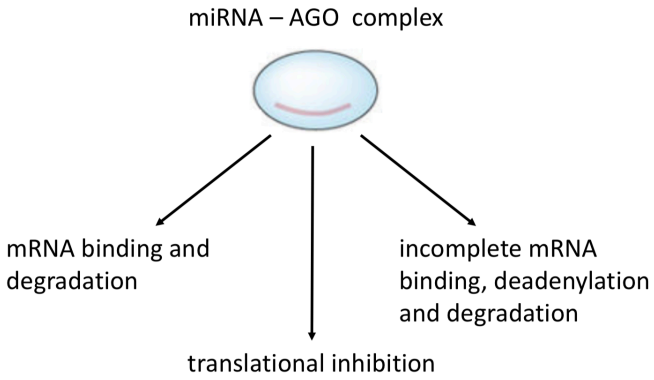


**Figure 1.10: Model of microRNA functions**
MicroRNAs use different mechanisms to induce translational repression.
*Adapted and merged from Höck and Meister [2008] 'The Argonaute protein family'. Genome biology. 9:2. p.210.1-210.8. and Ha and Kim [2014]'Regulation of microRNA biogenesis'. Nature Reviews. Molecular cell biology. 15:8. p.509-524.*

Besides the canonical pathways of microRNA induced repression, there are further ways how microRNAs influence homeostasis and regulate cell signaling. Some microRNAs induce gene transcription, e.g., miR-373 and miR-205 are described to recruit enzymes of translational activity to complementary promotor regions [Weiss and Ito, 2018]. This function inherits large potential for future research, but microRNA's translational activation is yet poorly understood [Weiss and Ito, 2018].

### 1.2.5 Role of microRNA in hematopoiesis with focus on myelopoiesis and leukemogenic progression

The understanding of microRNA's role in hematopoiesis has progressed continuously in recent years. Petriv et al. investigated microRNA clusters among many different hematopoietic cells and cells related to the hematopoietic system [Petriv et al., 2010]. They discovered, that microRNA expression of hematopoietic cells depends on the cell type and stage of differentiation. Thus, it is possible to group cells into clusters based on the expression of microRNA, and vice versa, measuring microRNA expression proved to be another way to distinguish between cell-types and between hierarchical stages of differentiation [Petriv et al., 2010].

MiR-223 is a well-characterized microRNA in hematopoiesis. In HSC, the miR-223 expression level is relatively low, but it increases with differentiation [O'Connell et al., 2011; Petriv et al., 2010]. This is caused by C/EBP$\alpha$ and NFI-A both competing for binding of a miR-223 promotor region and controlling miR-223 expression [Weiss and Ito, 2018]. C/EBP$\alpha$ induces miR-223 expression resulting in a repression of NFA-1 by miR-223. Vice versa when NFA-1 is expressed, it inhibits miR-223 and thus reduces granulocytic differentiation, so repression of NFA-1 by miR-223 is nothing else but a positive auto-regulatory feedback loop [O'Connell et al., 2011; Weiss and Ito, 2018]. Furthermore, miR-223 deficiency leads to granulocytic proliferation in mice, suggesting a second function of miR-223 as an inhibitor of proliferation [Weiss and Ito, 2018]. Another myeloid regulatory pathway of microRNAs is known, where PU.1 and C/EBP$\alpha$ cooperatively induce miR-223 expression more strongly than they would do it independently, and in contrast GATA1, a TF stimulating erythroid differentiation, represses miR-223 expression [Weiss and Ito, 2018].

Petriv et al. investigated further microRNAs, and found additional specific expression profiles, e.g., miR-125b is strongly expressed in hematopoietic stem and progenitor cells, and upon differentiation its expression level is reduced [Petriv et al., 2010]. The miR-125 family comprises of three independent miRs, -125a, -125b-1 and -2, and is involved in a wide range of oncologic processes [O'Connell

et al., 2011; Weiss and Ito, 2018]. Overexpression of miR-125b blocks the differentiation in cells from human leukemia cell lines (HL-60 and NB4) and in $CD34^+$ blasts obtained from patients and additionally cooperates with GATA1 to induce proliferation [Weiss and Ito, 2018]. This further indicates a close link between microRNA expression and their role for cell homeostasis and differentiation. Surdziel et al. found, that miR-125b negatively affected the differentiation induced by activated G-CSFR. It inhibited differentiation and supported proliferation of neutrophil progenitor cells, highlighting the importance of microRNA in myelopoiesis and myeloid cell homeostasis [Surdziel et al., 2011]. Other microRNAs were found to be especially highly expressed in myeloid cells like miR-25, -221 and as mentioned -223 [Petriv et al., 2010]. Petriv et al. reported, that particular microRNAs clustered by expression in biologically similar cells, e.g., it was found that expression of certain microRNAs subjected to very low variability in lymphoid $CD4^+$, $CD8^+$ and natural killer cells (NK). Thus, it was hypothesized, that microRNAs control important intracellular programs and clusters grouped according to similar expression of microRNAs that reflect functional similarities between the cells [Petriv et al., 2010]. Petriv and Kuchenbauer et al. also found similarities in the expression of microRNA clusters between cells of the same hierarchical level - in terms of their state of differentiation. Those similarities significantly changed or disappeared upon differentiation [Petriv et al., 2010]. As a result, cells can be distinguished by microRNA expression clusters and grouped according to their stage of differentiation and functional similarities.

Let-7 microRNA family was one of the first microRNAs discovered [Pasquinelli et al., 2000], and later reported to be expressed throughout myeloid differentiation [Petriv et al., 2010]. Let-7 is involved in an auto-regulatory feedback loop with lin-28 and Hmga2 which regulates HSC maintenance [Weiss and Ito, 2018].

The complex regulatory mechanisms involving miRNAs have a great potential for malfunction and disruption of crucial cellular processes. Hence, several miRNAs, known as oncomiRs, have oncogenic potential [Weiss and Ito, 2018]. There are three pathways of malignant transformation related to microRNAs: (1) microRNAs (oncomiRs) induce malignancies by over-expression, (2) microRNAs which

usually suppress oncogenes and induce malignancies when down-regulated, and (3) general disturbances in microRNA biogenesis can impair all microRNAs, thus lead to disease [Weiss and Ito, 2018].

Additionally to its role mentioned above, miR-125 plays a role in prostate cancer, and a microRNA cluster including miR-125b inherits oncogenic potential in AML [Klusmann et al., 2010; Weiss and Ito, 2018].

Among microRNAs involved in the orchestration of leukemogenesis and malignant transformation, is miR-139-5p which down-regulation is associated with childhood AML and poor outcome, whereas up-regulation of miR-139-5p indicates a better prognosis [Emmrich et al., 2015]. MiR-139-5p usually represses EIF4G2 and therefore leads to cell cycle arrest and apoptosis, thus, functioning as a tumor suppressor [Emmrich et al., 2014]. Its down-regulation leads to a contrary effect, and thus, promotes proliferation and malignant progression [Emmrich et al., 2015]. This effect was not only reported by Emmrich et al. in leukemia, but also in solid malignancies such as hepatocellular carcinoma (HCC). Thus, low miR-139 expression levels favor metastasis of cancerous cells, whereas an up-regulation of miR-139-5p is associated with a lower risk of metastatic spreading and a better prognosis in general [Emmrich et al., 2015; Luo et al., 2014; Wong et al., 2011]. Another microRNA involved in malignant diseases is miR-3151, which is located within the genomic region of BAALC (for brain and acute leukemia, cytoplasmic) on chromosome 8 [Eisfeld et al., 2012, 2014]. BAALC and miR-3151 are up-regulated in neural cells and undifferentiated hematopoietic cells [Eisfeld et al., 2014]. It has been described, that patients with overt leukemia or after stem-cell transplantation and high levels of BAALC expression had a worse prognosis and shorter remission intervals compared to patients without BAALC or miR-3151 expression. Eisfeld et al. hypothesized, that suppression of *TP53* by miR-3151 was responsible for leukemogenic progression in this AML group and the relatively worse outcome of the patients [Eisfeld et al., 2012]. In a later published article, they showed that over-expression of miR-3151 reduced p53 abundance, inhibited apoptosis and supported the proliferation of cells [Eisfeld et al., 2014]. Interestingly, they also observed that *BAALC* but not miR-3151 expression was induced

by RUNX1, which is known to be involved in leukemogenic progression in Congenital Neutropenia (CN) patients [Eisfeld et al., 2014; Skokowa et al., 2014] (sections 1.1.3 and 1.1.5). Of note, this reflects the potential clinical use of microRNAs as markers for diseases and predictors for the outcome.

A potential for clinical use of microRNAs and their role in diseases lays in the field of translational therapy, where targeting microRNA homeostasis and affected pathways could serve to manipulate pathologic conditions in patients where there is currently no or only inferior treatment available. For BAALC and miR-3151, Eisfeld et al. showed that Bortezomib (a proteasome inhibitor, used as drug in multiple myeloma patients) is a potential drug available for treatment. The authors found that Bortezomib disrupted SP1/NF-$\kappa$B and subsequently reduced miR-3151 and BAALC levels [Eisfeld et al., 2014]. Another example for translational therapy was a phase II trial, that has been conducted to target miR-122, a cofactor of HCV replication, by the drug Miravirsen, an antagomiR of miR-122 with the aim to reduce the viral load of HCV in 2014 [Weiss and Ito, 2018]. Antagonization of miR-122 repressed the protection that miR-122 provided HCV by inhibiting its degradation [Drury et al., 2017; Weiss and Ito, 2018]. It was shown that, following a few subcutaneous applications of Miravirsen, the viral load had been reduced significantly, but unfortunately started rising again in most patients after a few weeks [Drury et al., 2017]. In summary, targeting of microRNAs and the related pathways inherits a potential for future therapies and treatments, but it will take further research until drugs regulating or interfering with microRNA can be administered to patients on a regular basis.

## 1.3 Aims of the study

In this study, we aim to evaluate the mechanism of leukemogenic progression in congenital neutropenia.

1. We aimed to investigate mutated *RUNX1* allelic fraction abundance compared to *RUNX1* wild type fraction in patients at CN and CN-AML stage. This is a continuation of the project started by our group in previous years and published by Skokowa et al. [Skokowa et al., 2014]. Furthermore, we sought to establish a workflow allowing us to isolate DNA and identify targets of wild type RUNX1 versus mutated RUNX1 and obtain information about the binding behavior of RUNX1.

2. Our aim was to investigate the expression pattern of microRNAs in a CN patient cohort. Therefore, the present work was designed to establish a workflow for isolation and quantification of microRNA. Additionally, we wanted to investigate expression of 'miR-125b' and 'miR-3151' in hematopoietic cells obtained from CN patients and healthy donors.

*Luck is a matter of preparation*
*meeting opportunity.*

Lucius Annaeus Seneca

# 2

# Material and Methods

Materials and methods used for gathering the data presented in chapter 3.

## 2.1 Material

### 2.1.1 Cells and cell lines

The cells and cell lines mentioned in the **table 2.1** were used in this study. In total, twenty-three patients with CN, CyN or MDS/AML were analyzed. The study was performed with the signed informed consent of all subjects obtained through the respective institutional review boards and was approved by the Tübingen Medical School Institutional Review Board (966/2018B02, 929/2018B02, 814/2018B02). Mutated genes are depicted in *italic brackets* behind the patient ID.

**Table 2.1: Cells and cell lines**

| Name | Origin |
|---|---|
| Cells derived from CD34$^+$ BM MNC | AG Skokowa |
| HEK 293T | DSMZ |
| HL-60 | DSMZ |
| hiPSCs | AG Skokowa |
| Jurkat | DSMZ |
| K-562 | DSMZ |
| KG1-alpha | DSMZ |
| MDA-MB-231 | DSMZ |
| NB4 | DSMZ |
| CD33$^+$ cells from HD#4 | AG Skokowa |
| CD33$^+$ cells from HD#5 | AG Skokowa |
| CD33$^+$ cells from HD#12 | AG Skokowa |
| CD33$^+$ cells from HD#28 | AG Skokowa |
| CD33$^+$ cells from HD#28 | AG Skokowa |
| CD33$^+$ cells from HD#30 | AG Skokowa |
| CD33$^+$ cells from HD#31 | AG Skokowa |
| CD33$^+$ cells from patient #E14 CN *(ELANE)* | AG Skokowa |
| CD33$^+$ cells from patient #E14 CN-AML *(ELANE, CSF3R, RUNX1)* | AG Skokowa |
| CD33$^+$ cells from patient #E31 CN *(ELANE)* | AG Skokowa |
| CD33$^+$ cells from patient #E31 CN-AML *(ELANE, CSF3R, RUNX1)* | AG Skokowa |
| CD33$^+$ cells from patient #E32 CN *(ELANE)* | AG Skokowa |
| CD33$^+$ cells from patient #E32 CN-AML *(ELANE, CSF3R, RUNX1)* | AG Skokowa |
| CD33$^+$ cells from patient #H1 *(HAX1)* | AG Skokowa |
| CD33$^+$ cells from patient #H2 *(HAX1)* | AG Skokowa |

Continued on the next page

**Table 2.1: Cells and cell lines – continued from the previous page**

| Name | Origin |
|---|---|
| $CD33^+$ cells from patient #E1 *(ELANE)* | AG Skokowa |
| $CD33^+$ cells from patient #U1 *(genetically unclassified)* | AG Skokowa |
| $CD33^+$ cells from patient #U2 *(genetically unclassified)* | AG Skokowa |
| $CD33^+$ cells from patient #H3 *(HAX1)* | AG Skokowa |
| $CD33^+$ cells from patient #S1 *(SDS)* | AG Skokowa |
| $CD33^+$ cells from patient #E2 *(ELANE)* | AG Skokowa |
| $CD33^+$ cells from patient #E3 *(ELANE)* | AG Skokowa |
| $CD34^+$ cells from #HD28 | AG Skokowa |
| $CD34^+$ cells from #HD29 | AG Skokowa |
| $CD34^+$ cells from #HD30 | AG Skokowa |
| $CD34^+$ cells from #HD31 | AG Skokowa |
| $CD34^+$ cells from patient #H4 *(HAX1)* | AG Skokowa |
| $CD34^+$ cells from patient #U1 *(genetically unclassified)* | AG Skokowa |
| $CD34^+$ cells from patient #U2 *(genetically unclassified)* | AG Skokowa |
| $CD34^+$ cells from patient #E2 *(ELANE)* | AG Skokowa |
| $CD34^+$ cells from patient #H5 *(HAX1)* | AG Skokowa |
| hiPSCs #HDiPS | AG Skokowa |
| hiPSCs from patient #E14 L5-diff *(ELANE, CSF3R, RUNX1)* | AG Skokowa |
| hiPSCs from patient #E14 L6-diff *(ELANE, CSF3R, RUNX1)* | AG Skokowa |
| hiPSCs from patient #E14 L8-diff *(ELANE)* | AG Skokowa |
| hiPSCs from patient #E14 L10-diff *(ELANE, CSF3R, RUNX1)* | AG Skokowa |
| hiPSCs from patient #E14 L11-diff *(ELANE, CSF3R, RUNX1)* | AG Skokowa |
| hiPSCs from patient #E14 L13-diff *(ELANE, CSF3R, RUNX1)* | AG Skokowa |
| hiPSCs from patient #E14 L14-diff *(ELANE, CSF3R, RUNX1)* | AG Skokowa |
| hiPSCs from patient #E14 L15-diff *(ELANE, CSF3R, RUNX1)* | AG Skokowa |
| hiPSCs from patient #E14 L16-diff *(ELANE, CSF3R, RUNX1)* | AG Skokowa |
| hiPSCs from patient #E14 L6-diff *(ELANE, CSF3R, RUNX1)* | AG Skokowa |
| hiPSCs from patient #E14 L8-diff *(ELANE)* | AG Skokowa |

Continued on the next page

**Table 2.1: Cells and cell lines – continued from the previous page**

| Name | Origin |
|---|---|
| hiPSCs from patient #E14 L10-diff *(ELANE, CSF3R, RUNX1)* | AG Skokowa |

### 2.1.2 Equipment

**Table 2.2: Equipment**

| Name | Company |
|---|---|
| Agilent Bioanalyzer 2100 | Agilent |
| Neubauer chamber | Hecht |
| Centrifuge 5147R | Eppendorf |
| Centrifuge 5418 | Eppendorf |
| Centrifuge 5424 | Eppendorf |
| Centrifuge 5424R | Eppendorf |
| Centrifuge 5810R | Eppendorf |
| Centrifuge Megafuge 1.0 R | Heraeus |
| Centrifuge myFuge mini | Benchmark |
| Centrifuge Z160M | Hemde |
| Dual Flat Block™ GeneAmp PCR System 9700 | ThermoFisher Scientific |
| Film processor CP1000 | AGFA |
| Filmcasette | AGFA |
| Flow cytometer FACS Diva | BD Biosiences |
| Focused ultrasonicator M220 | Covaris |
| Freezer -80 °C | GFL |
| Fridge +4 °C and Freezer -20 °C Comfort | Liebher |
| Fridge +4 °C Comfort no freeze | Liebher |
| Gel electrophoresis running chamber | Bio Rad |
| Gel electrphoresis power unit E835 | Consort |

Continued on the next page

**Table 2.2: Equipment – continued from the previous page**

| Name | Company |
|---|---|
| Gel-documentation system | INTRAS Sience Imaging |
| Gelelectrophoresis hood | Heraeus |
| Hood DNA/RNA UV-Cleaner UVC/T-AR | Kisker-Biotech |
| Hood Safe 2020 | ThermoFisher Scientific |
| Icebuckets | Neolab |
| Icemaker AF100 | Scotsman |
| Incubator Hera cell | ThermoFisher Scientific |
| LightCycler™ 480 | Roche |
| Microscope CKX 41 | Olympus |
| Microscope Wilovert S | hund |
| Microwave | AEG |
| Mini Protean 3 cell | Bio Rad |
| Mini Trans Blot | Bio Rad |
| Mixer RCT basic | IKA |
| NanoDrop ND-1000 | Nano Technologies |
| PCR Cycler Master nexus GX2 | Eppendorf |
| PCR600 Workstation | Air Clean |
| Pipette research 0.5-10 ul | Eppendorf |
| Pipette research 10-100 ul | Eppendorf |
| Pipette research 100-1000 ul | Eppendorf |
| Pipette research 2-20 ul | Eppendorf |
| Pipette research 20-200 ul | Eppendorf |
| Pipetteboy | Integra Biosiences |
| Power Pack Basic | Bio Rad |
| QuantStudio™ 3D Digital PCR Chip Adapter Kit for Flat Block Thermal Cycler | ThermoFisher Scientific |
| QuantStudio™ 3D Digital PCR Chip Loader | ThermoFisher Scientific |

Continued on the next page

**Table 2.2: Equipment – continued from the previous page**

| Name | Company |
|---|---|
| QuantStudio™ 3D Digital PCR Instrument with Power Cord | ThermoFisher Scientific |
| QuantStudio™ 3D Digital PCR Thermal Pads | ThermoFisher Scientific |
| QuantStudio™ 3D Tilt Base | ThermoFisher Scientific |
| Rocker 'Rocky' | LTF |
| Rocker M3 | CMT |
| Steam Autoclave Type 022.022.050 | Wesa |
| Thermomixer 5436 | Eppendorf |
| Vortex Genie 2 | Bender & Horbein AG |
| Vortex MS3 basic | IKA |
| Waterbath 36° C | GFL |

**Table 2.3: Consumables**

| Name | Company |
|---|---|
| 96 Well Light Cycler plates | Sarstedt |
| Adhesive qPCR foil | Sarstedt |
| AFA Tubes | Covaris |
| Amersham Hyperfilm TM Gel | GE Healthcare |
| Biosphere extra long tips | Sarstedt |
| Biosphere filter tips (2.5; 10; 100; 1000 ul) | Sarstedt |
| CD33 Microbeads human | Miltenyi Biotec |
| CD34 PE-Cy7 Clone 8G12 antibody | BD |
| DMSO | Sigma |
| DNA Away solution | Carl Roth |
| DNA gel Loading Dye (6x) 5x1 ml | ThermoFisher Scientific |
| DNA LoBind Tube 1,5 ml | Eppendorf |

Continued on the next page

**Table 2.3: Consumables – continued from the previous page**

| Name | Company |
|---|---|
| Eppendorf DNA lo-bind (0.2; 0.5; 1.5; 2.0 ml) | Eppendorf |
| Eppendorf tubes (0.2; 0.5; 1.5; 2.0 ml) | Eppendorf |
| Flow cytometry tubes | BD Biosiences |
| TaqMan Assay reagents | ThermoFisher Scientific |
| Gel Red Nucleic Acid Gel stain | Biotrend |
| Immersion Fluid syringe | ThermoFisher Scientific |
| Low Binding SafeSeal-Tips (10; 100; 200; 1000; 1250 ml) | Bioyzm |
| Luminata Forte Western HRP Substrate | Millipore |
| Nitrocellulose 0,2 mm 1 roll 300 mm x 4 m | GE Healthcare |
| Page Ruler Pre-stained Protein Ladder, 10 to 180 kDa | ThermoFisher Scientific |
| Pierce Control Agarose Resin | ThermoFisher Scientific |
| Pierce ECL Western Blotting Substrate | ThermoFisher |
| Pierce IP lysis Buffer 250 ml | ThermoFisher Scientific |
| ProtranPremium Western blotting membranes, nitrocellulose | Amersham |
| QuantStudio™ 3D Digital PCR Chip Lid v2 | ThermoFisher Scientific |
| QuantStudio™ 3D Digital PCR Chip v2 | ThermoFisher Scientific |
| QuantStudio™ 3D Digital PCR Chip v2 Kit | ThermoFisher Scientific |
| QuantStudio™ 3D Digital PCR Master Mix v2 | ThermoFisher Scientific |
| QuantStudio™ 3D Digital PCR Sample Loading Blade | ThermoFisher Scientific |
| QuantStudio™ 3D Digital PCR Sample Loading Blade 8 | ThermoFisher Scientific |
| QuantStudio™ 3D Digital PCR Master Mix v2 | ThermoFisher Scientific |
| Quibit assay tubes | Invitrogen |
| Safe-Lock Tubes (0.5; 1.5; 2.0 ml) | Eppendorf |

Continued on the next page

**Table 2.3: Consumables – continued from the previous page**

| Name | Company |
|---|---|
| Sample Loading Guide 15 combs | Bio Rad |
| Serol. Pipette (5; 10; 25; 50 ml) | Sarstedt |
| TC-Flask (T25, T75 ml) | Sarstedt |
| Test tubes (15; 50 ml) | Greiner Bio-One |
| Whatman gel blotting paper, Grade GB003 58x60 cm | Sigma-Aldrich |

### 2.1.3 Reagents and chemicals

**Table 2.4: Reagents and chemicals**

| Reagents/chemicals | Company |
|---|---|
| 10x RT Buffer | Applied Biosystems |
| 2-Mercaptoethanol | Sigma |
| APEL serum-free differentiation medium | Stemcell technologies Inc. |
| Aqua ad iniectabilia | Braun |
| Basic fibroblast growth factor (bFGF) | Prepotech |
| Bovine serum albumin (BSA) | Milteney |
| Buffer AL (264 ml) | Qiagen |
| Calcium chloride | Merck |
| Chloroform | Roth |
| DMSO | Sigma |
| DMEM F12 | Sigma |
| dNTP Mix PCR Grade | Qiagen |
| Double destilled water (ddH2O) | Merck |
| Ethanol 100% | SAV |
| Ethanol 100% | Roth |
| Fetal Bovine Serum (FBS) Lot: 025M3361 500 ml | Sigma Aldrich |
| Fetal Calf Serum (FCS) | Biochrome |
| Gel Red | Biotium |
| Granulocyte Colony Stimulating Factor (G-CSF) | R&D Systems |
| Hydrochloric acid (HCl) | Carl Roth |
| Isopropanol | VWR Chemicals |
| IL-3 | R&D Systems |
| Knockout Serum Replacement | Invitrogen |

Continued on the next page

**Table 2.4: Reagents and chemicals – continued from the previous page**

| Reagents/chemicals | Company |
|---|---|
| L-Glutamine | R&D Systems |
| LE Agarose | Biozym |
| Matrigel | Corning |
| Methanol | Roth |
| Methanolfree Formaldehyde | ThermoFisher Scientific |
| Methocult H4435 Enriched medium | Stemcell Technologies |
| Mitomycin-C | Sigma |
| N,N,N',N'-tetramethyl-ethane-1.2-diamine (TEMED) | Sigma |
| Non-essential amino acids solution | Invitrogen |
| PBS 500 ml | Biozym |
| Penicillin/Streptomycin 100 ml | Biochrome |
| Prointeinase K | ThermoFisher Scientific |
| Protease Inhibitor cocktail | Roche |
| RNase A | Qiagen |
| RNaseZap | Ambion |
| ROCK Inhibitor | R&D |
| RPMI 1640 medium | Gibco |
| Stem cell factor (SCF) | R&D Systems |
| SDS 250 g >99.5% | Roth |
| Sterillium | Bode |
| Tris | Roth |
| Tween 20 | AppliChem |
| Vascular Endothelial Growth Factor (VEGF) | R&D Systems |

### 2.1.4 Kits

**Table 2.5: Kits**

| Name | Company |
|---|---|
| MACS MicroBead Technology | Miltenyi |
| miRNeasy Micro Kit | Qiagen |
| Omniscript RT Kit | Qiagen |
| Pierce Reversible Protein Stain-Kit | ThermoFisher Scientific |
| QIAamp DNA Mini Kit | Qiagen |
| QuantStudio™ 3D Digital PCR chip kit v.2 | ThermoFisher Scientific |
| Quibit dsDNA HS Assay Kit | Invitrogen |
| Quibit Protein Assay Kit | Invitrogen |
| Quibit RNA HS Assay Kit | Invitrogen |
| RNeasy Micro Kit | Qiagen |
| TaqMan Advanced mi RNA cDNA Synthesis Kit | ThermoFisher Scientific |

### 2.1.5 Primers

#### 2.1.5.1 Digital PCR primers

For digital PCR, custom TaqMan SNP Genotyping assays *(ThermoFisher Scientific, US)* were designed individually. The assays include specific primers and probes, labeled with VIC green or FAM blue dyes for detection. The sequence of the target gene was identified by means of (primer-) basic local alignment search tool (Primer-BLAST) and then two sequences were created, one for the wild-type sequence and one with the target mutation. Afterward, the resulting nucleotide sequences were processed by RepeatMasker software *(Institute for Systems Biology;* ***table 2.9***) and subsequently submitted to ThermoFisher Scientific. The TaqMan assays used for digital PCR are listed in **table 2.6**.

**Table 2.6: TaqMan SNP Genotyping Assay for digital PCR**

| **RUNX1 Mutation** | **Primer Sequence (Forward *'fwd'* and reverse *'rev'*; 5' to 3')** | **VIC Probe (wild type) (5' to 3')** | **FAM Probe (mutation) (5' to 3')** |
|---|---|---|---|
| p.R139G (CN-AML pat. #14) | *fwd*: AAA CGT GTT TCA AGC ATA GTT TTG ACA<br>*rev*: CAT GAA GAA CCA GGT TGC AAG ATT T | TCT TCC ACT TCG ACC GAC | CTT CCA CTT CCA CCG AC |
| p.D171N (CyN-AML pat. #1) | *fwd*: CAC CTAC CAC AGA GCC ATC AAA AT<br>*rev*: GGA TGC ACT TAC TTC GAG GTT CTC | CAC AGT GGA TGG GCC | CAC AGT GAA TGG GCC |
| p.R174L (CN-AML pat. #31) | *fwd*: CCA CAG AGC CAT CAA AAT CAC AGT<br>*rev*: CAG CCC CAA GTG GAT GCA | ATG GGC CCC GAG AAC | ATG GGC CCC TAG AAC |

**For all samples amino acid positions were used according to the RUNX1 protein variant UniProtKB:Q01196 (www.uniprot.org).*

#### 2.1.5.2 MicroRNA assays

For the detection and quantification of microRNA, the following 'TaqMan Advanced miRNA Assays' *(Thermo Fisher Scientific, US)* were used:

- hsa-miR-3151-5p for miRNA-3151
- hsa-miR-125b-5p for miRNA-125b subtypes
- hsa-let-7b-5p for miRNA-let-7b, which was described as constitutively expressed in hematopoietic cells by Petriv et al., served as endogeneous control and was used for normalization [Petriv et al., 2010].

#### 2.1.5.3 Real-time PCR primers

**Table 2.7: qPCR Primers for ChIP**

| Gene name | Primer Name | Primer sequence (5' to 3') | PCR-product length |
|---|---|---|---|
| RUNX3 | RUNX3PR_fwd | TGAGCTGAGGTTGGGTTGA | 150 |
| | RUNX3PR_rev | AGGCTCTGGTGGGTACGA | |
| RUNX3 | PK.RUNX3_fwd | TGTATCCGTCTAGGCAGTGGA | 258 |
| | PK.RUNX3_rev | CCCCACAGCCTGCGATTTTT | |
| UBE2M | UBE2M_fwd | GCTCGCGGTCACTTCATCTT | 188 |
| | UBE2M_rev | GAAGGTACTCGACCTCGCAC | |
| KHSR | KHSR_fwd | GTGCTTGTAAAGATGGGCAGC | 278 |
| | KHSR_rev | CGCTAATCCCCTCGCTGTCT | |
| GNA15 | GNA15_fwd | TAATTCTGAAGCCAGCGGGAG | 276 |
| | GNA15_rev | AACCGGATAGCAGCAACGA | |
| PKC-beta | PKCB_fwd | ATCCCATTGGTCATTCTGCA | 310 |
| | PKCB_rev | TATTGATCTACTGAAATCCTTCCTC | |

### 2.1.6 Antibodies

**Table 2.8: Antibodies for IP and Western Blot**

| Antibody | Origin | Company | Catalog number |
|---|---|---|---|
| alpha-Tubulin | Rabbit | Cell Signaling | CS2144 |
| anti-goat | Donkey | Santa Cruz | SC2020 |
| anti-mouse | HRP | Cell Signaling | CS7076 |
| anti-rabbit | Goat | Santa Cruz | SC2004 |
| beta-Actin | Mouse | Cell Signaling | CS3700 |
| ELANE | Goat | Santa Cruz | SC9520 |
| rabbit isotype control | Rabbit | Cell Signaling | CS2729S |
| RUNX1 | Rabbit | Abcam | ab23980 |
| RUNX1 | Rabbit | Cell Signaling | CS4334S |

### 2.1.7 Software

**Table 2.9: Software**

| Name | Source |
|---|---|
| Adobe Draw | Adobe Systems |
| Primer-BLAST | blast.ncbi.nlm.nih.gov |
| Excel | Microsoft |
| FACS Diva Software | BD Biosciences |
| FlowJo | flowjo.com |
| GraphPad Prism | graphpad.com/scientific-software/prism |
| LightCycler 480 Software | lifescience.roche.com |
| miRBASE | mirbase.org |
| PowerPoint | Microsoft |
| QuantStudio 3D AnalysisSuite Cloud Software | Thermo Fischer Scientific |
| RepeatMasker | repeatmasker.org |
| Smart Servier | smart.servier.com |

## 2.2 Methods

### 2.2.1 Cell biology methods

#### 2.2.1.1 Cell culture

All non-adherent cells were cultured in 25 ml or 75 ml TC-Flasks (Sarstedt, GER) in *RPMI 1640–Gibco* medium *(Life Technologies, US, CA)* supplemented with 10 % inactivated FCS and 1 % PBS in a *HERAcell incubator* (Heraeus, GER) at 37 °C and in a 5 % $CO_2$ environment. 293T cells were cultured in DMEM under the conditions mentioned above. The medium was changed depending on cell confluency. Non-adherent cells (all cells except for MDA-MB-231, breast-cancer cell line and 293T cell line) were centrifuged with 300 xg for 5 minutes, washed in PBS and new medium was added. Afterward, the supernatant was replaced by fresh medium. Cells were passaged twice a week. Non-adherent cells were centrifuged at 300 xg for 5 minutes, the supernatant was removed and 1–3 ml fresh medium was added, cells were counted in a Neubauer chamber (LO - Laboroptik Ltd, UK), $1x10^6 cells/15\ ml$ were seeded. Dead cells were excluded by Trypan blue staining. For the adherent cells, medium was removed and cells were incubated with a trypsin-EDTA solution at 37 °C for 5 minutes. After that, FCS was added to block enzymatic activity of trypsin, and cells were spun down by centrifugation, then the cell pellet was resuspended in fresh medium and cells were counted in a Neubauer chamber. Dead cells were excluded by Trypan blue staining. $1x10^6 cells/15\ ml$ were seeded.

#### 2.2.1.2 HiPSC cell culture

The h iPSCs were maintained on mitomycin-C treated SNL-feeder cells *(Public Health, England)* in iPSC-medium consisting of DMEM F12 *(Sigma)* supplemented with 20 Knockout Serum Replacement *(Invitrogen)*, 30 ng/ml bFGF *(Peprotech)*, 1% non-essential amino acids solution *(Invitrogen)*, 100 $\mu$M 2-Mercapto-Ethanol and 2 mM L-Glutamine.The iPSC-medium was replaced every day. The

hiPSCs were subcultured by manual colony-picking onto new SNL feeder cells every 10 days.

#### 2.2.1.3 EB-based hematopoietic differentiation of hiPSCs

HiPSCs were dissociated from SNL-feeders or Matrigel-coated plates *(Corning)* using PBS/EDTA (0.02%) for 5 min. EB induction was done via spin EBs (20 000 cell/EB) in 96-well plates using APEL serum-free differentiation medium *(Stemcell Technologies)* with bFGF (20 ng/ml) and ROCK Inhibitor *(R&D)*. The next day, BMP4 (40 ng/ml) was added to induce mesodermal differentiation. On day 4, EBs were plated on matrigel-coated 6-well-plates (10 EBs/well) in APEL medium supplemented with VEGF (40 ng/ml) + SCF (50 ng/ml) + IL-3 (50 ng/ml). For myeloid differentiation, the medium was changed 3 days later to APEL + IL3 (50 ng/ml) + GCSF (50 ng/ml). The first hematopoietic floating cells appeared on day 12 - 14. Floating cells were harvested every 3-4 days and used for qPCR, digital PCR, Western Blot analysis from day 14 to day 32.

#### 2.2.1.4 Colony forming unit (CFU) assay

10,000 floating cells from EB-based iPS differentiation at day 14 were used for CFU-Assay using Methocult H4435 Enriched medium *(Stemcell Technologies)*. Colonies were counted after 10 or 14 days.

### 2.2.2 Cell separation of $CD34^+$ and $CD33^+$ cells

Separation of $CD33^+$ and/or $CD34^+$ cells from bone marrow or peripheral blood samples was done by means of *MACS MicroBead Technology (Miltenyi, GER)* according to the protocol. At first, total cell number was determined then cells were centrifuged at 300 xg and supernatant was removed and cells were diluted in PBS-buffer. FcR Blocking Reagent and $CD34^+$ Micro Beads were added, and the cell suspension was incubated at +4 °C for 30 min. The PBS-buffer was added to the mixture and centrifuged at 300 xg for 10 min, then supernatant was removed, the cells were taken into solution with PBS-buffer, placed on the magnetic columns

and steadily rinsed with buffer. The flow-through was collected in an additional tube for $CD33^+$ separation. The $CD34^+$ fraction was eluted from the column in a new tube and cell purity was tested by means of FACS. Separation of $CD33^+$ cells followed the same principle except using $CD33^+$ Micro Beads instead of $CD34^+$ Micro Beads. A part of the supernatant from the column elution, the $CD33^+$ cells as well as the $CD34^+$ cells were kept for purity control with flow cytometry.

### 2.2.3 Molecular biology methods

#### 2.2.3.1 DNA isolation

DNA isolation from blood cells was performed according to the standard protocol using the QIAamp DNA Mini Kit *(Qiagen, Germany)*. The DNA purity and quantity was measured by *NanoDrop* (Thermo Fisher Scientific, US) or *Qubit (Life Technologies, GER)*.

#### 2.2.3.2 Total RNA isolation

RNA isolation was performed according to standard protocols using either RNeasy Micro Kit *(Qiagen, Germany)* or miRNeasy Micro Kit *(Qiagen, Germany)*. The RNA purity and quantity was measured by *NanoDrop* (Thermo Fisher Scientific, US) or *Qubit (Life Technologies, GER)*.

#### 2.2.3.3 Messenger RNA transcription to cDNA

RNA was transcribed using a standard protocol. The RNA transcription mix consists of 500 ng RNA, 27 ul $ddH_2O$, 2 ul random $Oligo(dT)_{18}$ Primer and 2 ul of Random Hexamers *(both ThermoFisher Scientific, US)*, 10x RT-buffer, 5 mM dNTPs and Omniscript Reverse Transcriptase *(QIAGEN, Germany)*. The resulting cDNA was either used immediately or kept at -80 °C until further use.

#### 2.2.3.4 cDNA synthesis for quantification of microRNAs

Total RNA isolated with miRNeasy Micro Kit was used to quantify microRNA abundance. It was processed according to the *TaqMan Advanced miRNA Assay's* protocol. Poly(A) tailing reaction was performed with the master mix from **table 2.10** at conditions from **table 2.11**. Next, ligation reaction master mix (**table 2.12**) was added and incubated at conditions depicted in **table 2.13**. After ligation, the resulting solution was used for reverse transcription with the mix from **table 2.14** at the conditions shown in **table 2.15**. Finally, the 5 ul of the obtained cDNA was amplified using amplification master mix (**table 2.16**) and incubated at the conditions from **table 2.17**. The amplified product was stored until further use at -20 °C.

**Table 2.10: Poly(A) tailing master mix**

| Name/Purpose | Volume (per one reaction) |
|---|---|
| 10 X Poly(A) Buffer | 0.5 ul |
| ATP | 0.5 ul |
| Poly A Enzyme | 0.3 ul |
| RNase-free water | 1.7 ul |

**Table 2.11: Poly(A) tailing conditions**

| Name/Purpose | Temperature | Duration |
|---|---|---|
| Polyadenylation | 37 °C | 45 min |
| Stop reaction | 65 °C | 10 min |
| Hold | 4 °C | hold |

**Table 2.12: Ligation reaction master mix**

| Name/Purpose | Volume (per one reaction) |
|---|---|
| 5 X DNA Ligase Buffer | 3.0 ul |
| 50% PEG 8000 | 4.5 ul |
| 25 X Ligation Adaptor | 0.6 ul |
| RNase-free water | 0.4 ul |
| RNA Ligase | 1.5 ul |

**Table 2.13: Ligation reaction conditions**

| Name/Purpose | Temperature | Duration |
|---|---|---|
| Ligation | 16 °C | 60 min |
| Hold | 4 °C | hold |

**Table 2.14: Reverse transcription master mix**

| Name/Purpose | Volume (per one reaction) |
|---|---|
| 5 X RT Buffer | 6.0 ul |
| dNTP Mix (25mM each) | 1.2 ul |
| 20 X Universal RT Primer | 1.5 ul |
| 10 X RT Enzyme Mix | 3.0 ul |
| RNase-free water | 3.3 ul |

**Table 2.15: Reverse transcription reaction conditions**

| Name/Purpose | Temperature | Duration |
|---|---|---|
| Reverse transcription | 42 °C | 15 min |
| Stop reaction | 85 °C | 5 min |
| Hold | 4 °C | hold |

**Table 2.16: microRNA amplification reaction master mix**

| Name/Purpose | Volume (per one reaction) |
|---|---|
| 2 X miR-Amp Master Mix | 25.0 ul |
| 20 X miR-Amp Primer Mix | 2.5 ul |
| RNase-free water | 17.5 ul |

**Table 2.17: microRNA amplification reaction cycler conditions**

| Cycling step | Temperature | Duration | Cycle repeats |
|---|---|---|---|
| Enzyme activation | 95 °C | 5 min | 1 X |
| Denaturation | 95 °C | 3 sec | 14 X |
| Annealing & Elongation | 60 °C | 30 sec | |
| Stop reaction | 99 °C | 10 min | 1 X |
| Hold | 4 °C | hold | 1 X |

#### 2.2.3.5 Digital PCR (dPCR)

Digital PCR was used for absolute endpoint quantification of gene copy numbers using TaqMan SNP Genotyping Assays *(ThermoFisher Scientific, US, MA)*. At first, isolated gDNA was diluted to approximately 7 ng/ul, then a master mix was set up according to the 'Rare mutation analysis protocol' from *ThermoFisher Scientific, US, MA*. 12 ul of diluted gDNA were added to the master mix (**table 2.18**) and incubated at the conditions depicted in **table 2.19**. Analysis of dPCR data was performed with QuantStudio 3D AnalysisSuite *(ThermoFisher Scientific, US, MA)* and Excel *(Microsoft, US, CA)*.

**Table 2.18:** Digital PCR master mix

| Name/Purpose | Volume for 2 chips (1 sample) |
|---|---|
| Master Mix v2 | 17.4 ul |
| TaqMan Assay 20X (primer/probe mix) | 1.74 ul |
| Molecular grade water | 3.66 ul |

**Table 2.19: Digital PCR cycling conditions**

| Cycling step | Temperature | Duration | Cycle repeats |
|---|---|---|---|
| Enzyme activation | 96 °C | 10 min | 1 X |
| Annealing & Extending | 60 °C | 30 sec | 39 X |
| Denaturation | 60 °C | 3 sec | |
| Stop reaction | 99 °C | 10 min | 1 X |
| Hold | 4 ° C | $\infty$ | 1 X |

#### 2.2.3.6 Real-time PCR (qPCR)

Real-time PCR (qPCR) was used for quantitative endpoint quantification of miRNA and gDNA abundance. This method uses *TaqMan Advanced miRNA Assays* or *SYBR Green dye* and primer pairs for the gDNA sequences. According to the amount of target substance, a fluorescent signal was generated and measured. Threshold difference between target subject and housekeeping control subject were calculated and normalization was performed using delta Ct method [Livak and Schmittgen, 2001]:

$$\Delta Ct = Ct[housekeeping] - Ct[target]$$

$$fold - change = 2^{-\Delta Ct}$$

a) Quantitative RT-PCR for miRNA was performed using the master mix from **table 2.20** and the cycling conditions shown in **table 2.21**. MicroRNA let-7b served as endogenous control.

**Table 2.20: microRNA-qPCR master mix**

| Component | Volume for one reaction |
|---|---|
| 2X TaqMan Universal master mix II | 5 ul |
| 20X TaqMan Advanced miRNA Assay | 0.5 ul |
| RNase-free water | 2 ul |
| transcribed miRNA | 2.5 ul |

**Table 2.21: Quantitative PCR cycling conditions for miRNA abundance**

| Cycling step | Temperature | Duration | Cycle repeats |
|---|---|---|---|
| Enzyme activation | 95 ° C | 10 min | 1 X |
| Denaturation | 95 ° C | 15 sec | 45 X |
| Annealing & Extending | 60 ° C | 60 sec | |
| Hold | 5 ° C | $\infty$ | 1 X |

b) Quantitative RT-PCR for gDNA abundance quantification following RUNX1 ChiP was performed using the master mix from **table 2.22** at the cycling conditions shown in **table 2.23**. DNA sequences of the genes were obtained from NCBI *(https://www.ncbi.nlm.nih.gov/)*, primers were designed using Primer-BLAST *(https://www.ncbi.nlm.nih.gov/tools/primer-blast/)* and reconfirmed using in-silico PCR. As a next step primers were tested with DNA from cell lines to confirm specificity (data not shown). gDNA was used in 1:50 dilution.

**Table 2.22: gDNA-qPCR master mix**

| Component | Volume for one reaction |
|---|---|
| 2X SYBR Green PCR mix | 5 ul |
| Forward/reverse Primer mix | 0.8 ul |
| gDNA | 4.2 ul |

**Table 2.23: Quantitative PCR conditions for RUNX1 binding target abundance**

| Cycling step | Detail | Temperature | Duration | Cycle repeats |
|---|---|---|---|---|
| Preincubation | | 95 °C | 10 min | 1 X |
| Amplification | Denaturation | 95 °C | 10 sec | 40 X |
| | Annealing | 63 °C | 10 sec | |
| | Elongation | 72 °C | 30 sec | |
| Meltingcurve | Interruption | 95 °C | 5 sec | 1 X |
| | Heating & Tm Analysis | 65 °C | 60 sec | 5 °C every 5 sec |
| Cooling | | 40 °C | 10 sec | hold |

#### 2.2.3.7 Flow cytometry and fluorescence-activated cell sorting (FACS)

Flow cytometry uses the principle of fluorescence, light emission and light excitation of fluorochromes that are specifically added to mark target structures, such as surface proteins. It produces multi-parameter data to specify and quantify the abundance of labeled target structures of the cells passing by the lasers and detectors. It was used for CD33 and CD34 surface protein to determine the purity of MACS sorting. Cells were stained with BD CD34 (8G12) Pe-Cy7 antibodies for $CD34^+$ cell separation and with BD CD33 (P67.6) Pe-Cy7 antibodies for isolation of $CD33^+$ cells. Afterward, stained cells were washed with PBS-buffer and used for analysis. Analysis was performed with FACS Diva II *(BD Biosiences)* and 'FlowJo' software *(FlowJo LLC, Ashland, Oregon)*.

### 2.2.4 Biochemistry methods

#### 2.2.4.1 Protein isolation

Cells were washed with PBS, spun down and supernatant was removed. The pellet was lysed in 5 X Laemmli–buffer.

**Table 2.24: Laemmli–Buffer**

| Name | Chemicals |
|---|---|
| 5 X Laemmli–Buffer | 300 mM Tris/HCl p.H 6.8 |
| | 3% DTT ($w/v$) |
| | 40% Glycerol ($v/v$) |
| | 2% SDS ($w/v$) |
| | 0.05% Bromphenol blue ($w/v$) |

#### 2.2.4.2 Western blot

Western Blot was performed in several steps. Equal amounts of total protein were loaded to an SDS page gel and run in 1 X running buffer in a BioRad running chamber at 80 V for 20 minutes, then voltage was increased to 120 V and run for

another 60 minutes. Afterward, the gel was placed in a stacking sandwich and transfer was done in 1 X wet transfer buffer in a BioRad transfer chamber with 100 V at +4 °C for 60 minutes. Subsequently, the membrane was washed three times in TBST for 5 minutes each. Following the washing step, reversible staining was performed with Pierce Reversible Staining Kit for Nitrocellulose Membranes (ThermoFisher Scientific, US, MA) according to the kit's protocol. The stained membrane was scanned and afterward staining was erased. Blocking was done in 5 % blocking-milk for 60 minutes followed by incubation in primary antibody (1:500 - 1:1000) in 5 % blocking-milk at 4 °C over night. Afterward, the membrane was washed three times in TBST and then incubated in secondary antibody (1:2000 - 1:4000) in 5 % blocking-milk at room temperature for 1 hour. Used antibodies are listed in **table 2.8**. After incubation with secondary antibody, the membrane was washed three times for 5 minutes in TBST and then incubated with either 'Pierce ECL Western Blotting Substrate' *(ThermoFisher Scientific, US)* or 'Luminata Forte Western HRP Substrate' *(Merck Millipore, GER)*. Subsequently, the membrane was analyzed with X-ray films. After the detection of protein bands, the membrane was washed three times with TBST for 10 minutes and incubated in stripping buffer for 15 minutes at RT. Following incubation with stripping buffer, the membrane was incubated in blocking solution and was then ready to detect different proteins. Developed films were scanned.

**Table 2.25: Western Blot buffers and solutions**

| Purpose/Name | Chemicals |
|---|---|
| 10 X Running Buffer | 25 mM Tris–Buffer |
| | 192 mM Glycine |
| | 1 % SDS ($w/v$) |
| | dd$H_2O$ to 2000 ml |
| | pH 8.3–8.5 |
| 10 X Wet Transfer Buffer | 250 mM Tris–Buffer |
| | 1.92 M Glycine |
| | dd$H_2O$ to 1000 ml |
| 1 X Wet Transfer Buffer | 10 X Wet Transfer Buffer |
| | 200 ml Methanol |
| | dd$H_2O$ to 1000 ml |
| 10 X TBS | 200 mM Tris–Base |
| | 1.37 M NaCl |
| | dd$H_2O$ to 1000 ml |
| | pH 7.6 |
| 1 X TBST | 10 X TBS |
| | 1 ml Tween 20 |
| | dd$H_2O$ to 1000 ml |
| 5 % Blocking–milk | 5 $g/100$ $ml$ skimmed milk powder |
| | dd$H_2O$ |

**Table 2.26: PAGE preparation**

| Purpose (Concentration) | Chemicals for 2 gels |
|---|---|
| Stacking gel (4 %) | 3.0 ml $ddH_2O$ |
| | 1.5 ml Tris–Buffer 0.5 M pH 6.8 |
| | 1.0 ml 30 % Acrylamide ($w/v$) |
| | 12 ul 20 %Ammonium persulfate |
| | 12 ul Temed ($w/v$) |
| Separation gel (12 %) | 2.6 ml $ddH_2O$ |
| | 3.0 ml Tris–Buffer 1.5 M pH 8.8 |
| | 5.0 ml 30 % Acrylamide ($w/v$) |
| | 1.4 ml 1 % SDS ($w/v$) |
| | 24 ul 20 %Ammonium persulfate ($w/v$) |
| | 24 ul Temed ($w/v$) |
| Separation gel (15 %) | 1.6 ml $ddH_2O$ |
| | 3.0 ml Tris–Buffer 1.5 M pH 8.8 |
| | 6.0 ml 30 % Acrylamide ($w/v$) |
| | 1.4 ml 1 % SDS ($w/v$) |
| | 24 ul 20 %Ammonium persulfate ($w/v$) |
| | 24 ul Temed |

#### 2.2.4.3 Chromatin immunoprecipitation (ChIP)

Chromatin immunoprecipitation was done according to the *truChIP™ Chromatin Shearing Reagent Kit* protocol and performed with *M220 Focused-ultrasonicator™* (Covaris, US, MA). The following instructions refer to the kit's protocol [Covaris, 2016] (For buffer composition see **table 2.27**). For each ChIP, 1 x $10^6$ cells were washed once with PBS then cross-linked with 1 X Fixing Buffer A and 11.1 % formaldehyde for 10 minutes at RT. Afterward, Quenching Buffer E was added and incubated for 5 minutes. Cells were centrifuged, the supernatant was removed and washed with 1 X PBS. Lysis Buffer B was added and the solution was incubated at 4°C for 10 minutes. Afterward, it was spun down, the supernatant was dis-

carded and the pellet was resuspended in 1 X Wash Buffer C. Subsequently, cells were incubated at 4 °C for 10 minutes, centrifuged, the supernatant was discarded and the pellet was resuspended in Shearing Buffer D3. Chromatin shearing was done by means of *M220 Focused-ultrasonicator™* (Covaris, US, MA) according to conditions listed in **table 2.28**, and aimed to produce fragments of *approx*. 200 - 300 bp length. Aliquots were taken after 10, 15 and 20 minutes of sonication and shearing efficiency was controlled using Bioanalyzer. The sheared chromatin was processed and immunoprecipitated with either RUNX1 *(Abcam, ab23980, US)* or rabbit IgG *(Cell Signaling, CS2729S, US)* antibody following the instructions of Lee et al. ChIP protocol was performed using magnetic 'uMACS Protein A MicroBeads' *(Miltenyi BioTec, GER)* and buffers listed in **table 2.27** [Lee et al., 2006]. The isolated DNA was purified using 'QIAquick PCR purification kit' *(QIAGEN, GER)*. ChIP efficiency was controlled by means of qPCR and melting curve analysis (see 2.2.3.6).

**Table 2.27: ChIP buffers, solutions and reagents**

| Name / Purpose | Volume per ChIP sample |
|---|---|
| 1X PBS | 2.0 ml PBS |
| Fixing Buffer A | 50 ul Fixing Buffer A<br>450 ul $H_2O$ |
| 11.1% Formaldehyde | 690 ul 16% Formaldehyde<br>310 ul $H_2O$ |
| Quenching Buffer E | 23 ul |
| 1X Lysis Buffer | 100 ul 5 X Lysis Buffer B<br>400ul $H_2O$<br>5ul 100X Buffer F |
| 1X Washing Buffer | 50ul 10 Wash Buffer C<br>450 ul $H_2O$<br>5 ul 100X Buffer F |

Continued on the next page

**Table 2.27: – continued from the previous page**

| Name / Purpose | Volume per ChIP sample |
|---|---|
| 1X Shearing Buffer D3 | 100ul 10X Shearing Buffer D3<br>900ul $H_2O$<br>10 ul 100X Buffer F |
| Low Salt Wash Buffer | 0.1% SDS<br>1% Triton X100<br>2mM EDTA<br>20 mM Tris- HCl pH 8.0<br>150mM NaCl |
| High Salt Washing Buffer | 0.1% SDS<br>1% Triton X100<br>2mM EDTA<br>20 mM Tris- HCl pH 8.0<br>500mM NaCl |
| LiCl Washing Buffer | 0.25M LiCl<br>1% NP-40<br>1% Sodium Deoxycholate<br>1 mM EDTA<br>10mM Tris-HCl pH 8.0 |
| Elution Buffer | 1% SDS<br>100 mM NaHCO3 |

**Table 2.28: ChIP Shearing conditions**

| Name | Settings |
|---|---|
| Target BP (Range) | 200–700 |
| Duty Cycle | 5% |
| Intensity peak power | 75 Watts |
| Cycles per Burst | 200 |
| Processing Time | empirical (5–30 minutes) |
| Bath Temperature | 7°C |

*Learning never exhausts the brain.*

Leonardo da Vinci

# 3 Results

## 3.1 *RUNX1* gene copy-number quantification

In 2014, our group reported on the cooperativity of *RUNX1* and *CSF3R* mutations in a CN patient cohort with overt MDS or AML [Skokowa et al., 2014]. Myeloid cell clones of CN patients were carrying the inherited mutations (e.g., *ELANE, HAX1, GPT1*) and positive for additional acquired mutations. Skokowa and colleagues observed a sequential gain of *CSF3R* mutations, followed by *RUNX1* mutations in CN individuals who developed a malignant phenotype. They postulated followed mechanism of malignant transformation in CN: inherited genetic lesions and lesions in *CSF3R* alone were not sufficient to induce leukemia, but further alterations - as mutations in *RUNX1* - were required [Skokowa et al., 2014].

We grouped the CN patients according to their *RUNX1* mutation types and searched for other associated chromosomal aberrations (**table 3.1**). In the patients' group with missense *RUNX1* mutations, seven patients were positive for trisomy 21 and no trisomy 21 was found in the six CN-AML patients with non-sense *RUNX1* mutations. Fisher's two-tailed t-test indicated non-random distribution of trisomy 21 occurrence between CN-AML missense *RUNX1* and non-sense

*RUNX1* mutation cohorts (p = 0.0515). Thus, we aimed to investigate the ratio of wild type and mutant *RUNX1* alleles in CN-AML patients positive for missense *RUNX1* and trisomy 21. Of note, all *RUNX1* mutations associated with trisomy 21 were located within the RHD. Subsequently, Sanger sequencing was performed on samples from 'CN-AML patient #14' and 'CyN-AML patient #1' obtained at CN and CN-AML stage.

**Table 3.1: Phenotypical and genetic characterizations of investigated CN patients with nonsense and missense *RUNX1* mutations**

| **Pat. ID.** | ***RUNX1* mutation position, AA** | **Karyotype** | **CN-associated mutation position, AA** |
|---|---|---|---|
| *nonsense* | | *RUNX1* | *mutations* |
| #21† | p.R174X<br>p.L294QfsX6 | 47, XX 1mar[8];<br>47, idem, del(10)(q32)) | *ELANE* p.G214R<br>*GFI1* |
| #13‡‡ | p.R139X<br>p.V137D | 46, XX | *ELANE* p.A79VfsX9 |
| #16‡ | p.R174X | 46, XY | *ELANE* p.G214R |
| #15§ | p.R139X | t(p1;q3) | *ELANE* p.C151Y |
| #20± | p.Q370X | 46,XX,add(2)(q37),<br>add(7)(q22)) | *WAS* |
| #10± | p.F13TrpfsX14<br>p.R139ProfsX47 | 45, XY, -7 [10];<br>46XY [5] | *HAX1* p.V44X |
| *missense* | | *RUNX1* | *mutations* |
| #14§ | p.R139G<br>p.M240I | 2010:<br>45,XY,-7[9]; 46,XY[11]<br>2011:<br>47,XY,**+21**[13]; 46,XY[2] | *ELANE* p.C151Y |
| #22§ | p.K83Q | 46,XY | *ELANE*<br>p.IVS411G>T |

Continued on next page

**Table 3.1– Continued from previous page**

| Pat. ID. | RUNX1 specifics | Karyotype | CN inflicting mutations |
|---|---|---|---|
| #18‡‡ | p.R64P | 46,XY,t(9;11) | *ELANE* p.N113K |
| #6†† | p.R80S | 45,XX,-7 | *ELANE* p.L152P |
| #11+ | p.R174L | 46,XY,**add(21q)** | *ELANE* p.A57V |
| #7¢ | p.R135K | 46,XY,-7,**+21** | *ELANE* p.S126L |
| #31£ | p.R174L | 47,XY,**+21**[14] /46,XY[4] | *ELANE* p.G174R |
| #1CyN | p.D171N | 46,XX,-7,**+21**[14] | *ELANE* p.A223P |
| #4$ | Intron4 c.415_427dup6, c.421_427dup7 | 45,XX,-7[12]; 46,XX[11] | *WAS* p.S478I |
| #26‡‡ | p.R80S | 45,XY,-7 | *WAS* p.L270P |
| #19= | p.L29S p.R64P | 46,XX | *HAX1* p.V44X |
| #17= | p.I22K | 46,XY | *HAX1* p.V44X |
| #25? | p.S114P p.Y380_G394delinsC | 46,XX,**dup(21)(q22.1q22.3)**[19] | n.a. |
| #12† | p.K83Q | 47,XX,**+21** | *GPT1* |

AML FAB subtypes:

$AML M0, §AML M1, †AML M2, ‡AML M4

††AML M5, ‡‡AML FAB NA, +AML/B-ALL, =MDS

¢MDS/AML M1, ±MDS/RAEB, ?MDS/RAEB-2

£RAEB-T/AML FAB NA

Adapted from Skokowa et al. [2014], *Blood, 2014*.

### 3.1.1 Sanger sequencing of *ELANE, RUNX1* and *CSF3R* mutations in CN-AML patient #14 and CyN-AML patient #1 at neutropenia and leukemia stage

Some of the data presented in section 3.1.1 and 3.1.2 were published in *Cell Stem Cell*: 'iPSC modeling of stage-specific leukemogenesis reveals BAALC as a key oncogene in severe congenital neutropenia' [Dannenmann et al., 2021]. A previous karyotyping of the myeloid cells of CN-AML patient #14 had revealed an additional chromosome 21 (Chr 21, i.e. trisomy 21) at the CN-AML stage, which was not observed in cells obtained at the CN stage one year earlier (**table 3.1**). Sanger sequencing was performed to confirm the presence of *ELANE, RUNX1* and *CSF3R* mutations at CN and CN-AML stages (**figure 3.1**). Since *RUNX1* is located on Chr 21, we were especially interested in the *RUNX1* wild type to mutant allele ratio. The comparison of nucleotide peak heights in *RUNX1* Sanger sequencing data allowed the initial evaluation of a mutant and wild type gene dosage. Sanger sequencing was performed with gDNA isolated from hiPSC derived $CD34^+$ cells from CN-AML pat. #14. The hiPSC derived $CD34^+$ patient cells were programmed to characterize the myeloid cell clones observed at the CN and CN-AML stage of the disease. CN cells were positive for the inherited *ELANE* mutation NP_001963.1:p.C151Y (**figure 3.1 A**). Additionally, the CN-AML clones were positive for *RUNX1* NP_001001890.1:p.R139G and *CSF3R* NP_000751.1:p.Q718X mutations (**figure 3.1B**; [Dannenmann et al., 2021]). The peak heights representing the mutant *RUNX1* allele exceeded those of wild type alleles.

In 2016, members of our group described the leukemogenic progression in a CyN patient for the first time [Klimiankou et al., 2016a]. Besides the *ELANE* mutation, they reported mutations in *CSF3R* and *RUNX1* as well as trisomy 21 in the leukemia cells of this patient [Klimiankou et al., 2016a]. We analyzed DNA isolated from BM MNC CFU cells of 'CyN patient #1' (**figure 3.1C**). Again, Sanger sequencing data depicted that the peak height resembling the mutant *RUNX1* allele (NP_001001890.1:p.D171N) was higher than the peak of wild type *RUNX1* allele. In summary, Sanger sequencing data indicated an increased dosage of

missense *RUNX1* mutant allele over wild type *RUNX1* allele for both patients investigated.

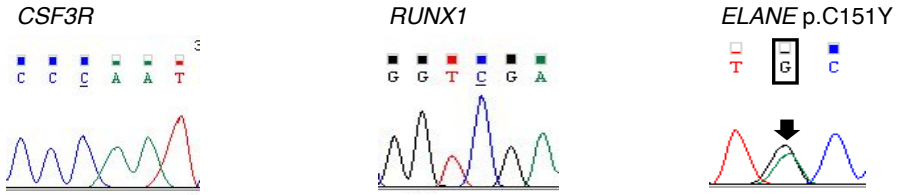


**(a)** CN-AML pat. # 14 - CN stage

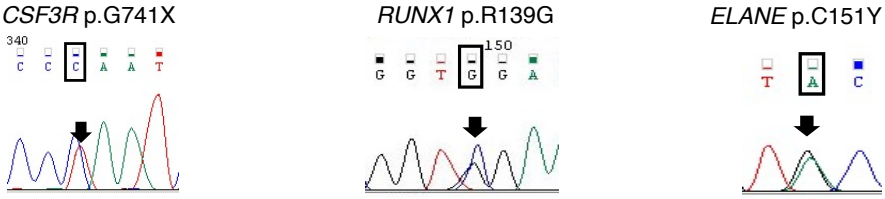


**(b)** CN-AML pat. # 14 - CN / AML stage

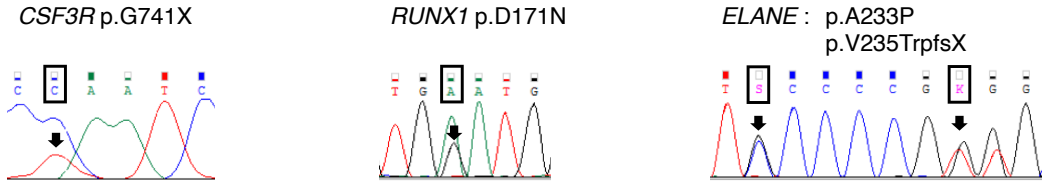


**(c)** CyN-AML pat. # 1 - CN / AML stage

**Figure 3.1: Sanger sequencing data for *ELANE, CSF3R* and *RUNX1* mutations of one CN and one CyN patient**

Figures A and B depict exemplary results of Sanger sequencing of hiPSC derived $CD34^+$ cell clones with similar characteristics of cells obtained at CN and CN-AML phenotype stage of CN-AML patient #14. The bottom row depicts Sanger sequencing results of CyN-AML patient #1 obtained from $CD34^+$ CFU cells with the same characteristics as the cells present at AML stage. Genetic characterization of inherited *ELANE* mutation and de novo *CSF3R* and *RUNX1* mutations are depicted. Black boxes and arrows indicate the mutation site with the resulting alteration in nucleotide sequence depicted above (colored) and amino acid position of the mutation (black). *Data kindly provided by the authors and adapted from Klimiankou et al. 'Two cases of cyclic neutropenia with acquired CSF3R mutations, with 1 developing AML', Blood 2016; 127:21; p.2638-2641; [Klimiankou et al., 2016a]. Adapted from Dannenmann et al., [2021].*

### 3.1.2 *RUNX1* mutant allele ratio quantification at CN and leukemia stage by means of digital PCR

To quantify the mutant to wild type *RUNX1* allele ratio, we performed digital PCR (dPCR), using samples of three different patients collected at CN and CN-AML

stages (**figures 3.2** to **3.6**). Each patient harbored a unique *RUNX1* missense mutation. We used custom SNP Genotyping assays from *Thermo Scientific* (see **table 2.6** for detailed assay information). The assays were designed for *RUNX1* mutations: NP_001 001 890 .1: p.R139G (CN-AML patient #14), p.D171N (CyN-AML patient #1) and p.R174L (CN-AML patient #31) **(figure 3.2)**. We measured the mutant to wild type *RUNX1* allele ratio in hiPSC derived $CD34^+$ cells. Those cells arise from a pure cell clone, whereas native patient samples at leukemia stage always represent a mixture of normal and malignant cells.

Firstly, we investigated gDNA of hiPSC derived samples obtained from CN-AML patient #14 (**figure 3.3A**). We found no *RUNX1* mutation in samples at CN stage. In CN-AML samples, we detected *RUNX1* NP_001 001 890 .1: p.R139G mutant allele. Digital PCR data show that the genomic amount of mutant *RUNX1* allele surpasses those of wild type *RUNX1* allele by approximately two-fold. HSPCS derived from two different CN-AML hiPSC clones (L6 and L10) which were examined provided similar results; in each sample, the mutated *RUNX1* p.R139G allelic fraction exceeded the wild type fraction by 1,82 (L10), or 1,97 (L6) times [Dannenmann et al., 2021].

To confirm this observation, we investigated gDNA from $CD34^+$ BM MNCs of the same patient obtained at CN and CN-AML stages (**figure 3.3B**). Interestingly, with a fraction of 14.73% mutated *RUNX1* was already detected in myeloid cells obtained at the CN stage. This proportion increased to 30.31% at CN-AML stage, but did not reach the formerly determined 2:1 ratio. Thus, we decided to examine gDNA isolated from CFU derived cells with confirmed *ELANE, CSF3R* and *RUNX1* mutations. In these cells, we observed again the 2:1 ratio between missense *RUNX1* p.R139G and wild type *RUNX1* alleles. In addition, we examined DNA obtained from seven hiPSC derived cell samples of the CN-AML patient #14; all showed the mutant to wild type *RUNX1* allele ratio of approximately 2:1 (**figure 3.4**).

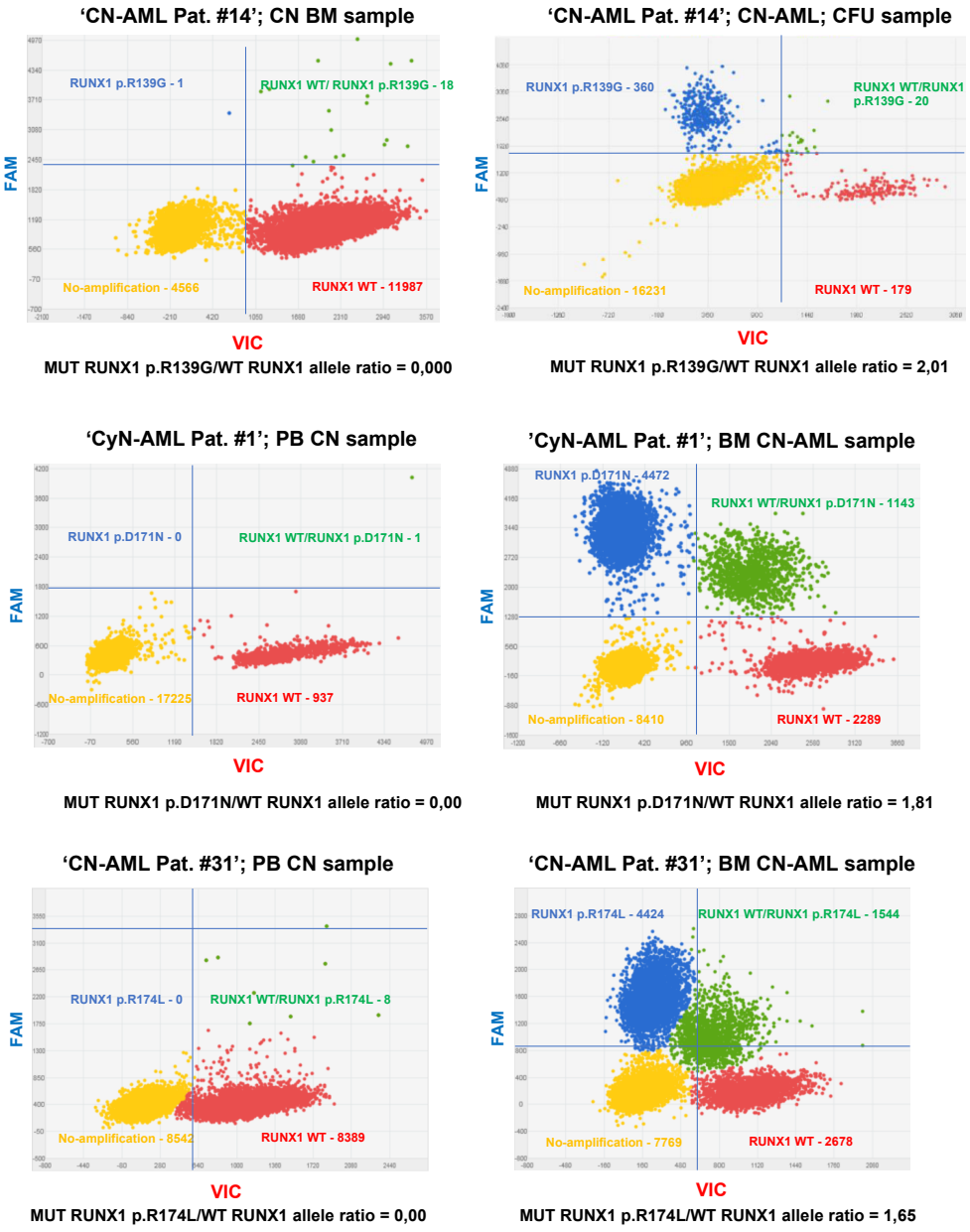


**Figure 3.2: Scatterplot of digital PCR results of CN patients (n = 3) collected at CN and CN-AML stages**

Representative images of digital PCR data plots for *RUNX1* wild type and mutation amplification and quantification. FAM reporter dye signals (mutant *RUNX1* allele = blue dots) are plotted on the Y-axis, VIC reporter dye signals (wild type *RUNX1* allele = red dots) are plotted on the X-axis. Green dots represent wells containing both PCR products, wild type and mutant *RUNX1* allele, whereas yellow dots represent empty wells. The ratio of mutant and wild type allele was calculated based on the number of FAM and VIC positive signals on the chip. For example: gDNA of samples from CN-AML Pat. #14 in CN and CN-AML phase were amplified and investigated using TaqMan Custom SNP assays *(Thermo Fisher Scientific, USA)* for wild type and *RUNX1* p.R139G allele. At CN phase, only wild type *RUNX1* allele was detectable (n= 11987), whereas at CN-AML phase, mutated *RUNX1* p.R139G was detected in 360 wells and wild type in 179 wells. Correspondingly, the ratio of mutant to wild type *RUNX1* is 2,01. *Adapted from Dannenmann et al., [2021]. All data were analyzed using the QuantStudio 3D Analysis Suite (Thermo Fisher Scientific, USA).*

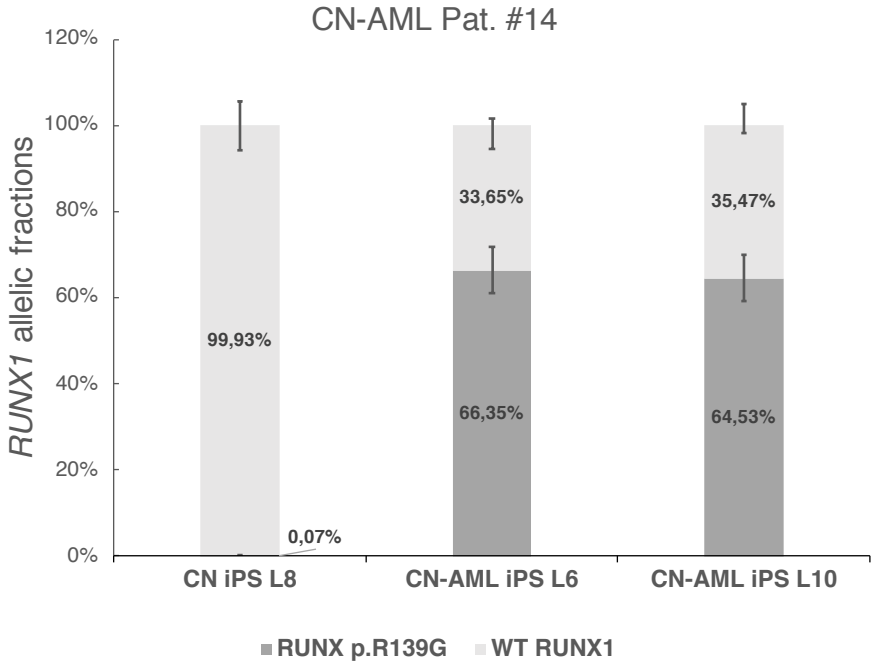


**(a)** hiPSC derived cells

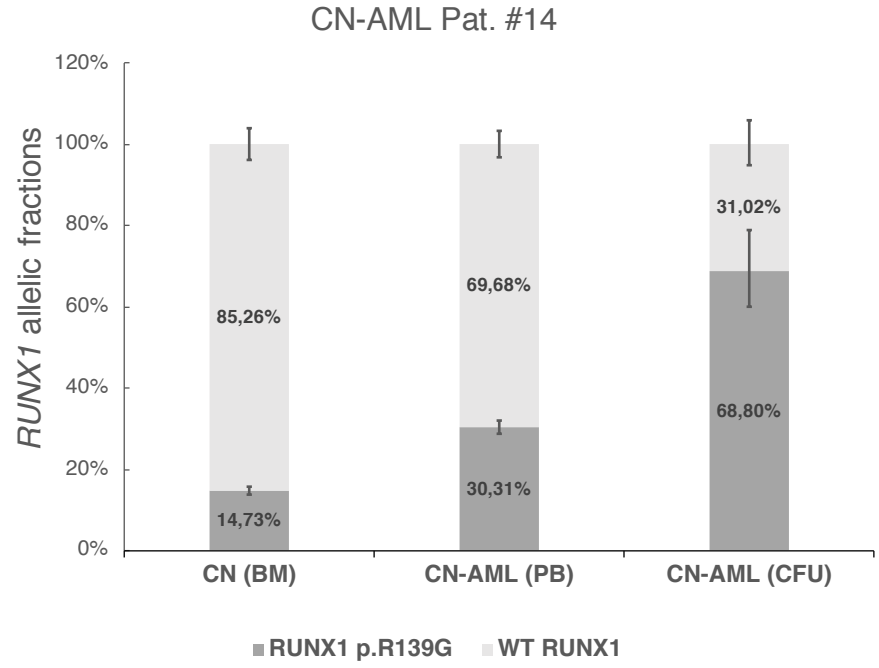


**(b)** Primary and CFU derived cells

**Figure 3.3: Digital PCR analysis of *RUNX1* mutant and wild type allelic fractions in hiPSC, CFU derived and primary cells of CN-AML pat. #14**
Fractions of wild type and mutant *RUNX1* p.R139G alleles - in 'a)' hiPSC derived cells or 'b)' primary and CFU derived cells at CN and leukemia (CN-AML) phase - are shown in light and dark grey, respectively. The frequency of mutant and wild type allele is given in percentage. Each bar represents a representative clone (L8, L6, L10, CFU) or native sample (CM, PB). *Adapted from Dannenmann et al., [2021]. All data were analyzed using the QuantStudio 3D Analysis Suite (Thermo Fisher Scientific, USA).*

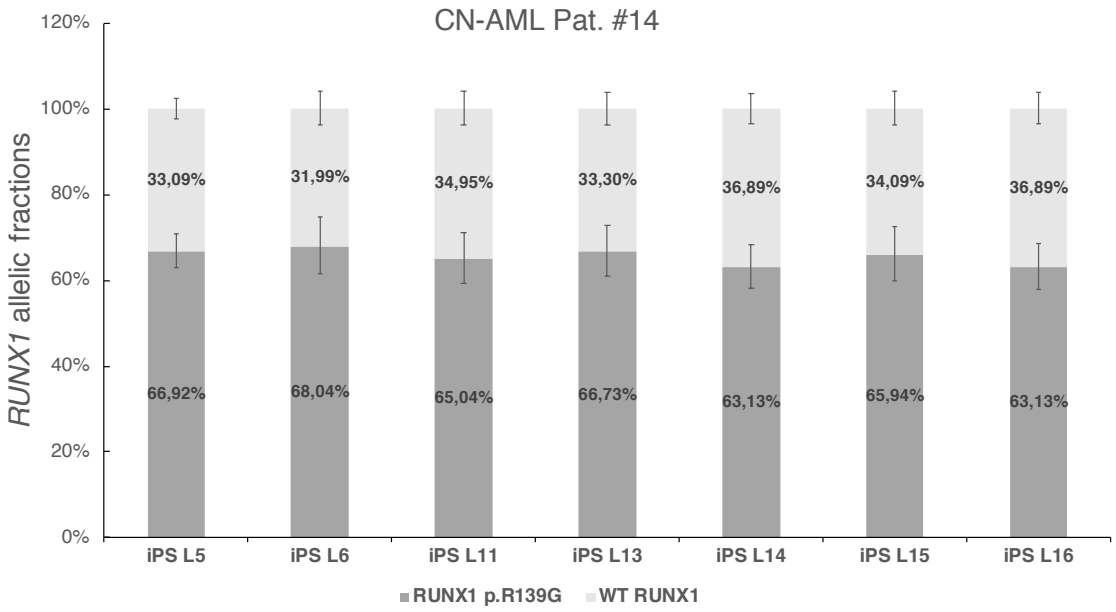


**Figure 3.4: Summarized digital PCR results of *RUNX1* mutant to wild type allelic fractions in hiPSC cells obtained from CN-AML patient #14**
Fractions of wild type and mutant *RUNX1* p.R139G alleles in samples derived from iPS cells of CN-AML patient #14 resembling CN-AML phase. The frequency of mutant (dark grey) and wild type (light gray) allele is expressed in percentage. Each bar represents one set of samples at CN-AML stage. In each sample, the mutant *RUNX1* exceeds the wild-type allele by about 2:1 with a ratio between 1.71 and 2.13.
*All data were analyzed using the QuantStudio 3D Analysis Suite (Thermo Scientific, USA).*

To confirm the gene dose increase of mutant *RUNX1* at CN-AML stage, we analyzed $CD34^+$ BM MNCs of two more patients - CN-AML patient #31 and CyN-AML patient #1- by means of dPCR. The results confirmed our previously obtained data (**figures 3.5a and 3.5b**). Again, the mutant *RUNX1* allelic fraction exceeded the frequency of wild type allele in a ratio of approximately 2:1 [Dannenmann et al., 2021]. An increase of mutated *RUNX1* allele had occurred in all three patients investigated (see summary in **figure 3.6**).

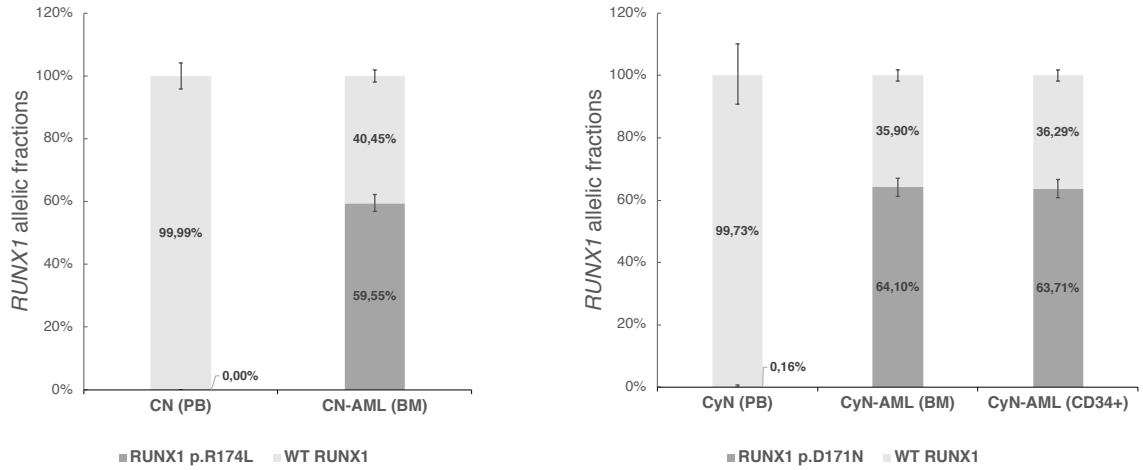


**(a)** CN-AML pat. #31 **(b)** CyN-AML pat. #1

**Figure 3.5: Digital PCR analysis of *RUNX1* mutant to wild type allelic fractions in CD34$^+$ BM MNC of CN-AML pat. #31 and CyN-AML pat. #1**

Fractions of wild type and mutant *RUNX1* alleles in samples from CN-AML pat. #31 and CyN-AML pat. #1, quantified by digital PCR. The frequencies of mutant and wild type allele are expressed in percentage. Each bar represents one set of clones at either CN/CyN or CN-AML/CyN-AML stage.

**a)** At CN stage (left bar), only wild type *RUNX1* allele was detectable, whereas in CN-AML phase mutant (*RUNX1* p.R174L) copy numbers reached approx. 59.55% of the total allelic fraction.

**b)** At CyN stage (left bar), only wild type *RUNX1* allele was detectable, whereas in CyN-AML phase mutant (*RUNX1* p.D171N) copy numbers reached approx. 64.10% in BM sample and approx. 63.71% in CD34$^+$ sample of the total allelic fraction.

*Adapted from Dannenmann et al., [2021]. All data were analyzed using the QuantStudio 3D Analysis Suite (Thermo Fisher Scientific, USA).*

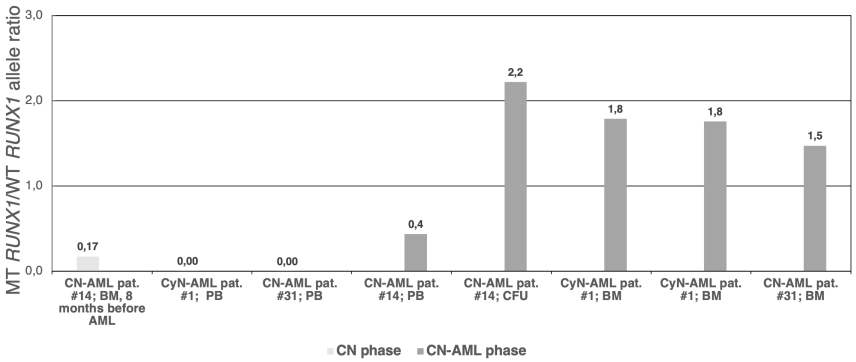


**Figure 3.6: Summary of digital PCR analysis of MT *RUNX1* to WT *RUNX1* ratio quantification in all investigated patients (n = 3)**

The graph depicts the ratio quantification analysis of missense *RUNX1* to wild type allelic fractions at CN (light gray) and CN-AML (dark gray) stages. Mutant to wild type allele ratio is the highest at CN-AML phase and lowest at CN stage. At CN-AML stage, the MT *RUNX1*/WT *RUNX1* ratio is about 66% (2:1 ratio).

## 3.2 RUNX1 binding pattern in NB4 and U937 cell lines

As a consequence of our findings obtained by dPCR, we aimed to establish a workflow, allowing us to investigate the binding pattern of wild type *RUNX1* in cell lines. In a longer perspective, this workflow could be adapted to study the effects of mutant *RUNX1* on the binding pattern of wild type RUNX1.

### 3.2.1 Selection of cell lines for RUNX1 chromatin immunoprecipitation (ChIP)

We focused on cell lines in which RUNX1 protein expression has already been described, or in which the expression of *RUNX1* is reported on *proteinatlas.org*. *Proteinatlas.org* indicated RUNX1 expression in NB4, U937 and 293T cells [Human Protein Atlas, 2019; Thul et al., 2017]; RUNX1 expression in Jurkat cells was described by Peterson et al. [2005]. To confirm the expression of RUNX1, we examined Jurkat, NB4, U937 and 293T cell lines using Western blot and results were normalized to $\alpha$-Tubulin. First, we compared the Abcam RUNX1-antibody (anti-RUNX1 antibody; ab23980) - validated for ChIP - to a RUNX1 antibody (*Cell Signaling; CS4334S)*, we had previously used for RUNX1 detection. Western blot analysis revealed RUNX1 expression in NB4, U937 and Jurkat cell lines (**figure 3.7**). Thus showed, that the Abcam antibody for ChIP had sufficiently detected RUNX1 protein (data not shown). Hence, we decided to conduct the further ChIP experiments in NB4 and U937 cell lines using this antibody.

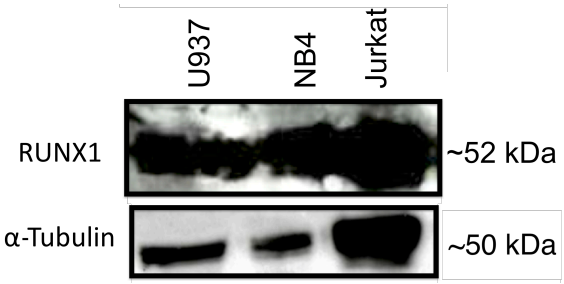


**Figure 3.7: RUNX1 expression in U937, NB4 and Jurkat cell lines**
Western blot analysis of RUNX1 in U937, NB4 and Jurkat cell lines. $\alpha$ -Tubulin was used as loading control. RUNX1 expression was detected in all three tested lines.
Following antibodies were used:
RUNX1: rabbit polyclonal anti-RUNX1 antibody (Abcam; ab23980). $\alpha$-Tubulin: rabbit polyclonal anti-$\alpha$-Tubulin antibody *(Cell Signaling; CS2144)*.

### 3.2.2 ChIP of RUNX1 in NB4 and U937 cell lines

ChIP was performed with NB4 and U937 cell lines and anti-RUNX1 antibody *(Abcam; ab23980)*, normal rabbit IgG *(Cell Signaling, CS 2729S)* served as isotype control. Western blotting with samples obtained subsequently and during ChIP workflow showed visible bands for RUNX1 (data not shown) - Thus we confirmed RUNX1 enrichment.

### 3.2.3 Enrichment of RUNX1 binding sites in ChIP measured by qRT-PCR in U937 cells

To further validate the efficiency of our ChIP protocol, we have selected previously identified RUNX1 binding sites from multiple genomic RUNX1 targets and confirmed the enrichment by quantitative real-time PCR (qRT-PCR) in U937 cells. The investigated RUNX1 binding sites, i.e. target genes, were: *RUNX3* (Chr 1), *PKC-beta* (Chr 16) and *GNA15* (Chr 19). RUNX1 binding sites in *RUNX3* gene were identified using the UCSC genome browser *(www.genome.ucsc.edu)* and ChIP-seq data from publications loaded as 'bigwig' file in the genome browser [Illendula et al., 2015; Kent et al., 2002a,b]. We identified two RUNX1-*RUNX3* binding sites: one extragenic , i.e. promoter region (*RUNX3*-promoter region), located on genome positions 24 965 034 - 24 965 183 and one intragenic site (*RUNX3-RUNX1 intragenic binding site*) on genome position 24 906 620 - 24 906

877. The *PKC-beta* and *GNA15* binding sites, both in the promoter regions, were identified in publications and located on genomic sites 23 846 605 - 23 846 914 [Hug et al., 2004] and 3 133 154 - 3 133 429 [Gardini et al., 2008], respectively. *TPO* sequence was used for normalization of the unspecific gDNA enrichment by ChIP. *TPO* is not expressed in myelopoietic cells, thus interaction of RUNX1 and *TPO* is highly unlikely [Human Protein Atlas, 2018; Uhlén et al., 2015].

QPCR analysis of the U937 RUNX1 ChIP sample compared to the U937 isotype-control ChIP sample (**figure 3.8**) indicated enrichment of one RUNX1-*RUNX3* (genome position: 24 965 034 - 24 965 183) and the RUNX1-*GNA15* binding site - the enrichment was 3.95- and 2.93-fold respectively. In contrast, no enrichment was detected for *PKC-beta* and the other RUNX1-*RUNX3* binding site. PCR product specificity was validated by melting curve analysis and gel electrophoresis (data not shown).

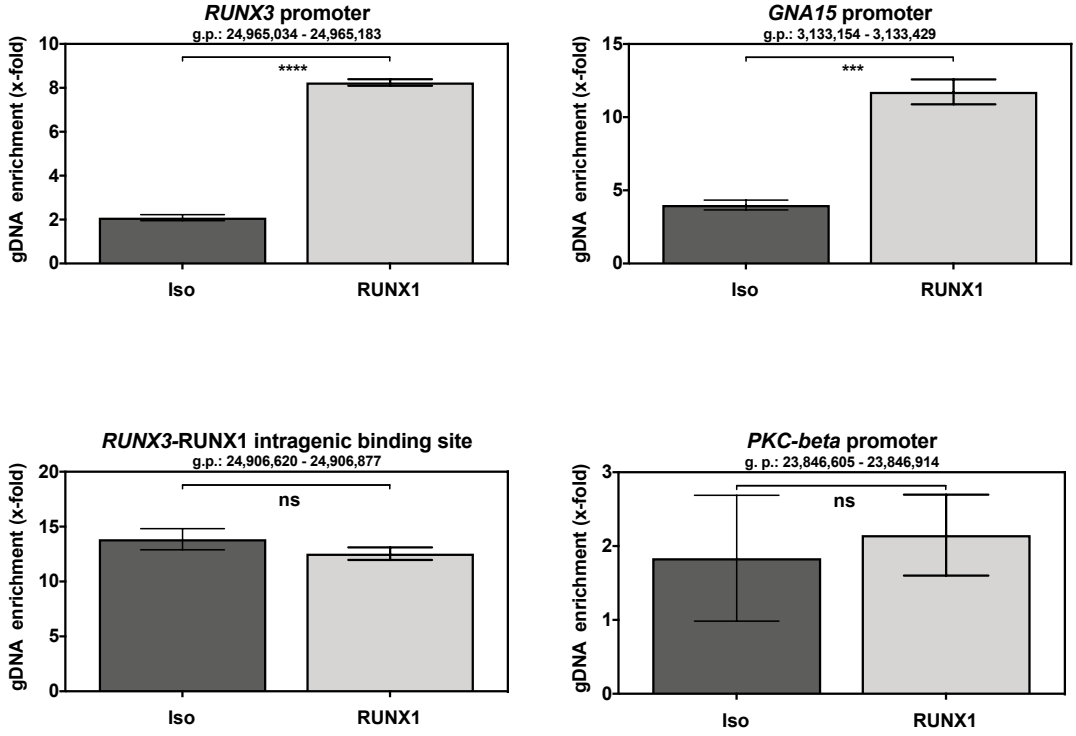


**Figure 3.8: qPCR analysis of the enrichment of RUNX1 binding sites in *RUNX3, GNA15* and *PKC-beta* in U937 cells**

Chromatin isolated from U937 cells was subjected to ChIP (see 3.2.2), performed with rabbit RUNX1 antibody (Abcam, ab23980) and rabbit IgG antibody (Cell signaling, CS2729S), which served as isotype control. ChIP output samples were analyzed by qPCR. Chromatin enrichment was calculated by the ΔCt method where chromatin enrichment of *TPO* sequence served as an endogeneous control for unspecific enrichment (data not shown). [Livak and Schmittgen, 2001]. Chromatin enrichment is depicted on the Y-axis, sample types (isotype control = iso, RUNX1 antibody = RUNX1) on the X-axis. Four target genes have been investigated: three promoter regions of *PKC-beta*[$], *GNA15*[*], *RUNX3* and one intragenic RUNX1 binding site in *RUNX3*.

[*] G protein subunit alpha 15

[$] Protein Kinase C beta

g.p.: genome position on respective chromosome

Data sets were tested for statistical significance using unpaired two-tailed t-test ([ns]: not significant, [***]: p=0,0001 and [****]: p<0,0001).

## 3.3 microRNA expression profiling in hematopoietic cells of CN patients (n = 10)

MicroRNAs have been described previously as versatile regulators in normal and malignant hematopoiesis, but their role in the pathogenesis of CN has not been investigated. Therefore, expression profiling of microRNA and the study of molec-

ular biological changes could improve our understanding of CN pathogenesis and progression to AML. We aimed to establish a workflow, that would allow us to isolate microRNAs from CN patients and investigate the expression profile of different microRNAs. We focused on two microRNAs: miR-125b, which is involved in the regulation of granulopoiesis [Surdziel et al., 2011], and miR-3151, which is associated with *BAALC* and whose upregulation is connected with a poor patient outcome in AML [Eisfeld et al., 2012]. We had previously observed upregulation of BAALC expression in hiPSC derived hematopoietic cells of CN-AML patient #14 at CN-AML stage (data not shown; see Dannenmann et al., [2021]). This finding supported the idea of BAALC and miR-3151 as relevant for the CN patient group, at least for those who progress to AML.

MicroRNA expression is highly variable, differs between distinct cell types and changes during differentiation [Petriv et al., 2010]. Therefore, we have investigated microRNA expression in bone marrow mononuclear cells (BM MNCs) of healthy donors and CN patients. We studied $CD33^+$ and $CD34^+$cells, and compared the expression levels between the groups: CN to healthy donor and $CD33^+$ to $CD34^+$ cells. Further information of the samples investigated, their mutation subtype and differentiation stage is provided in tables **3.2** and **3.3**. *TaqMan Advanced microRNA* assays (Abcam, *US*; material and methods 2.1.5) were used to determine miRNA expression profiles using qRT-PCR. MicroRNA let-7b was used as endogenous control.

### 3.3.1 Design and implementation of a microRNA investigation workflow

First, we aimed to establish a workflow that would allow us to isolate and process microRNA from primary BM and PB samples of CN patients. Following $CD34^+$ and $CD33^+$ cells isolation and separation using 'MACS separation protocol', as described in material and methods (section 2.2.2), sample purity was checked using flow cytometry. Only samples with a purity higher than 80% of live $CD34^+$ or $CD33^+$ cells were used for further analysis. Exemplary FACS purity control data is shown in **figure 3.9**. Cell samples were prepared according to our microRNA workflow (chapter 2.2.3) and quantified by means of qPCR. Products of qPCR

**Table 3.2: Overview of CN patient samples for microRNA quantification**
All native patient samples were bone marrow mononuclear cells.

| Patient ID | CN related gene (detailed mutation annotation) | cell type |
|---|---|---|
| HD12 | - | $CD33^+$ |
| HD28 | - | $CD33^+$ $CD34^+$ |
| HD29 | - | $CD34^+$ |
| HD30 | - | $CD33^+$ $CD34^+$ |
| HD31 | - | $CD34^+$ |
| E1 | *ELANE* (p.S126L) | $CD33^+$ |
| E2 | *ELANE* (p.R192GfsX21) | $CD33^+$ |
| E4 | *ELANE* (p.V190-F199del) | $CD33^+$ |
| H1 | *HAX1* (exon 2 p.W44X) | $CD33^+$ |
| H3 | *HAX1* (exon 2 p.W44X) | $CD33^+$ |
| H4 | *HAX1* (exon 2 p.W44X) | $CD34^+$ |
| H5 | *HAX1* (exon 2 p.W44X) | $CD34^+$ |
| S1 | *SDS* (not specified) | $CD33^+$ |
| U1 | genetically unclassified CN | $CD33^+$ $CD34^+$ |
| U2 | genetically unclassified CN | $CD33^+$ $CD34^+$ |

**Table 3.3: Overview of hiPSC derived CN patient samples for microRNA expression quantification**

| Patient ID | CN related gene (detailed mutation annotation) | cell type |
|---|---|---|
| CN-AML Pat. #14 iPS L8 | *ELANE* (exon 4; p.C151Y) | hiPSC |
| CN-AML Pat. #14 iPS L10 | *ELANE* (exon 4; p.C151Y) | hiPSC |
| HD iPS 1 | - | hiPSC |

were subjected to gel electrophoresis and analyzed using UV-light and 'GelRed Nucleic Acid Gel Stain' *(Biotinum, US)* (data not shown). The microRNA detection protocol was established in cell lines MDA-MB-231 and KG1-alpha. Once established, the workflow was used for primary patient samples. **Figure 3.10** shows Ct-values measured by qPCR for miR-125b expression in MDA-MB-231 and KG1-alpha cells. While we established and tested the workflow, normalization for miRNA expression was omitted.

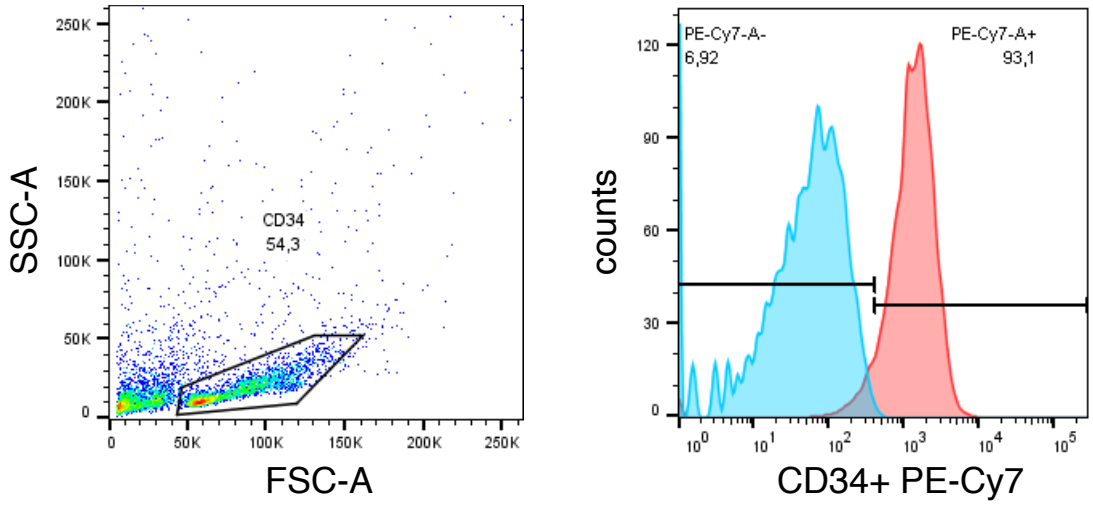


**Figure 3.9: Exemplary FACS purity assessment for CD34$^+$ cell fraction after MACS sorting**
Live CD34$^+$ cell fraction was defined by gating on side scatter (SSC-A) and forward scatter (FSC-A) properties excluding dead cells and debris (left). Histogram of flow cytometry cell counts labeled with CD34$^+$ PE-Cy7 antibody, clone 8G12 *(BD Biosciences, US)* (right).

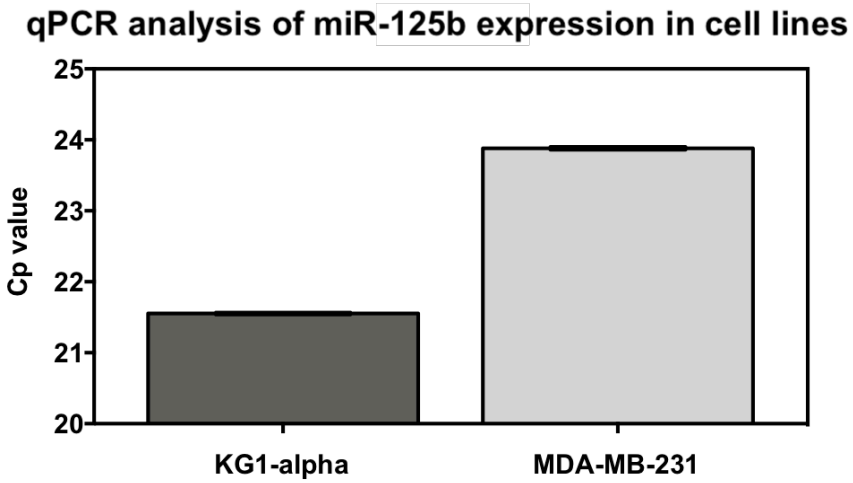


**Figure 3.10: Ct values of miR-125b in KG1-alpha and MDA-MB-231 cell lines** Ct values obtained by qRT-PCR results confirmed miRNA abundance. Total RNA was isolated from KG1-alpha and MDA-MB-231 cell lines. Subsequent to translation and amplification of microRNA, qRT-PCR was performed for miR-125b as validation of protocol efficiency. Ct-values are plotted on the Y-axis. During the process of establishing our workflow normalization and testing of statistical significance were omitted. qRT-PCR products were confirmed by gel electrophoresis (data not shown).

#### 3.3.1.1 MicroRNA expression profiling by qRT-PCR analysis in $CD33^+$ and $CD34^+$ cells of CN patients

Significant miR-125b and let-7b expression was observed in samples from 10 out of 21 investigated patients and 4 out of 5 healthy donors. The microRNA expression profile in $CD33^+$ cells, showed a variable pattern of expression for let-7b and miR-125b (**figure 3.11**). Further analysis, grouped according to genes with inherited mutations, showed no systematics or an ordered expression. Statistical testing using two-tailed t-test did not provide significant differences, neither between healthy donors and CN patients nor between CN subgroups ($p \gg 0.05$). No expression of miR-3151 was detected in any $CD33^+$ sample.

Let-7b and miR-125b expression profiling in $CD34^+$ cells revealed a homogeneous pattern of expression. MiR-125b expression exceeded let-7b expression in all investigated samples ($n = 8$; **figure 3.12**). Of note, no statistically significant difference could be found between the CN patient cohort and the healthy donor group. Analysis of relative miR-125b expression during differentiation revealed

downregulation of miR-125 upon differentiation from $CD34^+$ to $CD33^+$ cells. Furthermore, miR-3151 expression was not detected in $CD34^+$ cell fraction.

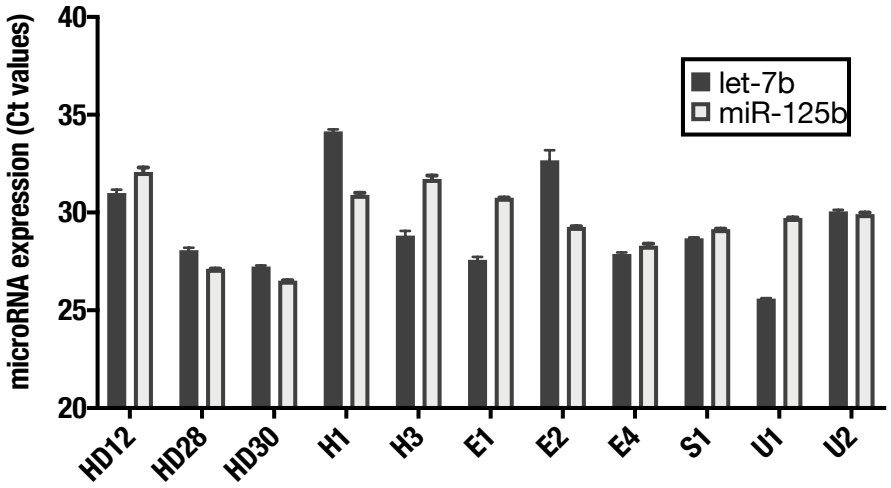


**(a)** qPCR analysis of miR-125b and let-7b expression in $CD33^+$ cells

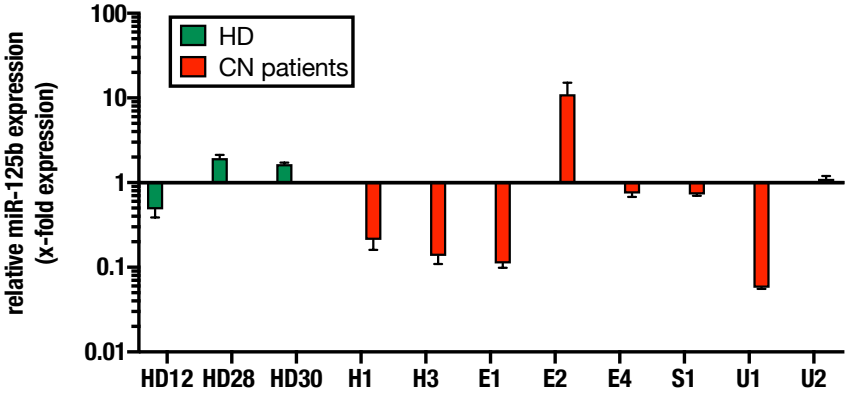


**(b)** miR-125b expression normalized to let-7b in $CD33^+$ cells

**Figure 3.11: Quantitative PCR analysis of miR-125b and let-7b expression in myeloid $CD33^+$ cells of CN patients and healthy donors**

a) Ct-values of MiR-125b and let-7b expression analysis by qRT-PCR in $CD33^+$ cells of CN patients with diverse mutations and healthy donors showed a very heterogeneous profile. The Samples are grouped by phenotype and genotype (table **3.2**). Dark columns represent let-7b expression and light grey columns represent microRNA-125b expression. Ct-values are plotted on the Y-axis, patient identifiers are plotted on the X-axis.

b) Normalization of miR-125b expression to let-7b confirmed the heterogenous profile indicated in 'a)'. Testing of statistical significance for differences in expression between healthy donors (green) and CN-patients (red) was omitted due to heterogeneous expression patterns. X-fold expression levels are plotted on the Y-axis (log scale), patient identifiers on the X-axis. Expression levels were calculated according to $2^{-\Delta Ct}$ method [Livak and Schmittgen, 2001]. Detailed data can be found in the appendix (**table 7.1**).

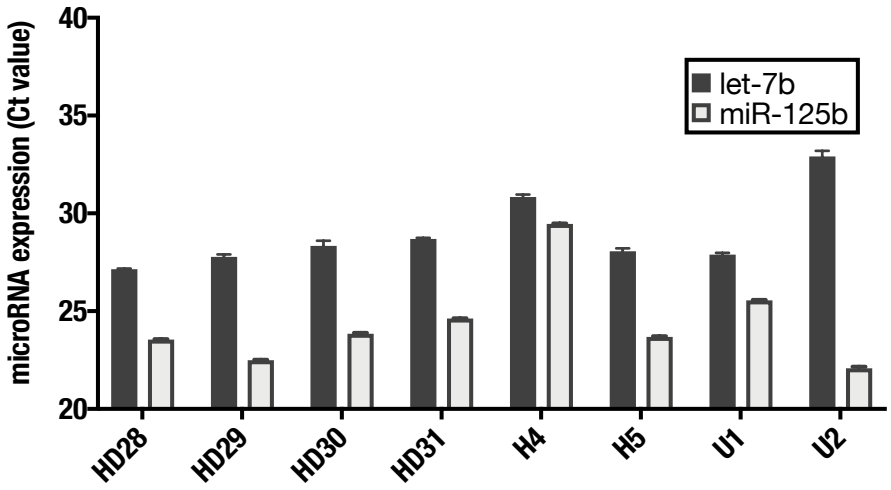


**(a)** qPCR analysis of miR-125b and let-7b expression in CD34$^+$ cells

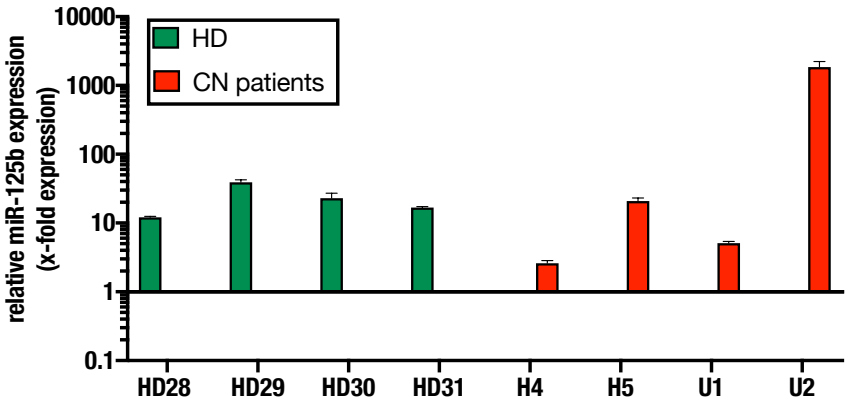


**(b)** miR125b-expression analysis in CD34$^+$ cells

**Figure 3.12: Quantitative PCR analysis of miR-125b and let-7b expression in myeloid CD34$^+$ cells of CN patients and healthy donors**

a) MiR-125b and let-7b expression analysis in CD34$^+$ cells of CN patients with diverse mutations and healthy donors showed miR-125b expression exceeding let-7b expression in every sample. Samples are grouped according to their phenotype and genotype (table **3.2**). Dark columns represent let-7b expression and light grey columns represent microRNA-125b expression. Ct-values are plotted on the Y-axis, patient identifiers are plotted on the X-axis.

b) Normalization of miR-125b expression to let-7b confirmed the upregulation of miR-125b compared to let-7b as indicated by values of 'a)'. Testing of statistical significance for differences in expression between healthy donors (green) and CN-patients (red) did not provide significance (Welch ungrouped t-test: $p>0.05$). X-fold expression levels are plotted on the Y-axis (log scale), patient identifiers on the X-axis. Expression levels were calculated according to $2^{-\Delta Ct}$ method [Livak and Schmittgen, 2001].

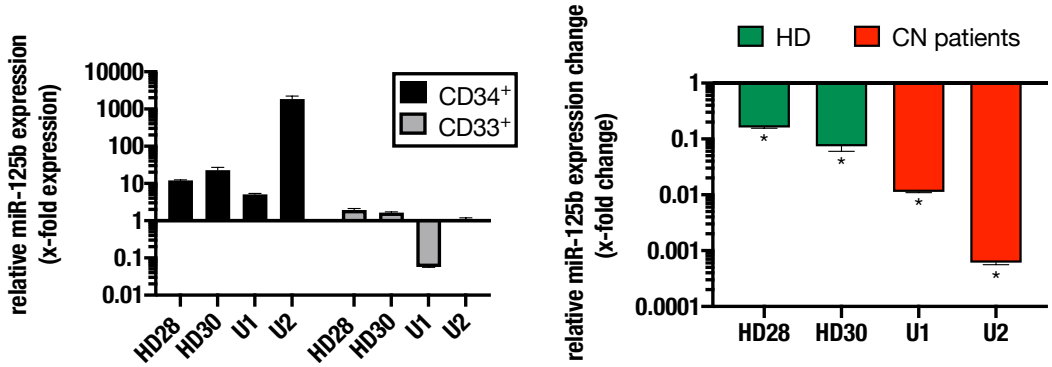


**Figure 3.13: Comparative analysis of relative miR-125b expression in CD34$^+$ and CD33$^+$ cells**

Change of relative miR-125b expression (normalized to let-7b) upon differentiation from CD34$^+$ to CD33$^+$ cells was calculated for four samples - two healthy donors, two CN patients - according to the $2^{-\Delta\ Ct}$ (left) and $2^{-\Delta\Delta\ Ct}$ method (right) [Livak and Schmittgen, 2001].
$^*$ unpaired t-test: $p < 0.05$

### 3.3.1.2 MicroRNA analysis in hiPSC derived cells

Quantitative PCR analysis of expression profiling of let-7b and miR-125b in hiPSC derived CD34$^+$ cells revealed a strong overexpression of miR-125b when compared to let-7b in all samples (**figure 3.14**). However, as in primary CD34$^+$ samples, no difference in the grade of miR-125b expression was observed between patient samples and healthy donor sample. Due to low sample numbers and high Ct-values of let-7b, normalization and testing for statistical significance was omitted (Data are shown in the 'Appendix' table **7.3**). Once again, miR-3151 expression was not detectable.

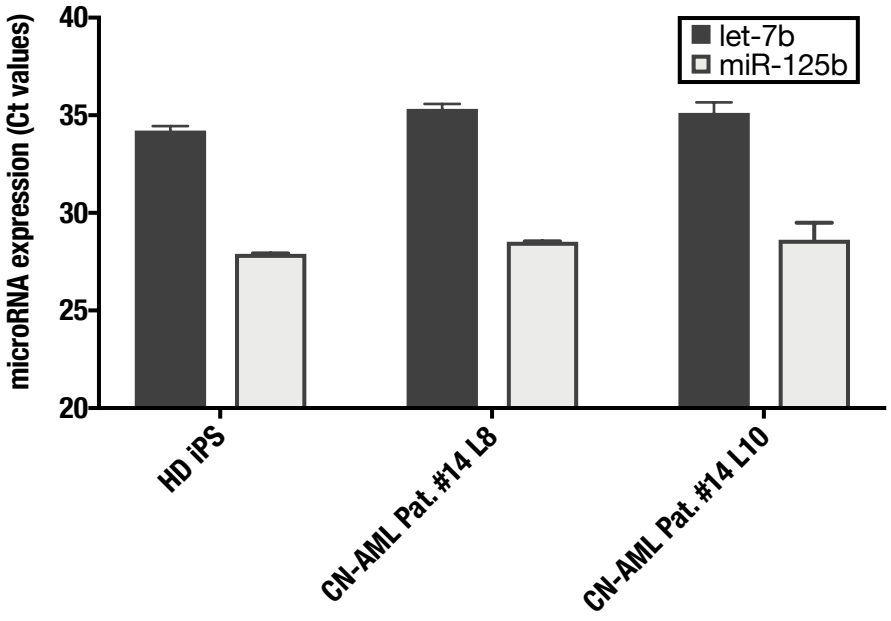


**Figure 3.14: Expression levels of miR-125b in hiPS derived CD34$^+$ cells of 'CN-AML pat. #14'**
Quantitative PCR data of miR-125b and let-7b expression analysis in hiPSC derived CD34$^+$ cells of a CN patient who developed leukemia and one healthy donor (HD) revealed continuous a higher abundance of miR-125b compared to let-7b. Both hiPSC derived cell lines of CN-AML pat. #14 were positive for *ELANE* mutations. Clone L8 resembled the CN phenotype and clone L10 resembled the CN-AML phase of the patient's disease, thus clone L10 was also positive for *CSF3R* and *RUNX1* mutations.

#### 3.3.1.3 Correlation analysis for miR-125b and let-7b in CD33$^+$ and CD34$^+$ cells of CN patients

To confirm independent expression of miR-125b and let-7b in CD33$^+$ and CD34$^+$ cells from our patient group, we performed correlation analysis by means of an XY-scatterplot. Scatterplot results of qPCR data for miR-125b and let-7b showed no correlation between the two microRNAs for both CD33$^+$ and CD34$^+$ cells (**figure 3.15**, detailed overview of Ct-values and standard deviation and correlation analysis is depicted in the Appendix **table 7.1** and **7.2**). Thus, further analysis and calculation of Pearson's coefficient proved to be insignificant and miR-125b and let-7b were assumed to be independently expressed. Of note, analysis was performed according to Rowe, P. [Rowe, 2012].

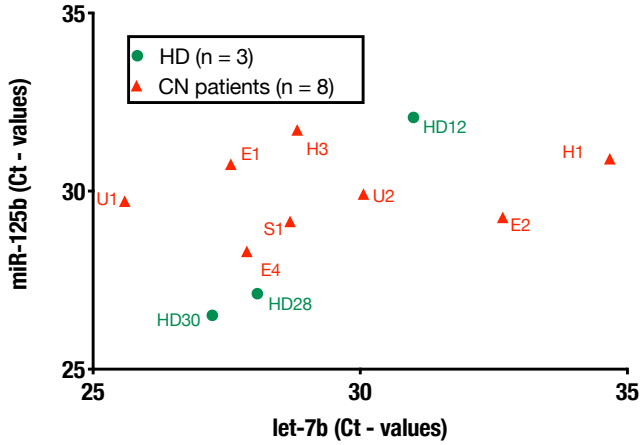


| Pearson r | |
|---|---|
| r | 0,3960 |
| 99% confidence interval | -0,4556 to 0,8692 |
| R squared | 0,1568 |
| Number of XY Pairs | 11 |

**(a)** CD33$^+$ cells

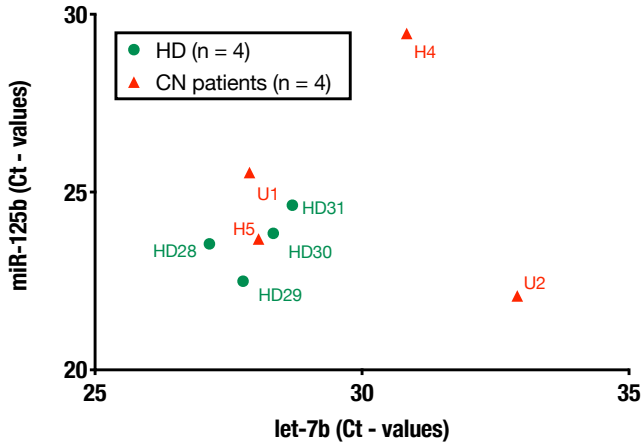


| Pearson r | |
|---|---|
| r | 0,1226 |
| 99% confidence interval | -0,7734 to 0,8552 |
| R squared | 0,01503 |
| Number of XY Pairs | 8 |

**(b)** CD34$^+$ cells

**Figure 3.15: Correlation analysis of let-7b and miR-125b in CD33$^+$ and CD34$^+$ cells of healthy donors and CN patients.**
Ct-values obtained by means of quantitative PCR for let-7b and miR-125b were plotted in an XY-scatterplot with let-7b expression plotted on the X-axis and miR-125b expression plotted on the Y-axis. Green plots mark Ct-values obtained from healthy donor samples, red plots mark Ct-values from CN patient samples. Letter code is explained in table **3.2**. Graph 'a)' shows the distribution for the investigated microRNAs in CD33$^+$ cells, whereas graph 'b)' shows the distribution in CD34$^+$ cells. *Calculation of Person's correlation showed no significance.*

The results presented in this section show a heterogeneous expression of microRNA -125b and let-7b in $CD33^+$ cells. In $CD34^+$ cells, when normalized to let-7b, we observed a miR-125b overexpression. It should be mentioned that in this project, our initial plan was also to investigate the microRNA expression in leukapheresis samples of healthy donors. Like our patient group, those donors were treated with clinical dosages of G-CSF, thus would have provided important data on the effect of G-CSF on microRNA homeostasis. Unfortunately, only trace amounts of microRNA could be obtained from leukapheresis samples by our experimental setup. Therefore we could not investigate this group and use the data to evaluate the effects of G-CSF on microRNA expression in myeloid cells. In addition, there was no sample in which miR-3151 expression was detected. Therefore, in the next chapter the results of this section will be discussed in more detail.

*Science is organized knowledge.*
*Wisdom is organized life.*

Immanuel Kant

# 4 Discussion

## 4.1 *RUNX1* gene copy number quantification

In continuation of a project published by Skokowa et al. in Blood 2014, the aim of this study was to expand the current knowledge regarding the underlying mechanism of malignant transformation in CN patients [Skokowa et al., 2014]. In 2014, our group reported about the cooperation between sporadic *CSF3R* (granulocyte colony-stimulating factor receptor) and *RUNX1* (Runt related transcription factor 1) mutations in a group of CN patients who progressed to MDS/AML on a large scale [Skokowa et al., 2014].

Malignant progression in blood cells, i.e. leukemogenesis, is a versatile process resulting of diverse genetic or epigenetic changes in the affected clones. The currently proposed multiple hit theory involves cooperating alterations which support proliferation, self-renewal and inhibit differentiation [Gilliland et al., 2004]. Exemplarily, those alterations can be chromosomal translocations resulting in fusion-proteins, mutations in tumor suppressor genes, gain of function mutations in oncogenes, misbalances in chromosomal amounts and mutations in epigenetic modifiers. In general, they can be grouped in type-I or type-II alterations which enhance

proliferation (e.g. alterations affecting *FLT3, KRAS, NRAS, KIT*) or inhibit differentiation (e.g. alterations affecting *CEPBa, RUNX1, HIPK2*), respectively [Gilliland et al., 2004; Harada and Harada, 2009; Röllig et al., 2018].

CN and familial platelet disorder with associated myeloid malignancy (FPD/AML) belong to the group of inherited bone-marrow failure syndromes (IBMFS); in addition to the disease-defining phenotypes, they have a significantly increased risk of malignant transformation [Skokowa et al., 2017; Song et al., 1999]. Since all IBMFS are susceptible to malignant progression, the mechanisms underlying malignant transformation might show similarities. Therefore, new insights on one type of IBMFS could help to understand the others. In most cases the cause of FPD/AML are heterozygous mutations and deletions of *RUNX1* - encoded on chromosome 21 (Chr 21) - and patients present with a low platelet count (below 100.000/ul), impaired platelet function and consequently prolonged bleeding time [Song et al., 1999]. On average, malignant transformation is observed in 35% of FPD/AML patients [Béri-Dexheimer et al., 2008; Perez Botero et al., 2017].

The underlying cause of CN are mutations in *ELANE* (neutrophil elastase; CN, 1, autosomal dominant (AD); OMIM: 202700 ), *GFI-1* (Growth Factor Independent Protein 1; CN, 2, AD; OMIM: 613107), *HAX1* (HCLS1-associated protein X-1; CN, 3, autosomal recessive (AR); OMIM: 610738) and *WAS* (Wiskott-Aldrich syndrome protein; CN, X-linked; OMIM: 300299) among others [Boztug et al., 2008; Skokowa et al., 2017; Triot et al., 2014; Ward et al., 1999; Zeidler et al., 2009]. Of note, there are other IBMFS also presenting with neutropenia such as Shwachman-Diamond syndrome (mutation in *SBDS*; Shwachman- Bodian- Diamond syndrome protein; OMIM: 260400) and cases of CN with yet unknown causes [Skokowa et al., 2017]. The mutations lead to a low absolute neutrophil count (ANC) of less than 500/ul by stopping the maturation of neutrophils at the promyelocyte stage [Welte et al., 2006]. Since neutrophils are needed for pathogen defense, especially against bacteria, patients with severely reduced ANC are vulnerable to bacterial infections and CN patients often have fever, pneumonia, skin abscesses and an increased sepsis rate [Skokowa et al., 2017; Welte and Dale, 1996]. Cyclic neutropenia (CyN) is also caused by *ELANE* mutations. In CyN, the

ANC fluctuates cyclically at a low level over a period of about 21 days, while the ANC is low, patients show the same symptoms as CN patients [Skokowa et al., 2017]. Both groups, CN and CyN patients, receive therapeutic doses of G-CSF, which leads to an increase in ANC of over 1000/ul; this provides sufficient protection against pathogens and leads to an almost normal life expectancy [Skokowa et al., 2017; Welte and Dale, 1996]. However, approximately 22% of CN patients progress towards MDS/AML [Skokowa et al., 2017]. Until 2016, CyN patients were expected to be spared from malignant transformation, but Klimiankou et al. reported a female CyN patient who developed AML at the age of 17 [Klimiankou et al., 2016a].

In this study, we re-analyzed the data of the patient cohort from 2014 and the CyN-AML patient from 2016 (For simplicity, CN-AML and CyN-AML are referred to as CN-AML in the following). When analyzing the cohort, we discovered that seven patients positive for *CSF3R* mutations (MT-*CSF3R*) and missense (Ms) *RUNX1* mutations had acquired trisomy 21. This was not detected in any of the patients with MT-*CSF3R* and nonsense (Ns) *RUNX1* mutation (n=6) (Fisher's t-test indicated a non-random distribution of the two defined constitutions; p = 0.0515; **table 3.1**) [Skokowa et al., 2014].

Constitutional trisomy 21 is the cause of Down's Syndrome (DS; OMIM: 190685), first described by John Langdon Down in 1862/66 [Cantor, 2015; Down, 1866]. Typically, people affected by trisomy 21 are of a small stature and suffer from delayed cognitive development and generally reduced intelligence. Besides congenital defects such as heart and gastrointestinal problems, they also have an increased risk for developing leukemia [Cantor, 2015]. In the first months of life, 4-18% of patients with DS develop 'Down syndrome associated transient abnormal myelopoiesis' (DS-TAM), which is either fatal or disappears in the months following presentation. 25% of patients who survive the DS-TAM phase develop leukemia - termed 'Down syndrome associated acute megakaryoblastic leukemia' (DS-AMKL) [Cantor, 2015]. Interestingly, in Down syndrome sporadic *RUNX1* mutations are very rare and are reported only in single cases [Cantor, 2015; Izraeli, 2006; Taketani et al., 2002].

Before mutations in *RUNX1* were reported, *RUNX1* was known as a translocation partner in t(8;21) AML FAB M2, where it induces its leukemogenic potential as a part of the chimeric protein RUNX1-RUNX1T1 [Miyoshi et al., 1991]. The first *RUNX1* mutations were reported by Osato et al. in AML patients of various subtypes, this first observation was followed by others reporting *RUNX1* mutations in FPD/AML, MDS, secondary AML, CML, CMML, FA (Fanconi Anemia; various FANC genes; OMIM: 227650), etc. [Imai et al., 2000; Osato et al., 1999; Preudhomme et al., 2000; Song et al., 1999]. Since 2016, there is a preliminary WHO entity for AML with mutated *RUNX1*, which takes into account the fact that AML with mutated *RUNX1* is associated with a worse response to treatment, a generally worse prognosis and requires special treatment [Haferlach et al., 2016; Stengel et al., 2018].

We aimed to investigate whether, in CN-AML patients, trisomy 21 was associated with an increase in the wild type or mutant *RUNX1* allele dosage. In contrast to the rare association of mutant *RUNX1* and trisomy 21 in Down Syndrome, in MDS/AML, trisomy 21 following *RUNX1* mutations is more frequent and associated with an increase of the mutant *RUNX1* allelic fraction [Preudhomme et al., 2000, 2009; Taketani et al., 2003].

In order to obtain first insights, we performed the Sanger sequencing of *RUNX1*, *ELANE* and *CSF3R* for hematopoietic cell samples of CN-AML pat. #14 [Dannenmann et al., 2021] and CyN pat. #1 [Klimiankou et al., 2016b] from CN and CN-AML stages (**figure 3.1**). In samples obtained at the CN stage, Sanger sequencing showed only the inherited *ELANE* mutations. At the CN-AML stage - where karyotyping of myeloid cells of both patients revealed trisomy 21 (data not shown) - Sanger sequencing revealed additional mutations in *CSF3R* and *RUNX1* [Dannenmann et al., 2021]. It is particularly remarkable, that in both patients the Sanger sequence data at the site of the *RUNX1* mutation showed elevated peaks with a mutant $>$ wild type allele ratio. This would be compatible with an additional mutant allele on the additional chromosome 21.

To validate this observation, we examined the gene copy number of mutant and wild type *RUNX1* in samples from three CN-AML patients - the two patients already

examined by Sanger sequencing and one additional patient (CN-AML pat. #31) - at the CN and CN-AML stage using digital PCR and custom TaqMan probes *(ThermoFisher Scientific, US, Ca)* (**figures 3.3** to **3.6**). Digital PCR allows the analysis of the gene copy number by a novel approach; in digital PCR the samples are distributed on a chip containing about 10,000 reaction wells, so each well contains about one copy of the target gene. PCR performed with fluorescence-labeled probes - different labels for mutant *RUNX1* (FAM dye) and wild type *RUNX1* (VIC dye) - amplifies and identifies the target genes and allows quantification and calculation of mutant to wild type ratio.

In total, we investigated six samples of CN-AML pat. #14, two of CN-AML pat. #31 and three of CyN-AML pat. #1 in duplicates and additionally screened seven hiPSC derived samples of CN-AML pat. #14 by means of digital PCR. For CN-AML pat. #14, we observed signals of mutant *RUNX1* allele in all native samples obtained at CN and CN-AML stage of disease and MT-*RUNX1*:WT-*RUNX1* ratio was significantly below 50%. To rule out the possibility of simultaneously examining non-leukemic and malignant cells in the same reaction, we decided to investigate pure cell clones which were either hiPSC or CFU derived [Dannenmann et al., 2021]. Investigation of these samples showed that at CN stage, MT-*RUNX1* was not detectable; and at CN-AML stage, MT-*RUNX1*:WT-*RUNX1* ratio reached levels around 2:1. Thus, we confirmed that trisomy 21, which had occurred after clones were positive for mutant *RUNX1*, led to an increase in the allelic fraction of mutant *RUNX1* [Dannenmann et al., 2021]. This was in line with observations by Preudhomme et al., who reported that in AML patients, trisomy 21 lead to additional alleles of mutated *RUNX1* [Preudhomme et al., 2000; Roumier et al., 2003].

Furthermore, we hypothesize that the association of trisomy 21 and missense *RUNX1* could reflect a variation of the underlying pathomechanism of leukemogenesis in CN patients proposed by Skokowa et al [Skokowa et al., 2014]. The functionally relevant *RUNX1* mutations (this excludes synonymous mutations and single nucleotide polymorphisms (SNP)) can be divided into four categories: (i) N-terminal point mutations that cluster in the RHD (Ms-RUNX1), (ii) frameshift mutations (Fs) and N-terminal (Nt) nonsense mutations, (iii) C-terminal (Ct) nonsense

mutations and (iv) frameshift mutations that result in an elongated RUNX1 protein. Previously reported functional studies of RUNX1 mutants indicated different effects of the altered RUNX1 proteins, and since Skokowa et al. have discovered Ms-, Nt- and Ct-RUNX1 mutations in our cohort, the discussion about their effects will focus on these mutations [Skokowa et al., 2014].

There have been inconsistent reports about the effects of Nt-RUNX1. On the one hand, Nt-RUNX1 was reported to have lost its ability to bind DNA and CBF-$\beta$, thus representing a loss of function; on the other hand, Michaud et al. reported a dominant negative effect for e.g. RUNX1 p.R174X compared to WT-RUNX1 [Harada et al., 2003; Imai et al., 2000; Michaud et al., 2002; Osato et al., 1999]. However, it is currently assumed that Nt-RUNX1 is degraded by nonsense mediated mRNA decay (NMD), thus not expressed in vivo, which results in haploinsufficiency of *RUNX1* [Cammenga et al., 2007; Christiansen et al., 2004; Maquat, 2004; Perez Botero et al., 2017; Song et al., 1999; Weischenfeldt et al., 2005; Zhao et al., 2012]. The same would be true for frameshift mutations resulting in Nt-RUNX1 proteins. In *RUNX1* mutant patients other than CN-AML, there were reports about Fs-mutations resulting in elongated RUNX1 proteins, which lack the transactivation domain (TAD) leading to a loss of function of the protein. For the remaining two mutations, Ms-RUNX1 and Ct-RUNX1, expression was confirmed *in vivo* and both were reported to act negatively dominant over WT-RUNX1 [Schmit et al., 2015]. Ms-RUNX1 is not able to bind to DNA and thus might repress WT-RUNX1 activity either by protein sequestration (e.g. of CBF-$\beta$ or others) or by disruption of other signaling pathways [Cammenga et al., 2007; Harada and Harada, 2009; Imai et al., 2000; Osato, 2004; Osato et al., 1999; Zhao et al., 2012]. It is important to note that it cannot be excluded that other, possibly not yet known functions, of wild type RUNX1 could still be executed by Ms-RUNX1. In addition to the experimentally obtained data, a further indication of the dominant potential of some *RUNX1* mutations in FPD/AML patients was derived by analyzing the malignant transformation rates. It was observed that more patients belonging to pedigrees positive for *RUNX1* mutations (K83E) with an assumed dominant negative potential progress to AML more frequently than patients belonging to

haploinsufficient *RUNX1* (deletion of one *RUNX1* allele) pedigrees - 54% versus 34% [Michaud et al., 2002]. It is known that Ct-RUNX1 retains both DNA and CBF-$\beta$ binding capacity but is not capable of transactivation due to impaired TAD, resulting in loss of function (haploinsufficiency) and possibly associated with protein sequestration [Zhao et al., 2012]. In the case of Ct-RUNX1, the absence of the VWRPY motif could also be of importance, this domain usually allows the suppression of RUNX1 via Groucho/TLE [Roumier et al., 2003]. Clinical observations also indicate functional differences between Ct- and Ms-RUNX1; the bone marrow of Ct-RUNX1 patients was hypercellular and additional mutations were found less frequently, while Ms-RUNX1 patients had hypocellular bone marrow and often had additional mutations [Harada and Harada, 2009].

Since Nt-RUNX1 acts via haploinsufficiency, Nt-*RUNX1* mutations reduce the available wild type RUNX1 amount by 50%. According to our observation, it can be hypothesized that this could be sufficient to induce leukemia in cells positive for both *CSF3R* mutations and *RUNX1* mutations. Complementing the mechanism postulated by Skokowa et al., that *CSF3R* mutations give the affected cells a survival advantage and the acquisition of *RUNX1* mutations would manifest their fate towards leukemia, Chin et al. reported that the haploinsufficiency of *RUNX1* increases the sensitivity of the cells to G-CSF, which promotes their proliferation and suppresses differentiation [Chin et al., 2016; Skokowa et al., 2014]. Although the experiments were performed with cells positive for WT-*CSF3R*, they implied that in our cohort, mutated *RUNX1* would contribute to the effects of mutated *CSF3R*, supported by the daily administration of G-CSF - which was reported by Ritter et al. in 2018 [Chin et al., 2016; Ritter et al., 2018]. Furthermore, *RUNX1*-haploinsufficient mice showed an increase of myeloid colonies (promoted proliferation) and a decrease in LT-HSCs numbers associated with an increased replating capacity reflecting the malignant potential of *RUNX1* haploinsufficiency [Sun and Downing, 2004]. Furthermore, reduced platelet numbers, as observed in FPD/AML patients, were also reported in this study [Sun and Downing, 2004]. The emergence of trisomy 21 after acquisition of *CSF3R* and missense *RUNX1* mutations suggests that the amounts of missense RUNX1 protein might not be suf-

ficient to cause fully developed leukemia in affected hematopoietic cells without trisomy 21. The increased amounts of missense RUNX1 protein due to trisomy 21 and two copies of mutated *RUNX1* would overcome this state, and the total negative dominant potential of the missense RUNX1 protein - expressed by the two alleles - could eventually provide sufficient suppression of wild type RUNX1 and induce the leukemic phenotype (**figure 4.1C**) [Roumier et al., 2003]. Assuming that Nt-RUNX1 exerts its malignant potential solely through the loss of diploidy, it is obvious that trisomy 21 would not increase the malignant potential of Nt-RUNX1. Furthermore, Harada et al. suggested, that Nt-RUNX1 could confer a greater malignant potential than Ms-RUNX1 and induce proliferation sufficient to mimic MDS/AML [Harada and Harada, 2009]. Of note, in the patient group presented by Skokowa et al. some patients were positive for further leukemia associated mutations such as mutations in *SUZ12, EP300, CBL, CREBBP, FLT3-ITD* and *Nras* [Skokowa et al., 2014]. Interestingly, as noted by the authors, the patient positive for the *Nras* mutation was negative for mutations in *RUNX1* and could represent a separate entity of leukemogenesis in CN [Skokowa et al., 2014]. The presence of additional mutations to the *RUNX1* mutations has been described as standard in AML patients and is consistent with the observations that mutated *RUNX1* alone is not sufficient to induce leukemia [Chin et al., 2016; Stengel et al., 2018]. The authors also reported that either the loss of the wild type allele or multiple *RUNX1* mutations negatively affected the prognosis and that a negative effect was seen by $\geqslant 2$ additional mutations and survival. Of note, in this particular study mutations in *CSF3R* were not investigated [Stengel et al., 2018]. In their report, Skokowa et al. also examined the CN-AML samples for mutations in *NPM1, FLT3-ITD, FLT3-TKD, CEBPA, NRAS, KRAS, CBL, TET2, IDH1, IDH2, DNMT3A, SUZ12, EP300* [Skokowa et al., 2014]. Regarding the leukemogenic potential of *RUNX1*, it would be of great interest to have whole genome analysis data available. Whole genome or exome analysis, preferably from samples taken at different points in time of the leukemogenic transformation, would clarify whether other mutations that cooperate with *RUNX1* and *CSF3R* are present, and if so, in what order they occur. Moreover, it would be of interest to further clarify the effects of missense

and Ct-nonsense RUNX1 mutations on their behavior.

To address the functional differences between wild type, missense and nonsense RUNX1 as suggested above, we started to investigate RUNX1 binding patterns using chromatin immunoprecipitation (ChIP). Our aim was to establish a workflow that would allow the enrichment of genomic regions bound by RUNX1 in the cell lines NB4 and U937. In this study, we achieved gDNA enrichment through our ChIP workflow for the already known RUNX1 targets *GNA15* and *RUNX3* in U937 cells (**figure 3.8**) [Gardini et al., 2008; Illendula et al., 2015]. It is important to note that the enrichment of the target genes was below the level we expected (achieved enrichment < 5 times). In accordance with our relatively low enrichment, Gardini et al., who performed ChIP for RUNX1-RUNX1T1, also described a low enrichment of GNA15 [Gardini et al., 2008]. Since Illendula et al. did not provide data for RUNX3 enrichment, the data we obtained for the enrichment of RUNX3 gDNA could not be compared with other data [Illendula et al., 2015]. In addition to low GNA15 and RUNX3 enrichment, we failed to enrich DNA of e.g. *PKC-β*. Since we used primers for *PKC-β* that have already been used and described by Hug et al., we assume that the problems encountered reflect problems in the ChIP experiment or are due to a lower, altered RUNX1 affinity in our cell lines and not the result of unspecific primers or errors in the qPCR [Hug et al., 2004]. Since enrichment levels were generally low, for future experiments, our workflow must be optimized in terms of sensitivity, and in terms of reliability; thus, the ChIP data provided must be treated with caution. Based on the underlying study, we hypothesize that in some CN-AML patients, missense *RUNX1* and trisomy 21 - leading to a 2:1 ratio of mutant to wild type *RUNX1* allelic fractions - might be sufficient to induce the malignants phenotype in the affected individuals. Besides probing our theory whenever possible, future studies will have to address the following questions. Firstly, are nonsense *RUNX1* mutations, in addition to either *CSF3R* mutations or the CN-causative mutation, sufficient to induce a leukemic phenotype? Secondly, do missense *RUNX1* mutations, that are not associated with trisomy 21, induce leukemic progression by another mechanism, or are they accompanied by further mechanisms that contribute to leukemia formation in these

patients? Hence, the future provides further potential for exiting scientific research in the field of CN.

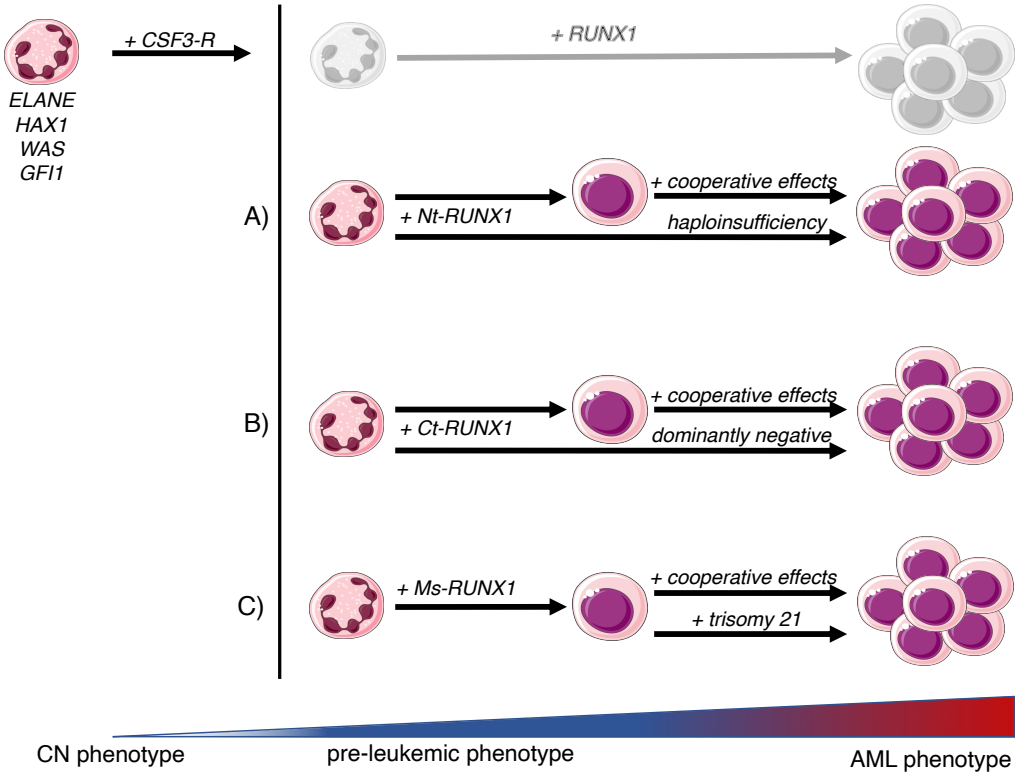


**Figure 4.1: Overview of possible mechanisms of malignant transformation depending on the underlying *RUNX1* mutation**
Following CN-associated mutations and *CSF3R* mutations, mutations in *RUNX1* are the most common genetic changes observed and published in CN. Our observation indicates different mechanisms of leukemogenesis for the different *RUNX1* mutations, whilst additional cooperating effects can not yet be excluded: (A) N-terminally truncated RUNX1 (Nt) - subjected to NMD - might exert its leukemic potential solely via haploinsufficiency; (B) C-terminally truncated RUNX1 (Ct) might act dominantly negatively over wild type RUNX1; (C) missense RUNX1 (Ms) might also contribute to leukemogenic progression via dominant negative suppression of wild type RUNX1 but requires an increased allelic fraction which is achieved by an occurrence of trisomy 21. Cooperating effects can for example comprise mutations in *SUZ12, EP300, CBL, CREBBP, FLT3-ITD* or *Nras*.
*Adapted from Skokowa et al., 'Cooperativity of RUNX1 and CSF3R mutations in severe congenital neutropenia: A unique pathway in myeloid leukemogenesis' [Skokowa et al., 2014]*

## 4.2 Expression analysis of microRNA-125b and miR-3151 in CD34$^+$ and CD33$^+$ cells of CN patients

This study aimed to lay the ground for the investigation of microRNA profiles in our CN patient group and to quantify the expression of microRNA-125b, miR-3151 in this patient cohort. On the longer perspective, this aims to increase the understanding of the mechanisms underlying the disease and to contribute to the knowledge about dysregulated intracellular signal transduction processes contributing to the high frequency of leukemogenic progression observed in the patient group.

Since their first description by Lee et al. in 1993, microRNAs, which are approximately 22 nt long non-coding RNAs, have become an important subject in molecular biology, such as in cell homeostasis and disease modeling - especially oncogenesis and leukemogenesis [Lee, 1993]. MicroRNAs exert their biological activity via several mechanisms which all involve Watson-Crick base pairing of matching nucleotides in or next to their seed region - a conserved RNA sequence spanning from nt position 2 to 8 - to mRNA or DNA [Bartel, 2018]. Their functional range includes the induction of mRNA degradation, the inhibition of translation, and supposedly transcriptional control over genes of both proteins and noncoding-RNA (ncRNA) [Bartel, 2018; Jonas and Izaurralde, 2015; Rasko and Wong, 2017; Weiss and Ito, 2018; Zardo et al., 2012].

MicroRNA expression profiles differ between distinct cell types and microRNA expression levels change upon differentiation even within the same cell type. For example, it was reported that in granulocytes, microRNA expression patterns were altered when cells were functionally active compared to inactive cells [Chen et al., 2004; Larsen et al., 2013; Petriv et al., 2010; Weiss and Ito, 2018]. As research on microRNA progressed, it became possible to use microRNA expression data to distinguish and group cells from both hierarchical and functional points of view, comparable to grouping by protein expression [Petriv et al., 2010]. Additionally, experimentally altered microRNA expression profiles made it possible to generate pluripotent stem cells from mature cells [De Haan and Lazare, 2018]. Moreover,

overexpression studies of specific microRNA (-clusters) have shown that altered microRNA expression levels had dramatic effects, such as a competitive advantage in replating experiments, eventually leading to a disease-like phenotype by affecting important cellular mechanisms e.g. apoptosis, or promoted a certain cell fate [Bousquet et al., 2010; Gerrits et al., 2012; O'Connell et al., 2010]. These observations and experiments highlight that microRNAs play an important role in cell homeostasis, as a consequence alterations in cell homeostasis have impact on the whole cell including its microRNA transcriptome. Vice-versa, alterations primarily affecting the microRNA transcriptome will eventually affect cell homeostasis. Prior works have noted the importance of considering the complexity of microRNA physiology when investigating microRNA expression [Shaham et al., 2012]. A great comprehensive insight of intracellular RNA dynamics is given by Chen et al. who illustrate the spatio-temporal interplay between the players involved in post-transcriptional mRNA regulation [Chen et al., 2018]. It is crucial to remember that biological effects of a given microRNA - besides its own expression level - is dependent on the availability of target structures as well as the expression of synergistic and antagonistic factors. This complexity leads to contra-intuitive observations: exemplarily miR-223, a microRNA involved in granulocytic differentiation, was reported to be upregulated during granulocytic differentiation, but knockout of miR-223 led to appearance of increased numbers of hypermature neutrophils, which indicates a sophisticated microRNA balance achieved in healthy cells and crucial for them to function properly [Fazi et al., 2005; Johnnidis et al., 2008; O'Connell et al., 2011; Stavast et al., 2018].

Early works in the field of hematopoiesis and hematological diseases - e.g. AML - pioneered the understanding of microRNA physiology and laid the foundation for the relatively broad knowledge of microRNA homeostasis in general, their involvement in cell differentiation and (hematological) disease modelling in particular. First reports stated that some microRNAs were predominantly expressed in hematopoietic tissue with almost mutually exclusive expression of miR-223 in the bone marrow and miR-181 in the thymus and B-lymphocytes [Chen et al., 2004]. It is especially interesting, that microRNAs often target early acting genes

- i.e. transcription factors and their regulators - such as *RUNX1*, *PU.1*, *C/EBPa*, *myb* and *Socs1*, adding a new dimension to this already manifold orchestration [O'Connell and Baltimore, 2012; Stavast et al., 2018]. By regulating early acting TFs, microRNAs are able to heavily impact the cell program with relatively small effort, thus affecting the heterochrony of cell maturation - i.e. the morphological aspects of the cells in a time-dependent manner [Rowe et al., 2016]. On HSC level, maintenance of the HSC pool is (co)mediated among others by miR-125 and let-7 family members. In more differentiated cells arisen from HSCs, on microRNA level lineage fate is mediated by e.g., miR-223, miR-150 and miR-181 [Zhao et al., 2012]. MiR-125b achieves HSC maintenance by supporting the proliferation of HSCs and myeloid progenitors whilst suppressing their apoptosis - relevant miR-125b targets are *LIN28A*, a pluripotency gene, *Bak1* and *Bmf*, both mediators of apoptosis [Bousquet et al., 2008, 2010; Chaudhuri et al., 2012; Emmrich et al., 2014]. Its involvement in those profound regulatory processes and in the pathogenesis of (trisomy 21 associated) leukemia, makes miR-125b an especially interesting subject in terms of its role in CN pathogenesis and malignant transformation [Klusmann et al., 2010; Skokowa et al., 2017]. Let-7 family of microRNA mediates the balance between HSC maintenance and differentiation via a regulatory mechanism including *LIN28* and *Hmga2* regulation, which both promote self-renewal. *LIN28* expression suppresses let-7, let-7 is able to suppress *Hmga2* expression; in this context, let-7 expression is associated with differentiation [Weiss and Ito, 2018]. In favor of cell maturation, some of those microRNAs involved in HSC maintenance are downregulated as miR-125b, whilst others, such as miR-223, are upregulated during differentiation, miR-223 reaches its highest expression levels in mature granulocytes [Petriv et al., 2010]. MiR-223 is embedded in a feedback loop between *C/EBPα* (CAAAT-enhancer box protein alpha) and *NF1-A* (nuclear factor 1 a; inducing erythroid cell fate in hematopoietic progenitor cells), which favor or repress granulocytic fate, respectively [Fazi et al., 2005; Fukao et al., 2007; Starnes et al., 2009; Stavast et al., 2018; Zardo et al., 2012]. Interestingly, C/EBP*α* exerts its function by inducing the expression of miR-223 which limits *E2F1* expression, a suppressor of miR-223 and functional opponent

of *C/EBPα* [Pulikkan et al., 2010; Stavast et al., 2018]. Another important myeloid transcription factor, PU.1, resides in the center of a microRNA regulatory network which also mediates myeloid differentiation eventually towards a monocytic fate. This network consists of microRNAs -342, -141, -200c and -223, and PU.1 induces miR-223 which acts as mentioned above [Stavast et al., 2018]. In cells expressing *C/EBPα*, thus primed for myeloid fate, miR-223 and members of the let-7 family, which were among the first identified microRNAs in C. elegans, are upregulated during myeloid differentiation and suppress the stemness as well as genes of the erythroid fate [Stavast et al., 2018]. In $CD34^+$ cells, *RUNX1* is involved in fate selection between monocytic and granulocytic fate. When suppressed via miR-129, it does not longer inhibit expression of *CSF3R*, i.e granulocytic differentiation, otherwise it favors monocytic fate via induction of *CSF1R* (M-CSF) [Stavast et al., 2018].

In this study, we aimed to isolate microRNA and quantify the expression of miR-125b and miR-3151 in CN patients and compare the results to cells obtained from healthy donors. Our workflow proved to be successful in terms of isolating microRNA from native patient samples. Furthermore, we observed the previously reported down-regulation of miR-125b expression upon myeloid differentiation from $CD34^+$ to $CD33^+$ cells, when microRNA expression results were normalized to let-7b (**figure 3.13**) [Petriv et al., 2010]. However, we did not observe significant differences between healthy donors and CN samples as well as no differences within the CN groups with distinct genetic backgrounds, indicating no different physiology of miR-125b and let-7b in these populations (**figures 3.11, 3.12** and **3.14**). Furthermore, we aimed to examine miR-3151 expression in our patient group. Approximately one third of microRNAs is transcribed and generated from intronic parts of protein-coding genes [Baskerville and Bartel, 2005]. MicroRNA miR-3151 is located in the intronic region of *BAALC* (brain and acute leukemia cytoplasmic) and previous studies have shown that their expression correlates with poor prognosis in AML patients [Eisfeld et al., 2012]. The first study focused solely on *BAALC* expression and revealed positive correlation with other prognostic markers, e.g. *C/EBPα* mutations in AML, but also showed that higher *BAALC*

expression was associated with lower complete remission rates and poor overall survival [Langer et al., 2008; Weber et al., 2014]. After the discovery of miR-3151, it was shown that miR-3151 had prognostic relevance in AML and high expression of both, miR-3151 and *BAALC*, was associated with inferior endpoints [Eisfeld et al., 2012; Schotte et al., 2011]. Subsequent studies reported *TP53* (tumor protein 53) as direct target of miR-3151, which regulates p53 mediated apoptosis [Eisfeld et al., 2014]. However, we did not confirm expression of miR-3151 in any sample, neither in samples obtained from CN patients or healthy donors nor in hiPSC derived cells. The lack of detection of miR-3151 can have several reasons. On the one hand, it is possible that miR-3151 is not expressed in our samples or in too small amounts for detection by our workflow. This would mean, that in the hiPSC model of our index patient, the expression of *BAALC* is not associated with the microRNA encoded in its intron, as reported by Eisfeld et al. [Dannenmann et al., 2021]. Unfortunately, on the other hand, we had no positive control for miR-3151, thus a failure of the TaqMan assay, although unlikely, cannot be excluded.

Caution towards our quantitative microRNA expression data is given based on several reasons: normalization, different genetic backgrounds and sample treatment. First of all, we have normalized our results using let-7b as endogeneous control, on the basis of a report by Petriv et al. who carefully examined microRNA expression in myeloid cells and showed that let-7b was constantly expressed among all cells at different stages during granulocytic differentiation [Petriv et al., 2010]. Hence, it is plausible to assume that changes of miR-125b expression reported by our workflow reflects the reported behavior of miR-125b in myeloid cells. However, partially contradicting the reports of Petriv et al., Rajasekhar et al. reported a down regulation of miR-125b in myeloid cells which was accompanied by an up-regulation of let-7b [Rajasekhar et al., 2018]. Furthermore, Raghavachari et al. also reported altered let-7b expression levels upon differentiation from $CD34^+$ cells into mature granulocytes [Raghavachari et al., 2014]. Of note, upon examination of the Ct-values in the raw data generated by qPCR, we observed indication for increased let-7b expression levels from $CD34^+$ to $CD33^+$ cells in two

of the four samples studied (Appendix **tables 7.1** and **7.2**). This is in line with the two reports. Although this was only observed in patient samples and not in healthy donors, due to the small sample size it is not possible to draw solid conclusions. Interestingly, in the report about the prognostic impact of *BAALC* and miR-3151 in AML patients, Eisfeld et al. observed a down-regulation of let-7b in cells with high *BAALC* expression and in a later report the authors reported a SNP in the *BAALC* which expression could be induced by *RUNX1* [Eisfeld et al., 2012, 2014]. Taken together, this implies the relevance of *BAALC* and miR-3151 in the leukemogenic progression in CN patients and in the context of mutant *RUNX1*. This might be of special interest in light of our index patient CN/AML pat. # 1, where we observed both elevated *BAALC* expression levels and mutant *RUNX1* [Dannenmann et al., 2021]. Finally, the question remains whether significance of miR-125b down-regulation from $CD34^+$ to $CD33^+$ cells is achieved by actual down-regulation of miR-125b or by simultaneous up-regulation of let-7b expression. To take into account the influence of G-CSF, we initially planned to include healthy cells obtained by leukapheresis. This would have allowed us to study healthy myeloid progenitor cells that have been exposed to G-CSF. Unfortunately, we were not able to isolate sufficient RNA amounts from leukapheresis samples for further investigation, thus we could not quantify the impact of G-CSF on the expression of the microRNA. This would have been especially interesting for the expression of miR-125b, since Surdziel et al. have reported increased expression of miR-125b by G-CSF treatment in 32D cells [Surdziel et al., 2011]. However, this is counter-intuitive since G-CSF promotes differentiation and miR-125b is usually down-regulated upon myeloid differentiation [Petriv et al., 2010; Shaham et al., 2012]. When they induced miR-125b expression to supraphysiologic levels, they observed alteration in G-CSFR signalling in the 32D cell line. Later, their observation of increased miR-125b expression upon G-CSF treatment in mice was not confirmed in human cells by Rajasekhar et al. They reported that upon G-CSF-triggered differentiation, miR-125b expression was decreased, as also reflected by our data [Rajasekhar et al., 2018]. Regarding that in this study, the miR-125b expression in cells of the same hierarchical level do not differ significantly based

on their origin - e.g. between $CD34^+$ cells from CN patients and healthy donors - we also urge caution. Since the reported data are a part of a completely new project aiming to study microRNA profiles in CN patients, and initially the sample size was very small, it makes it hard to reach significance or to draw general conclusions from the data obtained. Although a purity control by means of fluorescence-labelled flow cytometry of the living $CD34^+$ or $CD33^+$ fractions was performed for each sample after cell separation - purity levels of over 80% were achieved - we cannot exclude that residual impurities or the remaining heterogeneity within the isolated cell fractions may have influenced the observed microRNA expression levels [Notta et al., 2016; Velten et al., 2017; Wünsche et al., 2018].

To address potential improvements for the performance of microRNA studies in the future, we would suggest several recommendations. First of all, we would recommend selecting appropriate normalization modes. There are multiple ways to increase the reliability of the data obtained via endogeneous control or spike-in controls. Normalization with microRNA as endogeneous control offers the possibility to examine microRNA expression without the risk of misinterpreting data due to alterations affecting the whole microRNA machinery. For example, when an experimental set up affects the processing machinery of microRNAs (Dicer, Drosha, etc.), or when the microRNA biogenesis is initially affected, an endogenous control would possibly be affected to a similar degree as the target microRNA, hence false conclusions could be avoided [Lin and Gregory, 2015; Schwarzenbach et al., 2015]. Another way of endogeneous normalization of microRNA expression data is the usage of other RNA types, such as snoRNAs (small nucleolar RNAs), but more recently there have been reports urging caution because other RNA types underly a different physiology compared to microRNA, which could add bias to the data analysis and interpretation [Schwarzenbach et al., 2015]. Normalization of microRNA expression data using spike-in controls, which are normally added to the experimental set-up after RNA isolation and before reverse transcription, allows an objective quantification and normalization of microRNA expression with some caveats, like the increased risk of false positive results [Schwarzenbach et al., 2015]. The gold-standard to find appropriate candidates for normal-

ization would be an initial review of the literature followed by the experimental confirmation of steady expression for the different experimental conditions and normalization against multiple endogeneous controls as well as spike-in controls [Schwarzenbach et al., 2015]. Further possibilities are the usage of microarrays or next-generation sequencing techniques which initially do not need normalization [Schwarzenbach et al., 2015].

Although we used a MACS-based sorting strategy and performed purity control by fluorescence-labeled flow cytometry using $CD34^+$ and $CD33^+$ antibodies, those populations are still very heterogenous [Notta et al., 2016; Velten et al., 2017; Wünsche et al., 2018]. To address the possibility of data bias due to impurities in the cell fractions, for further experiments we recommend single cell approaches which are available and allow high resolution investigation of microRNA expression [Faridani et al., 2016]. Data obtained by those techniques are either suitable for screening purpose or to validate data obtained by workflows bearing the possibility of (slightly) impure samples but require more sophisticated data analysis skills than simple qPCR results. However, it should be investigated if and which microRNAs could be detected by single-cell RNA sequencing. Due to the fact that the expression of microRNA depends, among other factors, on the degree of cell differentiation, the cellular environment and the therapeutic agents, we recommend a careful selection of the control reference group, in which the differences to the study group are defined as precisely as possible [Schwarzenbach et al., 2015].

In CN, the research field of microRNA still holds many interesting perspectives that need to be explored. In the treatment of leukemia patients, good risk stratification lays the ground for selection of the appropriate treatment protocol. Factors that are already used for risk stratification in AML patients due to their prognostic value are among others *FLT3-ITD*, wild type *NPM1*, high *ERG* expression, and mutations resulting in drug resistance [Langer et al., 2008]. Reports show, that microRNAs can also serve as such markers and allow assumptions about the general prognosis or indicate relapse and malignant progression [Marcucci et al., 2011; Weiss and Ito, 2018]. E.g. low expression levels of let-7 family members

are accompanied by increased expression of *LIN28* family members - their counterpart - and can serve as markers for poor prognosis in intestinal cancer [Weiss and Ito, 2018]. As aforementioned, miR-3151 can be used alone or together with *BAALC* as a prognostic marker for various endpoints in AML patients [Díaz-Beyá et al., 2015; Eisfeld et al., 2012, 2014; Langer et al., 2008; Weber et al., 2014]. Furthermore, other microRNAs such as miR-155 and miR-181, as well as miR-223*, can be used for the purpose of risk-stratification in AML [Eisfeld et al., 2012; Marcucci et al., 2013; Schwind et al., 2010; Weiss and Ito, 2018]. In AML, miR-223* (the functional 3'-strand of miR-223) expression correlates with other prognostic markers and high miR-223* expression is usually found in low-risk groups [Kuchenbauer et al., 2011; Weiss and Ito, 2018]. However, throughout different cancer entities there are inconsistent reports about the prognostic implication of a given microRNA. For example, when down regulated, miR-124-1 is associated with an unfavorable prognosis in solid tumors; in AML a comparatively lower expression of miR-124-1 is associated with a longer relapse-free interval - i.e. a better prognosis [Wang et al., 2014; xing Chen et al., 2014]. Thus, in CN it would be desirable to identify markers which (i) could predict the G-CSF response, and either hereby would allow early risk stratification towards malignant progression thus allow adapting the therapy towards early allogenic HSC transplantation or (ii) as for other malignant diseases, would be one indicating malignant progression or relapse. In this sense, it would be of interest to review and confirm existing markers for their suitability in CN/AML and to discover new ones.

As already proven, microRNA physiology bears therapeutic potential such as the antagonization of oncogenic microRNAs (oncomiRs) via antagonistic microRNAs (antagomiRs) or administration of tumorsuppressive microRNAs [Wallace and O'Connell, 2017; Weiss and Ito, 2018]. One of the most prominent samples comes from 'Miravirsen' an antagomiR against miR-122 in hepatitis caused by HCV. There, 'Miravirsen' was initially able to decrease the viral load in human [Van Der Ree et al., 2016; Wallace and O'Connell, 2017; Weiss and Ito, 2018]. As studies and clinical trials already demonstrated proof of principle, it is necessary to obtain more knowledge about the contribution of microRNAs to the pathomecha-

nisms underlying CN and its malignant progression. First steps could be to search for altered microRNA expression profiles - i.e. altered microRNA clusters - in CN or CN/AML patients and to compare the obtained data with data from healthy individuals and throughout the course of CN. Depending on the results, further points addressed could include, e.g. investigation of the impact of mutated *CSF3R* or *RUNX1* on microRNA expression profiles.

In summary, a deeper knowledge about the role of microRNA in CN could contribute to the understanding of the underlying pathomechanisms and eventually lead to diagnostic or therapeutic agents and strategies that could be applicable in CN, e.g. similar to initial effects of the antagomiR 'Miravirsen' in HCV [Van Der Ree et al., 2016].

# 5

# Summary

The underlying study is based on the research work published in Blood by Skokowa et al. in 2014. The authors postulated a unique mechanism of leukemogenesis in a group of patients suffering from congenital neutropenia (CN), a disease characterized by a low absolute neutrophil count and a high susceptibility of malignant progression to MDS or AML, which occurs in approximately 20 % of CN patients [Skokowa et al., 2014, 2017]. They found that, in approximately 70 % of CN/AML patients, in addition to the inherited CN-associated mutations (*e.g., ELANE, HAX1, GPT1* and *WAS*), the AML phenotype was observed when hematopoietic cell clones were positive for sporadic *RUNX1* mutations which were acquired after sporadic *CSF3R* mutations. The authors postulated cooperating leukemogenic effects of *RUNX1* and *CSF3R* mutations.

In this Doctoral Thesis, we re-analyzed the CN/AML patients' group investigated in 2014. Among those patients who underwent malignant transformation, we found hints of non-random distribution for sporadic missense (n = 7) and nonsense (n = 6) *RUNX1* mutations (Fisher's t-test: p = 0.0515) at AML stage. Furthermore, samples positive for missense *RUNX1* mutations were also positive for trisomy 21. This was not observed in samples positive for nonsense *RUNX1* mutations

(**table 3.1**).

Since *RUNX1* is located on chromosome 21, it was of special interest to test whether trisomy 21 resulted in an increase of the mutant or the wild-type *RUNX1* allelic fraction. Thus, we performed Sanger sequencing and digital PCR on samples of three selected CN/AML individuals all positive for missense *RUNX1* mutations and trisomy 21 (UniProtKB:Q01196, p.R139G, p.D171N, p.R174L) (**figures 3.1** to **3.6**). We were able to confirm an increase of mutant *RUNX1* allelic fraction over wild type *RUNX1* allelic fraction in a 2:1 ratio in all three patients. Hence, we showed that the occurrence of trisomy 21 was accompanied by an increase of the mutant *RUNX1* allele. Since in our patient cohort nonsense *RUNX1* mutations were not associated with trisomy 21, we concluded that this was due to different mechanisms of leukemogenic progression between both groups (**figure 4.1**). Furthermore, we established a chromatin immunoprecipitation assay using a RUNX1 antibody which allows the identification of binding patterns of different mutated RUNX1 proteins to DNA or to other proteins, interaction partners of RUNX1 protein in the future. This might contribute to the better understanding of the patho-mechanisms underlying the effects of different *RUNX1* mutations in leukemogenesis.

The second objective reported in this thesis, was to investigate the role of microRNAs in CN pathogenesis. MicroRNAs are small, approximately 22 nts long noncoding RNAs, which exert diverse biologic functions including the post- transcriptional control of mRNAs [Lee, 1993]. First, we established a workflow for the isolation and expression quantification of microRNAs in CN patients. We were able to isolate and quantify microRNA-125b and let-7b and aimed to investigate microRNA-3151 (**figures 3.11** to **3.14**). We observed that miR-125b expression levels were down-regulated upon myeloid differentiation from $CD34^+$ hematopoietic stem and progenitor cells to $CD33^+$ promyelocytic cells. Those findings were in line with previous reports [O'Connell et al., 2011; Rajasekhar et al., 2018; Shaham et al., 2012]. Interestingly, we could not detect significant differences in miR-125b expression levels between healthy donors and CN patients, neither in $CD34^+$ nor in $CD33^+$ cell populations. This was also true for miR-125b expression lev-

els in CN samples, when grouped according to their inherited mutations (*ELANE, HAX1, etc.*). Of note, miR-3151 expression was not detected in any of the samples; either because it is not expressed by the cells investigated or due to technical issues of the methods used. In this study, we successfully identified and quantified microRNAs, known to be relevant for hematopoiesis, for the first time in our patient cohort. However, due to the small sample size and the small number of microRNAs examined, further research in this field is required in order to finally draw significant conclusions about the role of microRNA in CN pathogenesis.

In summary, this study expands the understanding of leukemogenic progression in CN and provides valuable workflows for further investigation of the role of RUNX1 proteins as well as microRNA profiles in CN.

# 6

# Zusammenfassung

Die vorliegende Arbeit basiert auf einer in 2014 von Skokowa et al. in Blood veröffentlichten Studie. In dieser postulierten die Autoren einen einzigartigen Mechanismus der Leukämogenese bei Patienten mit kongenitaler Neutropenie (CN). CN ist eine Krankheit, die durch eine niedrige absolute Neutrophilenzahl gekennzeichnet ist und mit einer hohen malignen Progressionsrate zu MDS oder AML einhergeht. Eine maligne Progression tritt bei etwa 20 % der CN Patienten auf [Skokowa et al., 2014, 2017]. Die Autoren fanden heraus, dass in ca. 70 % der CN/AML Patienten der AML- Phänotyp auftrat, wenn die hämatopoetischen Stammzellen, zusätzlich zu den vererbten CN assoziierten Mutationen (beispielsweise *ELANE, HAX1, GPT1* und *WAS*), positiv für sporadische *CSF3R* Mutationen, gefolgt von sporadischen *RUNX1* Mutationen waren. Die Autoren postulierten, dass in diesen Patienten, kooperierende leukämogene Effekte von *RUNX1* und *CSF3R* Mutationen verantwortlich für die Leukämie-Entwicklung sind.

In der vorliegenden medizinischen Doktorarbeit analysierten wir die in 2014 untersuchte CN/AML Patientengruppe erneut. Unter den Patienten, die eine maligne Transformation haben, fanden wir Hinweise auf eine nicht-zufällige Verteilung sporadischer missense (n = 7) und nonsense (n = 6) *RUNX1* Mutationen in AML

Blasten (Fisher's t-Test: p = 0,0515) (**Tabelle 3.1**). Darüber hinaus waren Proben, die positiv für missense *RUNX1* Mutationen waren, auch positiv für Trisomie 21. Dies wurde bei Proben, die positiv für nonsense *RUNX1* Mutationen waren, nicht beobachtet. Da *RUNX1* auf Chromosom 21 kodiert ist, war es von besonderem Interesse zu untersuchen, ob hierbei Trisomie 21 zu einer Erhöhung der mutierten oder der wildtypischen *RUNX1* Allelfraktion führt. Daher führten wir eine Sanger-Sequenzierung und digitale PCR an Proben von drei ausgewählten CN/AML Individuen durch, die alle positiv für missense *RUNX1* Mutationen und Trisomie 21 waren (UniProtKB: Q01196, p.R139G, p.D171N, p.R174L) (**Abbildungen 3.1** bis **3.6**). Wir konnten eine Erhöhung der mutierten *RUNX1* Allelfraktion gegenüber der Wildtyp *RUNX1* Allelfraktion in einem Verhältnis von 2:1 in Proben aller drei Patienten bestätigen. Somit konnten wir zeigen, dass das Auftreten der Trisomie 21 mit einem Anstieg des mutierten *RUNX1* Allels einhergeht. Da in unserer Patientenkohorte nonsense *RUNX1* Mutationen nicht mit Trisomie 21 assoziiert waren, folgerten wir, dass dies auf unterschiedliche Mechanismen der Leukämogenese in beiden Gruppen zurückzuführen war (**Abbildung 4.1**). Darüber hinaus etablierten wir ein Verfahren zur Chromatin-Immunpräzipitation von RUNX1 mittels RUNX1-Antikörper, das in Zukunft die Analyse von Bindungsmustern verschieden mutierter RUNX1 Proteine an DNA, andere Proteine, RUNX1-Interaktionspartner, ermöglicht. Dies könnte zum besseren Verständnis der Pathomechanismen, die den verschiedenen *RUNX1* Mutationen in der Leukämogenese zugrunde liegen, beitragen.

Der zweite Gegenstand dieser Arbeit, ist die Untersuchung der Rolle von microRNAs in der CN Pathogenese. MicroRNAs sind kleine, ca. 22 nt lange nichtkodierende RNAs, die verschiedene biologische Funktionen ausüben, darunter die post-transkriptionelle Kontrolle von mRNA [Lee, 1993]. Zunächst etablierten wir einen experimentellen Arbeitsablauf zur Isolierung und Expressionsquantifizierung von microRNAs bei CN Patienten. Wir waren in der Lage, microRNA-125b und let-7b zu isolieren und zu quantifizieren, weiterhin zielten wir auf die Untersuchung von microRNA-3151 ab (**Abbildungen 3.11** bis **3.14**). Wir beobachteten, dass die Expression von miR-125b bei der myeloischen Differenzierung

von $CD34^+$ hämatopoietischen Stamm- und Progenitorzellen zu $CD33^+$ Promyelozyten herunter reguliert wurde. Diese Befunde stimmten mit früheren Berichten überein [O'Connell et al., 2011; Rajasekhar et al., 2018; Shaham et al., 2012]. Interessanterweise konnten wir keine signifikanten Unterschiede in den miR-125b Expressionslevel zwischen gesunden Spendern und CN Patienten feststellen, weder in $CD34^+$ noch in $CD33^+$ Zellpopulationen. Dies galt auch für die miR-125b Expressionslevel in CN Proben, wenn sie nach ihren vererbten Mutationen gruppiert wurden (*ELANE, HAX1, etc.*). Eine Expression von miR-3151 wurde in keiner der Proben nachgewiesen; entweder weil miR-3151 in den untersuchten Zellen nicht exprimiert wird oder ihre Expression auf Grund technischer Probleme der angewendeten Methoden nicht nachgewiesen werden konnte. In dieser Studie ist es uns erstmalig in unserer Patientenkohorte gelungen, für die Hämatopoiese relevante microRNAs zu identifizieren und zu quantifizieren. Aufgrund der geringen Stichprobengröße und der geringen Anzahl von untersuchten microRNAs ist jedoch weitere Forschung auf diesem Gebiet erforderlich, um letztendlich signifikante Schlussfolgerungen über die Rolle von microRNAs in der Pathogenese der CN ziehen zu können.

Zusammenfassend trägt diese Studie zum Verständnis der leukämogenen Progression bei CN Patienten bei. Zusätzlich liefert sie experimentelle Methoden für die künftige Untersuchung von RUNX1 Proteinen und die Erstellung von microRNA-Profilen in CN.

# 7 Appendix

## 7.1 Supplementary data

**Table 7.1: Ct-values obtained by means of qPCR for let-7b and miR-125b expression in CD33$^+$ cells**

All values depicted are Ct-values obtained by means of qPCR and were rounded to three decimal places. Standard deviation is depicted in the column following the mean microRNA expression and labeled St. Dev.

| Pat. ID | let-7b | St. Dev | miR-125b | St. Dev |
|---|---|---|---|---|
| HD12 | 30.997 | 0.176 | 32.07 | 0.235 |
| HD28 | 28.077 | 0.126 | 27.12 | 0.017 |
| HD30 | 27.233 | 0.061 | 26.513 | 0.021 |
| H1 | 34.67 | 0.912 | 30.91 | 0.096 |
| H3 | 28.82 | 0.242 | 31.72 | 0.168 |
| E1 | 27.577 | 0.159 | 30.757 | 0.015 |
| E2 | 32.667 | 0.518 | 29.263 | 0.035 |
| E4 | 27.877 | 0.081 | 28.307 | 0.101 |
| S1 | 28.687 | 0.042 | 29.15 | 0.03 |
| U1 | 25.597 | 0.032 | 29.72 | 0.026 |
| U2 | 30.06 | 0.082 | 29.917 | 0.083 |

**Table 7.2: Ct-values obtained by means of qPCR for let-7b and miR-125b expression in CD34$^+$ cells**

All values depicted are Ct-values obtained by means of qPCR and were rounded to three decimal places. Standard deviation is depicted in the column following the mean microRNA expression and labeled St. Dev.

| Pat. ID | let-7b | St. Dev | miR-125b | St. Dev |
|---|---|---|---|---|
| HD28 | 27.143 | 0.040 | 23.547 | 0.025 |
| HD29 | 27.773 | 0.131 | 22.493 | 0.025 |
| HD30 | 28.340 | 0.260 | 23.840 | 0.056 |
| HD31 | 28.697 | 0.050 | 24.630 | 0.010 |
| H4 | 30.837 | 0.129 | 29.460 | 0.026 |
| H5 | 28.063 | 0.146 | 23.683 | 0.038 |
| U1 | 27.893 | 0.085 | 25.550 | 0.026 |
| U2 | 32.910 | 0.286 | 22.080 | 0.078 |

**Table 7.3: Ct-values obtained by qPCR for let-7b and miR-125b from iPS derived cells from 'CN-AML pat. #14' and healthy donor**

All values depicted are Ct-values obtained by means of qPCR and were rounded to three decimal places. Standard deviation is depicted in the column following the mean microRNA expression and labeled St. Dev.

| Pat. ID | let-7b | St. Dev. | miR-125b | St. Dev. |
|---|---|---|---|---|
| HD hiPSC | 34.213 | 0.239 | 79.90 | 0.85 |
| CN-AML pat. #14 L8 hiPSC | 35.33 | 0.251 | 112.79 | 1.62 |
| CN-AML pat. #14 L10 hiPSC | 35.127 | 0.538 | 106.296 | 42.796 |

**Table 7.4: Expression analysis of miR-125b normalized to let-7b by means of $2^{-\Delta Ct}$-values for CD33$^+$ cells from healthy donors and CN patients**

All values depicted are $2^{-\Delta Ct}$-values (miR-125b expression - let-7b-expression) obtained by means of qPCR and were rounded to three decimal places. Standard deviation was calculated according to *'Guide to Performing Relative Quantitation of Gene Expression Using Real-Time Quantitative PCR'* by Applied Biosystems (US) [Applied Biosystems, 2008].

| Pat. ID | $2^{-\Delta Ct}$ | St. Dev. |
|---|---|---|
| HD12 | 0.475 | 0.294 |
| HD28 | 1.941 | 0.127 |
| HD30 | 1.647 | 0.065 |
| H1 | 0.206 | 0.336 |
| H2 | 13.548 | 0.917 |
| H3 | 0.134 | 0.295 |
| E1 | 0.110 | 0.160 |
| E2 | 10.580 | 0.519 |
| E4 | 0.742 | 0.129 |
| S1 | 0.725 | 0.051 |
| U1 | 0.057 | 0.042 |
| U2 | 1.104 | 0.117 |

**Table 7.5: Expression analysis of miR-125b normalized to let-7b by means of $2^{-\Delta Ct}$-values for $CD34^+$ cells from healthy donors and CN patients**

All values depicted are $2^{-\Delta Ct}$-values (miR-125b expression - let-7b-expression) obtained by means of qPCR and were rounded to three decimal places. Standard deviation was calculated according to *'Guide to Performing Relative Quantitation of Gene Expression Using Real-Time Quantitative PCR'* by Applied Biosystems (US) [Applied Biosystems, 2008].

| Pat. ID | $2^{-\Delta Ct}$ | St. Dev. |
|---|---|---|
| HD28 | 12.098 | 0.048 |
| HD29 | 38.854 | 0.133 |
| HD30 | 23.013 | 5.931 |
| HD31 | 16.757 | 0.051 |
| H4 | 2.597 | 0.132 |
| H5 | 20.821 | 0.151 |
| U1 | 5.074 | 0.089 |
| U2 | 1820.35 | 0.297 |

**Table 7.6: Analysis of relative microRNA-125b expression change upon differentiation from $CD34^+$ to $CD33^+$ cells in four samples**

All values depicted were obtained by means of qPCR and calculated according to $2^{-\Delta\Delta Ct}$ - method (miR-125b target; let-7b control; all values rounded to three decimal places) [Livak and Schmittgen, 2001]. Standard deviation ('St. Dev.') was calculated according to *'Guide to Performing Relative Quantitation of Gene Expression Using Real-Time Quantitative PCR'* by Applied Biosystems (US) [Applied Biosystems, 2008].

| Pat. ID | $2^{-\Delta\Delta Ct}$ | St. Dev. |
|---|---|---|
| HD28 | 0.160 | 0.048 |
| HD30 | 0.073 | 0.266 |
| U1 | 0.0006 | 0.297 |
| U2 | 0.011 | 0.089 |

**Table 7.7: Testing power for the down regulation of miR-125b upon differentiation from $CD34^+$ to $CD33^+$ cells**

Quantification of testing power and statistical significance for qPCR results of miR-125b expression profiling indicated statistical significance in un-paired one-tailed t-test which was confirmed by unpaired two-tailed t-testing after removal of outliers.

| **Unpaired t test HD28** | |
|---|---|
| P value | <0.0001 |
| P value summary | **** |
| Significantly different (P < 0.05)? | Yes |
| One- or two-tailed P value? | Two-tailed |
| t, df | t=40.49, df=4 |

| **Unpaired t test HD30** | |
|---|---|
| P value | 0.0009 |
| P value summary | *** |
| Significantly different (P < 0.05)? | Yes |
| One- or two-tailed P value? | Two-tailed |
| t, df | t=8.757, df=4 |

| **Unpaired t test U1** | |
|---|---|
| P value | 0.0009 |
| P value summary | *** |
| Significantly different (P < 0.05)? | Yes |
| One- or two-tailed P value? | Two-tailed |
| t, df | t=27.75, df=4 |

| **Unpaired t test U2** | |
|---|---|
| P value | 0.0011 |
| P value summary | ** |
| Significantly different (P < 0.05)? | Yes |
| One- or two-tailed P value? | Two-tailed |
| t, df | t=8.463, df=4 |

# 8 References


Almeida M. I., Reis R. M., and Calin G. A. MicroRNA history: Discovery, recent applications, and next frontiers. *Mutation Research - Fundamental and Molecular Mechanisms of Mutagenesis*, 717(1-2):1–8, dec 2011. ISSN 00275107. doi: 10.1016/j.mrfmmm.2011.03.009.

Álvarez-Errico D., Vento-Tormo R., Sieweke M., and Ballestar E. Epigenetic control of myeloid cell differentiation, identity and function. *Nature reviews. Immunology*, 15(1):7–17, 2015. ISSN 1474-1741. doi: 10.1038/nri3777.

Ambros V., Bartel B., Bartel D. P., Burge C. B., Carrington J. C., Chen X., Dreyfuss G., Eddy S. R., Griffiths-Jones S., Marshall M., Matzke M., Ruvkun G., and Tuschl T. A uniform system for microRNA annotation. *Rna*, 9(3):277–279, 2003. ISSN 13558382. doi: 10.1261/rna.2183803.

Applied Biosystems . Guide to Performing Relative Quantitation of Gene Expression Using Real-Time Quantitative PCR, 2008. URL `https://assets.thermofisher.com/TFS-Assets/LSG/manuals/cms{_}042380.pdf[Dateaccessed2020-01-02]`.

Aprikyan A. A., Kutyavin T., Stein S., Aprikian P., Rodger E., Liles W. C., Boxer L. A., and Dale D. C. Cellular and molecular abnormalities in severe congenital neutropenia predisposing to leukemia. *Experimental Hematology*, 31(5):372–381, 2003. ISSN 0301472X. doi: 10.1016/S0301-472X(03)00048-1.

Bartel D. P. Metazoan MicroRNAs. *Cell*, 173(1):20–51, 2018. ISSN 10974172. doi: 10.1016/j.cell.2018.03.006.

Baskerville S. and Bartel D. P. Microarray profiling of microRNAs reveals frequent coexpression with neighboring miRNAs and host genes. *Rna*, 11(3):241–247, 2005. ISSN 13558382. doi: 10.1261/rna.7240905.

Bateman A. UniProt: A worldwide hub of protein knowledge. *Nucleic Acids Research*, 47(D1):D506–D515, 2019. ISSN 13624962. doi: 10.1093/nar/gky1049.

Beekman R. and Touw I. P. G-CSF and its receptor in myeloid malignancy. *Blood*, 115(25):5131–5136, jun 2010. ISSN 00064971. doi: 10.1182/blood-2010-01-234120.

Bellanné-Chantelot C., Clauin S., Leblanc T., Cassinat B., Rodrigues-Lima F., Beaufils S., Vaury C., Barkaoui M., Fenneteau O., Maier-Redelsperger M., Chomienne C., and Donadieu J. Mutations in the ELA2 gene correlate with more severe expression of neutropenia: A study of 81 patients from the French Neutropenia Register. *Blood*, 103(11):4119–4125, jun 2004. ISSN 00064971. doi: 10.1182/blood-2003-10-3518.

Bellissimo D. C. and Speck N. A. RUNX1 Mutations in Inherited and Sporadic Leukemia. *Frontiers in Cell and Developmental Biology*, 5, dec 2017. ISSN 2296-634X. doi: 10.3389/fcell.2017.00111.

Béri-Dexheimer M., Latger-Cannard V., Philippe C., Bonnet C., Chambon P., Roth V., Grégoire M. J., Bordigoni P., Lecompte T., Leheup B., and Jonveaux P. Clinical phenotype of germline RUNX1 haploinsufficiency: From point mutations to large genomic deletions. *European Journal of Human Genetics*, 16(8): 1014–1018, 2008. ISSN 10184813. doi: 10.1038/ejhg.2008.89.

Berman J. N. and Look A. T. Pediatric Myeloid Leukemia, Myelodysplasia, and Myeloproliferative Disease. In Orkin S. H., Fisher D. E., Look A. T., Lux S. E. I., Ginsburg D., and Nathan D. G., editors, *Nathan and Oski's Hematology and Oncology of Infancy and Childhood*, pages 1555–1613. Elsevier/Saunders, 8 edition, 2015. ISBN 9788578110796.

Bione S., D'Adamo P., Maestrini E., Gedeon A. K., Bolhuis P. A., and Toniolo D. A novel X-linked gene, G4.5. is responsible for Barth syndrome. *Nature Genetics*, 12(4):385–389, 1996. ISSN 10614036. doi: 10.1038/ng0496-385.

Blumenthal E., Greenblatt S., Huang G., Ando K., Xu Y., and Nimer S. D. Covalent modifications of RUNX proteins: Structure affects function. In Groner Y., Liu P., Speck N. A., Ito Y., Neil J. C., and Wijnen van A., editors, *Advances in Experimental Medicine and Biology*, volume 962, pages 33–44. Springer Nature Singa-

pore Pte Ltd., 2017. ISBN 978-981-10-3231-8. doi: 10.1007/978-981-10-3233-2_3.

Bonifer C., Levantini E., Kouskoff V., and Lacaud G. Runx1 structure and function in blood cell development. In Groner Y., Liu P., Speck N. A., Ito Y., Neil J. C., and Wijnen van A., editors, *Advances in Experimental Medicine and Biology*, volume 962, pages 65–81. Springer Nature Singapore Pte Ltd., 2017. doi: 10.1007/978-981-10-3233-2_5.

Bousquet M., Quelen C., Rosati R., Mas V. M. D., Starza R. L., Bastard C., Lippert E., Talmant P., Lafage-Pochitaloff M., Leroux D., Gervais C., Viguié F., Lai J. L., Terre C., Beverlo B., Sambani C., Hagemeijer A., Marynen P., Delsol G., Dastugue N., Mecucci C., and Brousset P. Myeloid cell differentiation arrest by miR-125b-1 in myelodysplasic syndrome and acute myeloid leukemia with the t(2;11)(p21;q23) translocation. *Journal of Experimental Medicine*, 205(11): 2499–2506, 2008. ISSN 00221007. doi: 10.1084/jem.20080285.

Bousquet M., Harris M. H., Zhou B., and Lodish H. F. MicroRNA miR-125b causes leukemia. *Proceedings of the National Academy of Sciences of the United States of America*, 107(50):21558–21563, 2010. ISSN 00278424. doi: 10.1073/pnas.1016611107.

Boxer L. A. How to approach neutropenia. *Hematology / the Education Program of the American Society of Hematology. American Society of Hematology. Education Program*, 2012:174–182, 2012. ISSN 15204383. doi: 10.1182/asheducation.v2012.1.174.3798251.

Boxer L. A., Stein S., Buckley D., Bolyard A. A., and Dale D. C. Strong evidence for autosomal dominant inheritance of severe congenital neutropenia associated with ELA2 Mutations. *Journal of Pediatrics*, 148(5):633–636, may 2006. ISSN 00223476. doi: 10.1016/j.jpeds.2005.12.029.

Boztug K., Appaswamy G., Ashikov A., Schäffer A. A., Salzer U., Diestelhorst J., Germeshausen M., Brandes G., Lee-Gossler J., Noyan F., Gatzke A.-K., Minkov M., Greil J., Kratz C., Petropoulou T., Pellier I., Bellanné-Chantelot C., Rezaei N., Mönkemöller K., Irani-Hakimeh N., Bakker H., Gerardy-Schahn R., Zeidler C., Grimbacher B., Welte K., and Klein C. A Syndrome with Congenital Neutropenia and Mutations in G6PC3. *New England Journal of Medicine*, 360(1):32–43, jan 2008. ISSN 0028-4793. doi: 10.1056/nejmoa0805051.

Bradley T. R. and Metcalf D. The growth of mouse bone marrow cells in vitro. *The Australian journal of experimental biology and medical science*, 44(3):287–99, 1966. ISSN 0004-945X. doi: 10.1038/icb.1966.28.

Brinkmann V. and Zychlinsky A. Neutrophil extracellular traps: Is immunity the second function of chromatin? *Journal of Cell Biology*, 198(5):773–783, 2012. ISSN 00219525. doi: 10.1083/jcb.201203170.

Budak H., Bulut R., Kantar M., and Alptekin B. MicroRNA nomenclature and the need for a revised naming prescription. *Briefings in Functional Genomics*, 15(1): 65–71, jul 2016. ISSN 20412657. doi: 10.1093/bfgp/elv026.

Cammenga J., Niebuhr B., Horn S., Bergholz U., Putz G., Buchholz F., Löhler J., and Stocking C. RUNX1 DNA-binding mutants, associated with minimally differentiated acute myelogenous leukemia, disrupt myeloid differentiation. *Cancer Research*, 67(2):537–545, jan 2007. ISSN 00085472. doi: 10.1158/0008-5472.CAN-06-1903.

Cantor A. B. Myeloid proliferations associated with Down syndrome. *Journal of Hematopathology*, 8(3):169–176, 2015. ISSN 18655785. doi: 10.1007/s12308-014-0225-0.

Chao J. R., Parganas E., Boyd K., Hong C. Y., Opferman J. T., and Ihle J. N. Hax1-mediated processing of HtrA2 by Parl allows survival of lymphocytes and neurons. *Nature*, 452(7183):98–102, 2008. ISSN 14764687. doi: 10.1038/nature06604.

Chaudhuri A. A., So A. Y. L., Mehta A., Minisandram A., Sinha N., Jonsson V. D., Rao D. S., O'Connell R. M., and Baltimore D. Oncomir miR-125b regulates hematopoiesis by targeting the gene Lin28A. *Proceedings of the National Academy of Sciences of the United States of America*, 109(11):4233–4238, 2012. ISSN 00278424. doi: 10.1073/pnas.1200677109.

Chen C. Z., Li L., Lodish H. F., and Bartel D. P. MicroRNAs Modulate Hematopoietic Lineage Differentiation. *Science*, 303(5654):83–86, jan 2004. ISSN 00368075. doi: 10.1126/science.1091903.

Chen P., Liao K., and Xiao C. MicroRNA says no to mass production. *Nature Immunology*, 19(10):1040–1042, 2018. ISSN 15292916. doi: 10.1038/s41590-018-0215-y.

Chin D. W., Sakurai M., Nah G. S., Du L., Jacob B., Yokomizo T., Matsumura T., Suda T., Huang G., Fu X. Y., Ito Y., Nakajima H., and Osato M. RUNX1

haploinsufficiency results in granulocyte colony-stimulating factor hypersensitivity. *Blood Cancer Journal*, 6(November 2015), 2016. ISSN 20445385. doi: 10.1038/bcj.2015.105.

Christiansen D. H., Andersen M. K., and Pedersen-Bjergaard J. Mutations of AML1 are common in therapy-related myelodysplasia following therapy with alkylating agents and are significantly associated with deletion or loss of chromosome arm 7q and with subsequent leukemic transformation. *Blood*, 104(5):1474–1481, 2004. ISSN 00064971. doi: 10.1182/blood-2004-02-0754.

Chuang L. S. H., Ito K., and Ito Y. RUNX family: Regulation and diversification of roles through interacting proteins. *International Journal of Cancer*, 132(6): 1260–1271, 2013. ISSN 00207136. doi: 10.1002/ijc.27964.

Ciau-Uitz A., Wang L., Patient R., and Liu F. ETS transcription factors in hematopoietic stem cell development. *Blood Cells, Molecules, and Diseases*, 51(4):248–255, dec 2013. ISSN 10799796. doi: 10.1016/j.bcmd.2013.07.010.

Collins J. and Dokal I. Inherited bone marrow failure syndromes. In Orkin S. H., Fisher D. E., Ginsburg D., Look A. T., Lux S. E., and Nathan D. G., editors, *Hematology*, volume 20, chapter 7, pages 433–434. Elsevier/Saunders, 2015. ISBN 9788578110796. doi: 10.1179/1024533215z.000000000381.

Covaris . PROTOCOL truChIP™ Chromatin Shearing Kit, 2016. URL `http://covarisinc.com/wp-content/uploads/pn{_}`010179`.pdf[lastaccess`2017/09/01`]`.

Crane G. M., Jeffery E., and Morrison S. J. Adult haematopoietic stem cell niches. *Nature Reviews Immunology*, 17(9):573–590, jun 2017. ISSN 14741741. doi: 10.1038/nri.2017.53.

Dale D. C. The discovery, development and clinical applications of granulocyte colony-stimulating factor. *Transactions of the American Clinical and Climatological Association*, 109:27–38, 1998. ISSN 0065-7778.

Dale D. C. and Welte K. Cyclic and chronic neutropenia. *Cancer Treatment and Research*, 157:97–108, 2011. ISSN 09273042. doi: 10.1007/978-1-4419-7073-2_6.

Dannenmann B., Zahabi A., Mir P., Oswald B., Bernhard R., Klimiankou M., Morishima T., Schulze-Osthoff K., Zeidler C., Kanz L., Lachmann N., Moritz T., Welte K., and Skokowa J. Human iPSC-based model of severe congenital neutropenia reveals elevated UPR and DNA damage in CD34 + cells preceding leukemic

transformation. *Experimental Hematology*, 71:51–60, 2019. ISSN 18732399. doi: 10.1016/j.exphem.2018.12.006.

Bruijn de M. and Dzierzak E. Runx transcription factors in the development and function of the definitive hematopoietic system. *Blood*, 129(15):2061–2069, 2017. ISSN 1528-0020. doi: 10.1182/blood-2016-12-689109.

De Haan G. and Lazare S. S. Aging of hematopoietic stem cells. *Blood*, 131(5): 479–487, 2018. ISSN 15280020. doi: 10.1182/blood-2017-06-746412.

Díaz-Beyá M., Brunet S., Nomdedéu J., Cordeiro A., Tormo M., Escoda L., Ribera J. M., Arnan M., Heras I., Gallardo D., Bargay J., Queipo De Llano M. P., Salamero O., Martí J. M., Sampol A., Pedro C., Hoyos M., Pratcorona M., Castellano J. J., Nomdedeu M., Risueño R. M., Sierra J., Monzó M., Navarro A., and Esteve J. The expression level of BAALC-associated microRNA miR-3151 is an independent prognostic factor in younger patients with cytogenetic intermediate-risk acute myeloid leukemia. *Blood Cancer Journal*, 5:e352, 2015. ISSN 20445385. doi: 10.1038/bcj.2015.76.

Dinauer M. C., Newburger P. E., and Borregaard N. Phagocyte system and disorders of granulopoiesis and granulocyte function. In Orkin S. H., Fisher D. E., Ginsburg D., Look A. T., Lux S. E., and Nathan D. G., editors, *Nathan and Oski´s hematology and oncology of infancy and childhood*, chapter 22, pages 773–847. Elsevier/Saunders, 8 edition, 2015. ISBN 9788578110796.

Donadieu J., Beaupain B., Mahlaoui N., and Bellanné-Chantelot C. Epidemiology of Congenital Neutropenia. *Hematology/Oncology Clinics of North America*, 27 (1):1–17, feb 2013. ISSN 08898588. doi: 10.1016/j.hoc.2012.11.003.

Dong F. and Larner A. C. Activation of Akt kinase by granulocyte colony-stimulating factor (G- CSF): Evidence for the role of a tyrosine kinase activity distinct from the janus kinases. *Blood*, 95(5):1656–1662, 2000. ISSN 00064971. doi: 10.1182/blood.v95.5.1656.005k29_1656_1662.

Dong F., Buitenen van C., Pouwels K., Hoefsloot L. H., Löwenberg B., and Touw I. P. Distinct cytoplasmic regions of the human granulocyte colony-stimulating factor receptor involved in induction of proliferation and maturation. *Molecular and Cellular Biology*, 13(12):7774–7781, 1993. ISSN 0270-7306. doi: 10.1128/mcb.13.12.7774.

Dong F., Hoefsloot L. H., Schelen A. M., Broeders L. C., Meijer Y., Veerman A. J., Touw I. P., and Lowenberg B. Identification of a nonsense mutation in the

granulocyte-colony- stimulating factor receptor in severe congenital neutropenia. *Proceedings of the National Academy of Sciences of the United States of America*, 91(10):4480–4484, 1994. ISSN 00278424. doi: 10.1073/pnas.91.10.4480.

Dong F., Brynes R. K., Tidow N., Welte K., Löwenberg B., and Touw I. P. Mutations in the Gene for the Granulocyte Colony-Stimulating–Factor Receptor in Patients With Acute Myeloid Leukemia Preceded By Severe Congenital Neutropenia. *New England Journal of Medicine*, 333(8):487 – 493, 1995. doi: 10.1056/NEJM199508243330804.

Dong F., Larner A., Grimley P. M., Liu X., Henninghausen L., De Koning J. P., and Touw I. P. Stimulation of Stat5 by granulocyte colony-stimulating factor (G-CSF) is modulated by two distinct cytoplasmic regions of the G-CSF receptor. *Journal of Immunology*, 161(12):6503–6509, 1998. ISSN 0022-1767.

Doulatov S., Notta F., Laurenti E., and Dick J. E. Hematopoiesis: A human perspective. *Cell Stem Cell*, 10(2):120–136, 2012. ISSN 19345909. doi: 10.1016/j.stem.2012.01.006.

Down J. L. Observations on an ethnic classification of idiots. *London Hospital Reports*, 3:259–262, feb 1866. ISSN 0047-6765.

Drissen R., Buza-Vidas N., Woll P., Thongjuea S., Gambardella A., Giustacchini A., Mancini E., Zriwil A., Lutteropp M., Grover A., Mead A., Sitnicka E., Jacobsen S. E. W., and Nerlov C. Distinct myeloid progenitor–differentiation pathways identified through single-cell RNA sequencing. *Nature Immunology*, 17(6):666–676, 2016. ISSN 1529-2908. doi: 10.1038/ni.3412.

Drury R. E., O'Connor D., and Pollard A. J. The clinical application of MicroRNAs in infectious disease. *Frontiers in Immunology*, 8(SEP), sep 2017. ISSN 16643224. doi: 10.3389/fimmu.2017.01182.

Dwivedi P. and Greis K. D. Granulocyte colony-stimulating factor receptor signaling in severe congenital neutropenia, chronic neutrophilic leukemia, and related malignancies. *Experimental Hematology*, 46:9–20, 2017. ISSN 18732399. doi: 10.1016/j.exphem.2016.10.008.

Eisfeld A. K., Marcucci G., Maharry K., Schwind S., Radmacher M. D., Nicolet D., Becker H., Mrózek K., Whitman S. P., Metzeler K. H., Mendler J. H., Wu Y. Z., Liyanarachchi S., Patel R., Baer M. R., Powell B. L., Carter T. H., Moore J. O., Kolitz J. E., Wetzler M., Caligiuri M. A., Larson R. A., Tanner S. M., De La Chapelle A., and Bloomfield C. D. miR-3151 interplays with its host gene

BAALC and independently affects outcome of patients with cytogenetically normal acute myeloid leukemia. *Blood*, 120(2):249–258, 2012. ISSN 00064971. doi: 10.1182/blood-2012-02-408492.

Eisfeld A. K., Schwind S., Patel R., Huang X., Santhanam R., Walker C. J., Markowitz J., Hoag K. W., Jarvinen T. M., Leffel B., Perrotti D., Carson W. E., Marcucci G., Bloomfield C. D., and De La Chapelle A. Intronic miR-3151 within BAALC drives leukemogenesis by deregulating the TP53 pathway. *Science Signaling*, 7(321):ra36, apr 2014. ISSN 19379145. doi: 10.1126/scisignal.2004762.

Emmrich S., Rasche M., Schöning J., Reimer C., Keihani S., Maroz A., Xie Y., Li Z., Schambach A., Reinhardt D., and Klusmann J. H. miR-99a/100~125b tricistrons regulate hematopoietic stem and progenitor cell homeostasis by shifting the balance between TGF$\beta$ and Wnt signaling. *Genes and Development*, 28(8): 858–874, apr 2014. ISSN 15495477. doi: 10.1101/gad.233791.113.

Emmrich S., Engeland F., El-Khatib M., Henke K., Obulkasim A., Schöning J., Katsman-Kuipers J. E., Michel Zwaan C., Pich A., Stary J., Baruchel A., Haas de V., Reinhardt D., Fornerod M., Heuvel-Eibrink van den M. M., and Klusmann J. H. miR-139-5p controls translation in myeloid leukemia through EIF4G2. *Oncogene*, 35(14):1822–1831, apr 2015. ISSN 1476-5594. doi: 10.1038/onc.2015.247.

Faridani O. R., Abdullayev I., Hagemann-Jensen M., Schell J. P., Lanner F., and Sandberg R. Single-cell sequencing of the small-RNA transcriptome. *Nature Biotechnology*, 34(12):1264–1266, dec 2016. ISSN 15461696. doi: 10.1038/nbt.3701.

Fazi F., Rosa A., Fatica A., Gelmetti V., De Marchis M. L., Nervi C., and Bozzoni I. A minicircuitry comprised of microRNA-223 and transcription factors NFI-A and C/EBP$\alpha$ regulates human granulopoiesis. *Cell*, 123(5):819–831, 2005. ISSN 00928674. doi: 10.1016/j.cell.2005.09.023.

Friedman A. D. Transcriptional control of granulocyte and monocyte development. *Oncogene*, 26(47):6816–6828, oct 2007. ISSN 0950-9232. doi: 10.1038/sj.onc.1210764.

Friedman A. D. Cell cycle and developmental control of hematopoiesis by Runx1. *Journal of Cellular Physiology*, 219(3):520–524, jun 2009. ISSN 00219541. doi: 10.1002/jcp.21738.

Fukao T., Fukuda Y., Kiga K., Sharif J., Hino K., Enomoto Y., Kawamura A., Nakamura K., Takeuchi T., and Tanabe M. An Evolutionarily Conserved Mechanism for MicroRNA-223 Expression Revealed by MicroRNA Gene Profiling. *Cell*, 129(3):617–631, 2007. ISSN 00928674. doi: 10.1016/j.cell.2007.02.048.

Gardini A., Cesaroni M., Luzi L., Okumura A. J., Biggs J. R., Minardi S. P., Venturini E., Zhang D. E., Pelicci P. G., and Alcalay M. AML1/ETO oncoprotein is directed to AML1 binding regions and co-localizes with AML1 and HEB on its targets. *PLoS Genetics*, 4(11):e1000275, nov 2008. ISSN 15537390. doi: 10.1371/journal.pgen.1000275.

Germeshausen M., Grudzien M., Zeidler C., Abdollahpour H., Yetgin S., Rezaei N., Ballmaier M., Grimbacher B., Welte K., and Klein C. Novel HAX1 mutations in patients with severe congenital neutropenia reveal isoform-dependent genotype-phenotype associations. *Blood*, 111(10):4954–4957, 2008. ISSN 00064971. doi: 10.1182/blood-2007-11-120667.

Germeshausen M., Zeidler C., Stuhrmann M., Lanciotti M., Ballmaier M., and Welte K. Digenic mutations in severe congenital neutropenia. *Haematologica*, 95(7):1207–1210, 2010. ISSN 15928721. doi: 10.3324/haematol.2009.017665.

Germeshausen M., Deerberg S., Peter Y., Reimer C., Kratz C. P., and Ballmaier M. The Spectrum of ELANE Mutations and their Implications in Severe Congenital and Cyclic Neutropenia. *Human Mutation*, 34(6):905–914, jun 2013. ISSN 10597794. doi: 10.1002/humu.22308.

Gerrits A., Walasek M. A., Olthof S., Weersing E., Ritsema M., Zwart E., Van Os R., Bystrykh L. V., and De Haan G. Genetic screen identifies microRNA cluster 99b/let-7e/125a as a regulator of primitive hematopoietic cells. *Blood*, 119(2): 377–387, 2012. ISSN 00064971. doi: 10.1182/blood-2011-01-331686.

Ghemlas I., Li H., Zlateska B., Klaassen R., Fernandez C. V., Yanofsky R. A., Wu J., Pastore Y., Silva M., Lipton J. H., Brossard J., Michon B., Abish S., Steele M., Sinha R., Belletrutti M., Breakey V. R., Jardine L., Goodyear L., Sung L., Dhanraj S., Reble E., Wagner A., Beyene J., Ray P., Meyn S., Cada M., and Dror Y. Improving diagnostic precision, care and syndrome definitions using comprehensive next-generation sequencing for the inherited bone marrow failure syndromes. *Journal of Medical Genetics*, 52(9):575–584, 2015. ISSN 14686244. doi: 10.1136/jmedgenet-2015-103270.

Gibson C. and Berliner N. How we evaluate and treat neutropenia in adults. *Blood*, 124(8):1251–1258, 2014. ISSN 15280020. doi: 10.1182/blood-2014-02-482612.

Gilliland D. G., Jordan C. T., and Felix C. A. The molecular basis of leukemia. *Hematology / the Education Program of the American Society of Hematology. American Society of Hematology. Education Program*, pages 80–97, 2004. ISSN 15204391. doi: 10.1182/asheducation-2004.1.80.

Gilman P. A., Jackson D. P., and Guild H. G. Congenital Agranulocytosis: Prolonged Survival and Terminal Acute Leukemia. *Blood*, 36(5):576 – 585, 1970.

Gits J., Leeuwen van D., Carroll H. P., Touw I. P., and Ward A. C. Multiple pathways contribute to the hyperproliferative responses from truncated granulocyte colony-stimulating factor receptors. *Leukemia*, 20(12):2111–2118, 2006. ISSN 14765551. doi: 10.1038/sj.leu.2404448.

Grenda D. S., Johnson S. E., Mayer J. R., McLemore M. L., Benson K. F., Horwitz M., and Link D. C. Mice expressing a neutrophil elastase mutation derived from patients with severe congenital neutropenia have normal granulopoiesis. *Blood*, 100(9):3221–3228, 2002. ISSN 00064971. doi: 10.1182/blood-2002-05-1372.

Grenda D. S., Murakami M., Ghatak J., Xia J., Boxer L. A., Dale D., Dinauer M. C., and Link D. C. Mutations of the ELA2 gene found in patients with severe congenital neutropenia induce the unfolded protein response and cellular apoptosis. *Blood*, 110(13):4179–4187, 2007. ISSN 00064971. doi: 10.1182/blood-2006-11-057299.

Griffiths-Jones S. miRBase: microRNA sequences, targets and gene nomenclature. *Nucleic Acids Research*, 34(90001):D140–D144, 2005. ISSN 0305-1048. doi: 10.1093/nar/gkj112.

Gupta K., Kuznetsova I., Klimenkova O., Klimiankou M., Meyer J., Moore M. A., Zeidler C., Welte K., and Skokowa J. Bortezomib inhibits STAT5-dependent degradation of LEF-1, inducing granulocytic differentiation in congenital neutropenia CD34 + cells. *Blood*, 123(16):2550–2561, 2014. ISSN 15280020. doi: 10.1182/blood-2012-09-456889.

Ha M. and Kim V. N. Regulation of microRNA biogenesis. *Nature reviews. Molecular cell biology*, 15(8):509–524, jul 2014. ISSN 1471-0080. doi: 10.1038/nrm3838.

Haferlach T., Stengel A., Eckstein S., Perglerová K., Alpermann T., Kern W., Haferlach C., and Meggendorfer M. The new provisional WHO entity 'RUNX1 mutated AML' shows specific genetics but no prognostic influence of dysplasia. *Leukemia*, 30(10):2109–2112, 2016. ISSN 0887-6924. doi: 10.1038/leu.2016.150.

Harada H., Harada Y., Tanaka H., Kimura A., and Inaba T. Implications of somatic mutations in the AML1 gene in radiation-associated and therapy-related myelodysplastic syndrome/acute myeloid leukemia. *Blood*, 101(2):673–680, 2003. ISSN 00064971. doi: 10.1182/blood-2002-04-1010.

Harada Y. and Harada H. Molecular pathways mediating MDS/AML with focus on AML1/RUNX1 point mutations. *Journal of Cellular Physiology*, 220(1):16–20, 2009. ISSN 00219541. doi: 10.1002/jcp.21769.

Hermans M. H., Antonissen C., Ward A. C., Mayen A. E., Ploemacher R. E., and Touw I. P. Sustained receptor activation and hyperproliferation in response to granulocyte colony-stimulating factor (G-CSF) in mice with a severe congenital neutropenia/acute myeloid leukemia-derived mutation in the G-CSF receptor gene. *Journal of Experimental Medicine*, 189(4):683–691, 1999. ISSN 00221007. doi: 10.1084/jem.189.4.683.

Herold G. Erkrankungen der weißen Blutzellen und der blutbildenen Organe. In Herold G., editor, *Innere Medizin : eine vorlesungsorientierte Darstellung : unter Berücksichtigung des Gegenstandskataloges für die Ärztliche Prüfung : mit ICD 10-Schlüssel im Text und Stichwortverzeichnis*, pages 63 – 73. Herold, 2016. ISBN 9783981466058.

Höck J. and Meister G. The Argonaute protein family. *Genome Biology*, 9(2): 210, 2008. ISSN 14747596. doi: 10.1186/gb-2008-9-2-210.

Horwitz M. S., Duan Z., Korkmaz B., Lee H. H., Mealiffe M. E., and Salipante S. J. Neutrophil elastase in cyclic and severe congenital neutropenia. *Blood*, 109(5): 1817–1824, 2007. ISSN 00064971. doi: 10.1182/blood-2006-08-019166.

Hug B. A., Ahmed N., Robbins J. A., and Lazar M. A. A Chromatin Immunoprecipitation Screen Reveals Protein Kinase C$\beta$ as a Direct RUNX1 Target Gene. *Journal of Biological Chemistry*, 279(2):825–830, jan 2004. ISSN 00219258. doi: 10.1074/jbc.M309524200.

Hughes S. and Woollard A. RUNX in invertebrates. In Groner Y., Liu P., Speck N. A., Ito Y., Neil J. C., and Wijnen van A., editors, *Advances in Experimental Medicine and Biology*, volume 962, pages 3–18. Springer Nature Singapore Pte Ltd., 2017. doi: 10.1007/978-981-10-3233-2_1.

Human Protein Atlas . www.proteinatlas.org, 2018. URL https://www.proteinatlas.org/ENSG00000115705-TPO/tissue[Zugriff05.11.2018].

Human Protein Atlas . proteinatlas.org - RUNX1, 2019. URL https://www.proteinatlas.org/ENSG00000159216-RUNX1/cell[Zugriff05.11.2018].

Hunter M. G. and Avalos B. R. Granulocyte colony-stimulating factor receptor mutations in severe congenital neutropenia transforming to acute myelogenous leukemia confer resistance to apoptosis and enhance cell survival. *Blood*, 95(6): 2132–2137, 2000. ISSN 00064971. doi: 10.1182/blood.v95.6.2132.

Hyde R. K., Liu P., and Friedman A. D. RUNX1 and CBF$\beta$ mutations and activities of their wild-type alleles in AML. In Groner Y., Liu P., Speck N. A., Ito Y., Neil J. C., and Wijnen van A., editors, *Advances in Experimental Medicine and Biology*, volume 962, chapter 17, pages 265–282. Springer Nature Singapore Pte Ltd., 2017. doi: 10.1007/978-981-10-3233-2_17.

Illendula A., Pulikkan J. A., Zong H., Grembecka J., Xue L., Sen S., Zhou Y., Boulton A., Kuntimaddi A., Gao Y., Rajewski R. A., Guzman M. L., Castilla L. H., and Bushweller J. H. A small-molecule inhibitor of the aberrant transcription factor CBF$\beta$-SMMHC delays leukemia in mice. *Science*, 347(6223):779–784, 2015. ISSN 10959203. doi: 10.1126/science.aaa0314.

Imai Y., Kurokawa M., Izutsu K., Hangaishi A., Takeuchi K., Maki K., Ogawa S., Chiba S., Mitani K., and Hirai H. Mutations of the AML1 gene in myelodysplastic syndrome and their functional implications in leukemogenesis. *Blood*, 96(9): 3154–60, nov 2000. ISSN 0006-4971.

Izraeli S. Perspective: Chromosomal aneuploidy in leukemia - Lessons from Down Syndrome. *Hematological Oncology*, 24(1):3–6, 2006. ISSN 02780232. doi: 10.1002/hon.758.

Jacobson L. O. and Marks E. K. The role of the spleen in radiation injury. *Proceedings of the Society for Experimental Biology and Medicine. Society for Experimental Biology and Medicine (New York, N.Y.)*, 70(4):740–2, apr 1949. ISSN 0037-9727.

Johnnidis J. B., Harris M. H., Wheeler R. T., Stehling-Sun S., Lam M. H., Kirak O., Brummelkamp T. R., Fleming M. D., and Camargo F. D. Regulation of progenitor cell proliferation and granulocyte function by microRNA-223. *Nature*, 451(7182): 1125–1129, 2008. ISSN 14764687. doi: 10.1038/nature06607.

Jonas S. and Izaurralde E. Towards a molecular understanding of microRNA-mediated gene silencing. *Nature Reviews Genetics*, 16(7):421–433, jun 2015. ISSN 1471-0056. doi: 10.1038/nrg3965.

Kalra R., Dale D., Freedman M., Bonilla M. A., Weinblatt M., Ganser A., Bowman P., Abish S., Priest J., Oseas R. S., Olson K., Paderanga D., and Shannon K. Monosomy 7 and activating RAS mutations accompany malignant transformation in patients with congenital neutropenia. *Blood*, 86(12):4579–86, 1995. ISSN 0006-4971.

Karamitros D., Stoilova B., Aboukhalil Z., Hamey F., Reinisch A., Samitsch M., Quek L., Otto G., Repapi E., Doondeea J., Usukhbayar B., Calvo J., Taylor S., Goardon N., Six E., Pflumio F., Porcher C., Majeti R., Göttgens B., and Vyas P. Single-cell analysis reveals the continuum of human lympho-myeloid progenitor cells article. *Nature Immunology*, 19(1):85–97, 2018. ISSN 15292916. doi: 10.1038/s41590-017-0001-2.

Kent W., Sugnet C., Furey T., Roskin K., Pringle T., Zahler A., and Haussler D. The human genome browser at UCSC, 2002a. URL https://genome.ucsc.edu/cgi-bin/hgTracks?db=hg38{&}lastVirtModeType=default{&}lastVirtModeExtraState={&}virtModeType=default{&}virtMode=0{&}nonVirtPosition={&}position=chr1{%}3A24906620-24906877{&}hgsid=720347639{_}EJMzaGREyTqsBPQHpt9TjHUaGZ2G[lastaccessed:04/08/2019].

Kent W., Sugnet C., Furey T., Roskin K., Pringle T., Zahler A., and Haussler D. The human genome browser at UCSC, 2002b. URL https://genome.ucsc.edu/cgi-bin/hgTracks?db=hg38{&}lastVirtModeType=default{&}lastVirtModeExtraState={&}virtModeType=default{&}virtMode=0{&}nonVirtPosition={&}position=chr1{%}3A24965034-24965183{&}hgsid=720351789{_}ZOvxJH48O8PyHoduUVnfYkBwmXJN[lastaccessed:04/10/2019].

Klein C., Grudzien M., Appaswamy G., Germeshausen M., Sandrock I., Schäffer A. A., Rathinam C., Boztug K., Schwinzer B., Rezaei N., Bohn G., Melin M., Carlsson G., Fadeel B., Dahl N., Palmblad J., Henter J. I., Zeidler C., Grimbacher B., and Welte K. HAX1 deficiency causes autosomal recessive severe congenital neutropenia (Kostmann disease). *Nature Genetics*, 39(1):86–92, 2007. ISSN 10614036. doi: 10.1038/ng1940.

Klimiankou M., Mellor-Heineke S., Klimenkova O., Reinel E., Uenalan M., Kandabarau S., Skokowa J., Welte K., and Zeidler C. Two cases of cyclic neutropenia

with acquired CSF3R mutations, with 1 developing AML. *Blood*, 127(21):2638–2641, 2016a. ISSN 15280020. doi: 10.1182/blood-2015-12-685784.

Klimiankou M., Mellor-Heineke S., Zeidler C., Welte K., and Skokowa J. Role of CSF3R mutations in the pathomechanism of congenital neutropenia and secondary acute myeloid leukemia. *Annals of the New York Academy of Sciences*, 1370(1):119–125, 2016b. ISSN 17496632. doi: 10.1111/nyas.13097.

Klusmann J. H., Li Z., Böhmer K., Maroz A., Koch M. L., Emmrich S., Godinho F. J., Orkin S. H., and Reinhardt D. miR-125b-2 is a potential oncomiR on human chromosome 21 in megakaryoblastic leukemia. *Genes and Development*, 24(5):478–490, 2010. ISSN 08909369. doi: 10.1101/gad.1856210.

Knudson A. G. Mutation and cancer: statistical study of retinoblastoma. *Proceedings of the National Academy of Sciences of the United States of America*, 68(4):820–3, 1971. ISSN 0027-8424. doi: 10.1073/pnas.68.4.820.

Köllner I., Sodeik B., Schreek S., Heyn H., Von Neuhoff N., Germeshausen M., Zeidler C., Krüger M., Schlegelberger B., Welte K., and Beger C. Mutations in neutrophil elastase causing congenital neutropenia lead to cytoplasmic protein accumulation and induction of the unfolded protein response. *Blood*, 108(2):493–500, 2006. ISSN 00064971. doi: 10.1182/blood-2005-11-4689.

Kostmann R. Infantile genetic agranulocytosis; agranulocytosis infantilis hereditaria. *Acta paediatrica. Supplementum*, 45(Suppl 105):1–78, 1956. ISSN 0803-5253. doi: 10.1111/j.1651-2227.1956.tb06875.x.

Krol J., Loedige I., and Filipowicz W. The widespread regulation of microRNA biogenesis, function and decay. *Nature Reviews Genetics*, 11(9):597–610, 2010. ISSN 14710056. doi: 10.1038/nrg2843.

Kuchenbauer F., Mah S. M., Heuser M., McPherson A., Rüschmann J., Rouhi A., Berg T., Bullinger L., Argiropoulos B., Morin R. D., Lai D., Starczynowski D. T., Karsan A., Eaves C. J., Watahiki A., Wang Y., Aparicio S. A., Ganser A., Krauter J., Döhner H., Döhner K., Marra M. A., Camargo F. D., Palmqvist L., Buske C., and Humphries R. K. Comprehensive analysis of mammalian miRNA*species and their role in myeloid cells. *Blood*, 118(12):3350–3358, 2011. ISSN 00064971. doi: 10.1182/blood-2010-10-312454.

Lam K. and Zhang D. E. RUNX1 and RUNX1-ETO: Roles in hematopoiesis and leukemogenesis. *Frontiers in Bioscience*, 17(3):1120–1139, 2012. ISSN 10939946. doi: 10.2741/3977.

Langer C., Radmacher M. D., Ruppert A. S., Whitman S. P., Paschka P., Mrózek K., Baldus C. D., Vukosavljevic T., Liu C. G., Ross M. E., Powell B. L., De La Chapelle A., Kolitz J. E., Larson R. A., Marcucci G., and Bloomfield C. D. High BAALC expression associates with other molecular prognostic markers, poor outcome, and a distinct gene-expression signature in cytogenetically normal patients younger than 60 years with acute myeloid leukemia: A Cancer and Leukemia Group B (CALGB) st. *Blood*, 111(11):5371–5379, 2008. ISSN 00064971. doi: 10.1182/blood-2007-11-124958.

Larsen M. T., Hother C., Häger M., Pedersen C. C., Theilgaard-Mönch K., Borregaard N., and Cowland J. B. MicroRNA Profiling in Human Neutrophils during Bone Marrow Granulopoiesis and In Vivo Exudation. *PLoS ONE*, 8(3), 2013. ISSN 19326203. doi: 10.1371/journal.pone.0058454.

Lawrence S. M., Corriden R., and Nizet V. The Ontogeny of a Neutrophil: Mechanisms of Granulopoiesis and Homeostasis. *Microbiology and Molecular Biology Reviews*, 82(1):e00057–17, mar 2018. ISSN 1092-2172. doi: 10.1128/mmbr.00057-17.

Lee R. C. The C. elegans Heterochronic Gene lin-4 Encodes Small RNAs with Antisense Complementarity to lin-14. *Cell*, 75:843–854, 1993. ISSN 0092-8674. doi: 10.1016/0092-8674(93)90529-Y.

Lee T. I., Johnstone S. E., and Young R. A. Chromatin immunoprecipitation and microarray-based analysis of protein location. *Nature Protocols*, 1(2):729–748, 2006. ISSN 17542189. doi: 10.1038/nprot.2006.98.

Lin S. and Gregory R. I. MicroRNA biogenesis pathways in cancer. *Nature Reviews Cancer*, 15(6):321–333, 2015. ISSN 14741768. doi: 10.1038/nrc3932.

Lin S., Mulloy J. C., and Goyama S. RUNX1-ETO leukemia. *Advances in Experimental Medicine and Biology*, 962:151–173, 2017. ISSN 22148019. doi: 10.1007/978-981-10-3233-2_11.

Livak K. J. and Schmittgen T. D. Analysis of relative gene expression data using real-time quantitative PCR and the 2-ΔΔCT method. *Methods*, 25(4):402–408, dec 2001. ISSN 10462023. doi: 10.1006/meth.2001.1262.

Luo H. N., Wang Z. H., Sheng Y., Zhang Q., Yan J., Hou J., Zhu K., Cheng Y., Xu Y. L., Zhang X. H., Xu M., and Ren X. Y. MiR-139 targets CXCR4 and inhibits the proliferation and metastasis of laryngeal squamous carcinoma cells. *Medical Oncology*, 31(1):789, jan 2014. ISSN 13570560. doi: 10.1007/s12032-013-0789-z.

MacFarlane L.-A. and R. Murphy P. MicroRNA: Biogenesis, Function and Role in Cancer. *Current Genomics*, 11(7):537–561, nov 2010. ISSN 13892029. doi: 10.2174/138920210793175895.

Makaryan V., Zeidler C., Bolyard A. A., Skokowa J., Rodger E., Kelley M. L., Boxer L. A., Bonilla M. A., Newburger P. E., Shimamura A., Zhu B., Rosenberg P. S., Link D. C., Welte K., and Dale D. C. The diversity of mutations and clinical outcomes for ELANE-associated neutropenia. *Current Opinion in Hematology*, 22(1):3–11, 2015. ISSN 15317048. doi: 10.1097/MOH.0000000000000105.

Maquat L. E. Nonsense-mediated mRNA decay: Splicing, translation and mRNP dynamics. *Nature Reviews Molecular Cell Biology*, 5(2):89–99, 2004. ISSN 14710072. doi: 10.1038/nrm1310.

Marcucci G., Mrózek K., Radmacher M. D., Garzon R., and Bloomfield C. D. The prognostic and functional role of microRNAs in acute myeloid leukemia. *Blood*, 117(4):1121–1129, 2011. ISSN 00064971. doi: 10.1182/blood-2010-09-191312.

Marcucci G., Maharry K. S., Metzeler K. H., Volinia S., Wu Y. Z., Mrozek K., Nicolet D., Kohlschmidt J., Whitman S. P., Mendler J. H., Schwind S., Becker H., Eisfeld A. K., Carroll A. J., Powell B. L., Kolitz J. E., Garzon R., Caligiuri M. A., Stone R. M., and Bloomfield C. D. Clinical role of microrna s in cytogenetically normal acute myeloid leukemia: MiR-155 Upregulation independently identifies high-risk patients. *Journal of Clinical Oncology*, 31(17):2086–2093, 2013. ISSN 15277755. doi: 10.1200/JCO.2012.45.6228.

Massullo P., Druhan L. J., Bunnell B. A., Hunter M. G., Robinson J. M., Marsh C. B., and Avalos B. R. Aberrant subcellular targeting of the G185R neutrophil elastase mutant associated with severe congenital neutropenia induces premature apoptosis of differentiating promyelocytes. *Blood*, 105(9):3397–3404, 2005. ISSN 00064971. doi: 10.1182/blood-2004-07-2618.

Maston G. A., Evans S. K., and Green M. R. Transcriptional Regulatory Elements in the Human Genome. *Annual Review of Genomics and Human Genetics*, 7(1): 29–59, 2006. ISSN 1527-8204. doi: 10.1146/annurev.genom.7.080505.115623.

Metcalf D. The granulocyte-macrophage colony-stimulating factors. *Science*, 229(4708):16–22, jul 1985. ISSN 00368075. doi: 10.1126/science.2990035.

Metcalf D. Hematopoietic cytokines. *Blood*, 111(2):485–491, jan 2008. ISSN 00064971. doi: 10.1182/blood-2007-03-079681.

Metzeler K. H. and Bloomfield C. D. Clinical relevance of RUNX1 and CBFB alterations in acute myeloid Leukemia and other hematological disorders. In Groner Y., Liu P., Speck N. A., Ito Y., Neil J. C., and Wijnen van A., editors, *Advances in Experimental Medicine and Biology*, volume 962, pages 175–199. Springer Nature Singapore Pte Ltd., 2017. doi: 10.1007/978-981-10-3233-2_12.

Mevel R., Draper J. E., Lie-A-Ling M., Kouskoff V., and Lacaud G. RUNX transcription factors: Orchestrators of development. *Development (Cambridge)*, 146: 1–19, 2019. ISSN 14779129. doi: 10.1242/dev.148296.

Michaud J., Wu F., Osato M., Cottles G. M., Yanagida M., Asou N., Shigesada K., Ito Y., Benson K. F., Raskind W. H., Bossier C., Antonarakis S. E., Israels S., McNicol A., Weiss H., Horwitz M., and Scott H. S. In vitro analyses of known and novel RUNX1/AML1 mutations in dominant familial platelet disorder with predisposition to acute myelogenous leukemia: Implications for mechanisms of pathogenesis. *Blood*, 99(4):1364–1372, 2002. ISSN 00064971. doi: 10.1182/blood.V99.4.1364.

Michaud J., Scott H. S., and Escher R. AML1 interconnected pathways of leukemogenesis. *Cancer Investigation*, 21(1):105–136, 2003. ISSN 07357907. doi: 10.1081/CNV-120018821.

MiRBase . MiRBase.org, 2018. URL `www.mirbase.org/[Zugriff:08.04.2018]`.

Miyoshi H., Shimizu K., Kozu T., Maseki N., Kaneko Y., and Ohki M. (8;21) breakpoints on chromosome 21 in acute myeloid leukemia are clustered within a limited region of a single gene, AML1. *Proceedings of the National Academy of Sciences of the United States of America*, 88(23):10431–10434, 1991. ISSN 00278424. doi: 10.1073/pnas.88.23.10431.

Morishima T., Watanabe ichiro K., Niwa A., Hirai H., Saida S., Tanaka T., Kato I., Umeda K., Hiramatsu H., Saito M. K., Matsubara K., Adachi S., Kobayashi M., Nakahata T., and Heike T. Genetic correction of HAX1 in induced pluripotent stem cells from a patient with severe congenital neutropenia improves defective granulopoiesis. *Haematologica*, 99(1):19–27, 2014. ISSN 03906078. doi: 10.3324/haematol.2013.083873.

Munshi H. G. and Montgomery R. B. Severe neutropenia: A diagnostic approach. *Western Journal of Medicine*, 172(4):248–252, 2000. ISSN 00930415. doi: 10.1136/ewjm.172.4.248.

Nasri M., Ritter M., Mir P., Dannenmann B., Aghaallaei N., Amend D., Makaryan V., Xu Y., Fletcher B., Bernhard R., Steiert I., Hahnel K., Berger J., Koch I., Sailer

B., Hipp K., Zeidler C., Klimiankou M., Bajoghli B., Dale D. C., Welte K., and Skokowa J. CRISPR/Cas9 mediated ELANE knockout enables neutrophilic maturation of primary hematopoietic stem and progenitor cells and induced pluripotent stem cells of severe congenital neutropenia patients. *Haematologica*, page haematol.2019.221804, 2019. ISSN 0390-6078. doi: 10.3324/haematol.2019.221804.

Nayak R. C., Trump L. R., Aronow B. J., Myers K., Mehta P., Kalfa T., Wellendorf A. M., Valencia C. A., Paddison P. J., Horwitz M. S., Grimes H. L., Lutzko C., and Cancelas J. A. Pathogenesis of ELANE-mutant severe neutropenia revealed by induced pluripotent stem cells. *Journal of Clinical Investigation*, 125(8):3103–3116, 2015. ISSN 15588238. doi: 10.1172/JCI80924.

Newburger P. E., Pindyck T. N., Zhu Z., Bolyard A. A., Aprikyan A. A., Dale D. C., Smith G. D., and Boxer L. A. Cyclic neutropenia and severe congenital neutropenia in patients with a shared ELANE mutation and paternal haplotype: Evidence for phenotype determination by modifying genes. *Pediatric Blood and Cancer*, 55(2):314–317, 2010. ISSN 15455009. doi: 10.1002/pbc.22537.

Notta F., Zandi S., Takayama N., Dobson S., Gan O. I., Wilson G., Kaufmann K. B., McLeod J., Laurenti E., Dunant C. F., McPherson J. D., Stein L. D., Dror Y., and Dick J. E. Distinct routes of lineage development reshape the human blood hierarchy across ontogeny. *Science*, 351(6269):aab2116 – aab2116–9, 2016. ISSN 0036-8075. doi: 10.1126/science.aab2116.

Nustede R., Klimiankou M., Klimenkova O., Kuznetsova I., Zeidler C., Welte K., and Skokowa J. ELANE mutant-specific activation of different UPR pathways in congenital neutropenia. *British Journal of Haematology*, 172(2):219–227, 2016. ISSN 13652141. doi: 10.1111/bjh.13823.

O'Connell R. M. and Baltimore D. MicroRNAs and Hematopoietic Cell Development. *Current Topics in Developmental Biology*, 99:145–174, 2012. ISSN 00702153. doi: 10.1016/B978-0-12-387038-4.00006-9.

O'Connell R. M., Chaudhuri A. A., Rao D. S., Gibson W. S., Balazs A. B., and Baltimore D. MicroRNAs enriched in hematopoietic stem cells differentially regulate long-term hematopoietic output. *Proceedings of the National Academy of Sciences of the United States of America*, 107(32):14235–14240, 2010. ISSN 00278424. doi: 10.1073/pnas.1009798107.

O'Connell R. M., Zhao J. L., and Rao D. S. MicroRNA function in myeloid biology. *Blood*, 118(11):2960–2969, 2011. ISSN 00064971. doi: 10.1182/blood-2011-03-291971.

Ohlsson E., Schuster M. B., Hasemann M., and Porse B. T. The multifaceted functions of C/EBP$\alpha$ in normal and malignant haematopoiesis. *Leukemia*, 30(4):767–775, 2016. ISSN 14765551. doi: 10.1038/leu.2015.324.

Orkin S. H. and Zon L. I. Hematopoiesis: an evolving paradigm for stem cell biology. *Cell*, 132(4):631–44, feb 2008. ISSN 1097-4172. doi: 10.1016/j.cell.2008.01.025.

Orkin S. H., Fisher D. E. D. E., Ginsburg D. H., Look A. T., Lux S. E., and Nathan D. G. *Nathan and Oski's hematology and oncology of infancy and childhood*. Elsevier/Saunders, 8 edition, 2015. ISBN 9781455754144.

Osato M. Point mutations in the RUNX1/AML1 gene: Another actor in RUNX leukemia. *Oncogene*, 23(24):4284–4296, may 2004. ISSN 09509232. doi: 10.1038/sj.onc.1207779.

Osato M., Asou N., Abdalla E., Hoshino K., Yamasaki H., Okubo T., Suzushima H., Takatsuki K., Kanno T., Shigesada K., and Ito Y. Biallelic and heterozygous point mutations in the runt domain of the AML1/PEBP2alphaB gene associated with myeloblastic leukemias. *Blood*, 93(6):1817–24, mar 1999. ISSN 0006-4971.

Ostuni R., Natoli G., Cassatella M. A., and Tamassia N. Epigenetic regulation of neutrophil development and function. *Seminars in Immunology*, 28(2):83–93, 2016. ISSN 10963618. doi: 10.1016/j.smim.2016.04.002.

Parikh S. and Bessler M. Recent insights into inherited bone marrow failure syndromes. *Current opinion in pediatrics*, 24(1):23–32, feb 2012. ISSN 1531-698X. doi: 10.1097/MOP.0b013e32834eca77.

Pasquinelli A. E., Reinhart B. J., Slack F., Martindale M. Q., Kuroda M. I., Maller B., Hayward D. C., Ball E. E., Degnan B., Müller P., Spring J., Srinivasan A., Fishman M., Finnerty J., Corbo J., Levine M., Leahy P., Davidson E., and Ruvkun G. Conservation of the sequence and temporal expression of let-7 heterochronic regulatory RNA. *Nature*, 408(6808):86–89, 2000. ISSN 00280836. doi: 10.1038/35040556.

Paul F., Arkin Y., Giladi A., Jaitin D. A., Kenigsberg E., Keren-Shaul H., Winter D., Lara-Astiaso D., Gury M., Weiner A., David E., Cohen N., Lauridsen F. K. B., Haas S., Schlitzer A., Mildner A., Ginhoux F., Jung S., Trumpp A., Porse B. T.,

Tanay A., and Amit I. Transcriptional Heterogeneity and Lineage Commitment in Myeloid Progenitors. *Cell*, 163(7):1663–1677, 2015. ISSN 10974172. doi: 10.1016/j.cell.2015.11.013.

Perez Botero J., Chen D., Cousin M. A., Majerus J. A., Coon L. M., Kruisselbrink T. M., Klee E. W., Lazaridis K. N., Pruthi R. K., and Patnaik M. M. Clinical characteristics and platelet phenotype in a family with RUNX1 mutated thrombocytopenia. *Leukemia and Lymphoma*, 58(8):1963–1967, 2017. ISSN 10292403. doi: 10.1080/10428194.2016.1265118.

Person R. E., Li F. Q., Duan Z., Benson K. F., Wechsler J., Papadaki H. A., Eliopoulos G., Kaufman C., Bertolone S. J., Nakamoto B., Papayannopoulou T., Grimes H. L., and Horwitz M. Mutations in proto-oncogene GFI1 cause human neutropenia and target ELA2. *Nature Genetics*, 34(3):308–312, 2003. ISSN 10614036. doi: 10.1038/ng1170.

Peterson L. F., Boyapati A., Ranganathan V., Iwama A., Tenen D. G., Tsai S., and Zhang D.-E. The hematopoietic transcription factor AML1 (RUNX1) is negatively regulated by the cell cycle protein cyclin D3. *Molecular and cellular biology*, 25(23):10205–10219, dec 2005. ISSN 0270-7306. doi: 10.1128/MCB.25.23.10205-10219.2005.

Petriv O. I., Kuchenbauer F., Delaney A. D., Lecault V., White A., Kent D., Marmolejo L., Heuser M., Berg T., Copley M., Ruschmann J., Sekulovic S., Benz C., Kuroda E., Ho V., Antignano F., Halim T., Giambra V., Krystal G., Takei C. J. F., Weng A. P., Piret J., Eaves C., Marra M. A., Humphries R. K., and Hansen C. L. Comprehensive microRNA expression profiling of the hematopoietic hierarchy. *Proceedings of the National Academy of Sciences of the United States of America*, 107(35):15443–8, aug 2010. ISSN 1091-6490. doi: 10.1073/pnas.1009320107.

Pittermann E., Lachmann N., MacLean G., Emmrich S., Ackermann M., Göhring G., Schlegelberger B., Welte K., Schambach A., Heckl D., Orkin S. H., Cantz T., and Klusmann J. H. Gene correction of HAX1 reversed Kostmann disease phenotype in patient-specific induced pluripotent stem cells. *Blood Advances*, 1 (14):903–914, 2017. ISSN 24739537. doi: 10.1182/bloodadvances.2016003798.

Preudhomme C., Warot-Loze D., Roumier C., Grardel-Duflos N., Garand R., Lai J. L., Dastugue N., Macintyre E., Denis C., Bauters F., Kerckaert J. P., Cosson A., and Fenaux P. High incidence of biallelic point mutations in the Runt domain of the AML1/PEBP2 alpha B gene in Mo acute myeloid leukemia and in myeloid

malignancies with acquired trisomy 21. *Blood*, 96(8):2862–9, oct 2000. ISSN 0006-4971.

Preudhomme C., Renneville A., Bourdon V., Philippe N., Roche-Lestienne C., Boissel N., Dhedin N., André J. M., Cornillet-Lefebvre P., Baruchel A., Mozziconacci M. J., and Sobol H. High frequency of RUNX1 biallelic alteration in acute myeloid leukemia secondary to familial platelet disorder. *Blood*, 113(22): 5583–5587, 2009. ISSN 00064971. doi: 10.1182/blood-2008-07-168260.

Pulikkan J. A., Dengler V., Peramangalam P. S., Peer Zada A. A., Müller-Tidow C., Bohlander S. K., Tenen D. G., and Behre G. Cell-cycle regulator E2F1 and microRNA-223 comprise an autoregulatory negative feedback loop in acute myeloid leukemia. *Blood*, 115(9):1768–1778, 2010. ISSN 00064971. doi: 10.1182/blood-2009-08-240101.

Qiu Y., Zhang Y., Hu N., and Dong F. A truncated Granulocyte Colony-stimulating Factor Receptor (G-CSFR) inhibits apoptosis induced by neutrophil elastase G185R mutant: Implication for understanding CSF3R gene mutations in severe congenital neutropenia. *Journal of Biological Chemistry*, 292(8):3496–3505, 2017. ISSN 1083351X. doi: 10.1074/jbc.M116.755157.

Raghavachari N., Liu P., Barb J. J., Yang Y., Wang R., Nguyen Q. T., and Munson P. J. Integrated analysis of miRNA and mRNA during differentiation of human CD34+ cells delineates the regulatory roles of microRNA in hematopoiesis. *Experimental Hematology*, 42(1):14–27.e2, 2014. ISSN 18732399. doi: 10.1016/j.exphem.2013.10.003.

Rajasekhar M., Schmitz U., Flamant S., Wong J. J., Bailey C. G., Ritchie W., Holst J., and Rasko J. E. Identifying microRNA determinants of human myelopoiesis. *Scientific Reports*, 8(1), 2018. ISSN 20452322. doi: 10.1038/s41598-018-24203-7.

Rasko J. E. and Wong J. J. Nuclear microRNAs in normal hemopoiesis and cancer. *Journal of Hematology and Oncology*, 10(1), 2017. ISSN 17568722. doi: 10.1186/s13045-016-0375-x.

Ritter M. U., Klimenkova O., Klimiankou M., Schmidt A. E., Stocking C., Kanz L., Zeidler C., Link D. C., Welte K., and Skokowa J. Understanding the Role of CSF3R and Runx1 Runt Homology Domain Missense Mutations in Leukemic Transformation of Hematopoietic Stem Cells. *Blood*, 132(Suppl 1):1101–1101, nov 2018. ISSN 0006-4971. doi: 10.1182/BLOOD-2018-99-118644.

Röllig C., Beelen D. W., Jan Braess R. G., Niederwieser D., Passweg J., Reinhardt D., and Schlenk R. F. DGHO - Leitline: Akute Myeloische Leukämie (AML) - www.onkopedia.com/de, 2018. URL https://www.onkopedia.com/de/onkopedia/guidelines/akute-myeloische-leukaemie-aml/@@view/html/index.html[Zugriff:24.04.2019].

Rosales C. Neutrophil: A cell with many roles in inflammation or several cell types? *Frontiers in Physiology*, 9(FEB):113, feb 2018. ISSN 1664042X. doi: 10.3389/fphys.2018.00113.

Rosenbauer F. and Tenen D. G. Transcription factors in myeloid development: Balancing differentiation with transformation. *Nature Reviews Immunology*, 7(2): 105–117, 2007. ISSN 14741733. doi: 10.1038/nri2024.

Rosenberg P. S., Alter B. P., Bolyard A. A., Bonilla M. A., Boxer L. A., Cham B., Fier C., Freedman M., Kannourakis G., Kinsey S., Schwinzer B., Zeidler C., Welte K., and Dale D. C. The incidence of leukemia and mortality from sepsis in patients with severe congenital neutropenia receiving long-term G-CSF therapy. *Blood*, 107(12):4628–4635, jun 2006. ISSN 00064971. doi: 10.1182/blood-2005-11-4370.

Rosenberg P. S., Zeidler C., Bolyard A. A., Alter B. P., Bonilla M. A., Boxer L. A., Dror Y., Kinsey S., Link D. C., Newburger P. E., Shimamura A., Welte K., and Dale D. C. Stable long-term risk of leukaemia in patients with severe congenital neutropenia maintained on G-CSF therapy. *British Journal of Haematology*, 150 (2):196 – 199, apr 2010. ISSN 00071048. doi: 10.1111/j.1365-2141.2010.08216.x.

Roumier C., Fenaux P., Lafage M., Imbert M., Eclache V., and Preudhomme C. New mechanisms of AML1 gene alteration in hematological malignancies. *Leukemia*, 17(1):9–16, 2003. ISSN 08876924. doi: 10.1038/sj.leu.2402766.

Rowe P. Korrelation und Regression - Zusammenhang zwischen Messwerten. In *Statistik für Mediziner und Pharmazeuten*, pages 167 – 191. Wiley-VCH, Weinheim, 1. aufl. edition, 2012. ISBN 9783527331192.

Rowe R. G., Mandelbaum J., Zon L. I., and Daley G. Q. Engineering Hematopoietic Stem Cells: Lessons from Development. *Cell Stem Cell*, 18(6):707–720, 2016. ISSN 18759777. doi: 10.1016/j.stem.2016.05.016.

Schmit J. M., Turner D. J., Hromas R. A., Wingard J. R., Brown R. A., Li Y., Li M. M., Slayton W. B., and Cogle C. R. Two novel RUNX1 mutations in a patient with congenital thrombocytopenia that evolved into a high grade myelodysplastic

syndrome. *Leukemia Research Reports*, 4(1):24–27, 2015. ISSN 22130489. doi: 10.1016/j.lrr.2015.03.002.

Schnittger S., Dicker F., Kern W., Wendland N., Sundermann J., Alpermann T., Haferlach C., and Haferlach T. RUNX1 mutations are frequent in de novo AML with noncomplex karyotype and confer an unfavorable prognosis. *Blood*, 117(8): 2348–2357, 2011. ISSN 00064971. doi: 10.1182/blood-2009-11-255976.

Schotte D., Moqadam F. A., Lange-Turenhout E. A., Chen C., Van Ijcken W. F., Pieters R., and Den Boer M. L. Discovery of new microRNAs by small RNAome deep sequencing in childhood acute lymphoblastic leukemia. *Leukemia*, 25(9): 1389–1399, 2011. ISSN 08876924. doi: 10.1038/leu.2011.105.

Schwarzenbach H., Da Silva A. M., Calin G., and Pantel K. Data normalization strategies for microRNA quantification, 2015. ISSN 15308561.

Schwind S., Maharry K., Radmacher M. D., Mrózek K., Holland K. B., Margeson D., Whitman S. P., Hickey C., Becker H., Metzeler K. H., Paschka P., Baldus C. D., Liu S., Garzon R., Powell B. L., Kolitz J. E., Carroll A. J., Caligiuri M. A., Larson R. A., Marcucci G., and Bloomfield C. D. Prognostic significance of expression of a single microRNA, miR-181a, in cytogenetically normal acute myeloid leukemia: A cancer and leukemia group B study. *Journal of Clinical Oncology*, 28(36):5257–5264, 2010. ISSN 0732183X. doi: 10.1200/JCO.2010.29.2953.

SCNIR . SCNIR- Internationales Register für schwere chronische Neutropenien, 2018. URL `http://www.severe-chronic-neutropenia.org/[Zugriff:08.04.2018]`.

Shaham L., Binder V., Gefen N., Borkhardt A., and Izraeli S. MiR-125 in normal and malignant hematopoiesis. *Leukemia*, 26:2011 – 2018, 2012. doi: 10.1038/leu.2012.90.

Sieff C. A., Daley G. Q., and Zon L. I. Anatomy and Physiology of Hematopoiesis. In Orkin S. H., Fisher D. E., Look A. T., Lux S. E. I., Ginsburg D., and Nathan D. G., editors, *Nathan and Oski's Hematology and Oncology of Infancy and Childhood*, chapter 1, pages 3–51.e21. Elsevier/Saunders, 8 edition, 2015. ISBN 9781455754144.

Sizemore G. M., Pitarresi J. R., Balakrishnan S., and Ostrowski M. C. The ETS family of oncogenic transcription factors in solid tumours. *Nature Reviews Cancer*, 17(6):337–351, 2017. ISSN 14741768. doi: 10.1038/nrc.2017.20.

Skokowa J. and Welte K. Defective G-CSFR Signaling Pathways in Congenital Neutropenia. *Hematology/Oncology Clinics of North America*, 27(1):75–88, feb 2013. ISSN 08898588. doi: 10.1016/j.hoc.2012.11.001.

Skokowa J., Cario G., Uenalan M., Schambach A., Germeshausen M., Battmer K., Zeidler C., Lehmann U., Eder M., Baum C., Grosschedl R., Stanulla M., Scherr M., and Welte K. LEF-1 is crucial for neutrophil granulocytopoiesis and its expression is severely reduced in congenital neutropenia. *Nature Medicine*, 12(10):1191–1197, 2006. ISSN 1078-8956. doi: 10.1038/nm1484.

Skokowa J., Fobiwe J. P., Dan L., Thakur B. K., and Welte K. Neutrophil elastase is severely down-regulated in severe congenital neutropenia independent of ELA2 or HAX1 mutations but dependent on LEF-1. *Blood*, 114(14):3044–3051, 2009. ISSN 00064971. doi: 10.1182/blood-2008-11-188755.

Skokowa J., Klimiankou M., Klimenkova O., Lan D., Gupta K., Hussein K., Carrizosa E., Kusnetsova I., Li Z., Sustmann C., Ganser A., Zeidler C., Kreipe H. H., Burkhardt J., Grosschedl R., and Welte K. Interactions among HCLS1, HAX1 and LEF-1 proteins are essential for G-CSF-triggered granulopoiesis. *Nature Medicine*, 18(10):1550–1559, 2012. ISSN 10788956. doi: 10.1038/nm.2958.

Skokowa J., Steinemann D., Katsman-Kuipers J. E., Zeidler C., Klimenkova O., Klimiankou M., Ünalan M., Kandabarau S., Makaryan V., Beekman R., Behrens K., Stocking C., Obenauer J., Schnittger S., Kohlmann A., Valkhof M. G., Hoogenboezem R., Göhring G., Reinhardt D., Schlegelberger B., Stanulla M., Vandenberghe P., Donadieu J., Zwaan C. M., Touw I. P., Van Den Heuvel-Eibrink M. M., Dale D. C., and Welte K. Cooperativity of RUNX1 and CSF3R mutations in severe congenital neutropenia: A unique pathway in myeloid leukemogenesis. *Blood*, 123(14):2229–2237, 2014. ISSN 15280020. doi: 10.1182/blood-2013-11-538025.

Skokowa J., Dale D. C., Touw I. P., Zeidler C., and Welte K. Severe congenital neutropenias. *Nature Reviews Disease Primers*, 3:17032, jun 2017. ISSN 2056-676X. doi: 10.1038/nrdp.2017.32.

Song W. J., Sullivan M. G., Legare R. D., Hutchings S., Tan X., Kufrin D., Ratajczak J., Resende I. C., Haworth C., Hock R., Loh M., Felix C., Roy D. C., Busque L., Kurnit D., Willman C., Gewirtz A. M., Speck N. A., Bushweller J. H., Li F. P., Gardiner K., Poncz M., Maris J. M., and Gilliland D. G. Haploinsufficiency of CBFA2 causes familial thrombocytopenia with propensity to develop acute myelogenous leukaemia. *Nature Genetics*, 23(2):166–175, 1999. ISSN 10614036. doi: 10.1038/13793.

Spoor J., Farajifard H., and Rezaei N. Congenital neutropenia and primary immunodeficiency diseases. *Critical Reviews in Oncology/Hematology*, 133 (October 2018):149–162, 2019. ISSN 18790461. doi: 10.1016/j.critrevonc.2018.10.003.

Starnes L. M., Sorrentino A., Pelosi E., Ballarino M., Morsilli O., Biffoni M., Santoro S., Felli N., Castelli G., De Marchis M. L., Mastroberardino G., Gabbianelli M., Fatica A., Bozzoni I., Nervi C., and Peschle C. NFI-A directs the fate of hematopoietic progenitors to the erythroid or granulocytic lineage and controls $\beta$-globin and G-CSF receptor expression. *Blood*, 114(9):1753–1763, 2009. ISSN 00064971. doi: 10.1182/blood-2008-12-196196.

Stavast C. J., Leenen P. J., and Erkeland S. J. The interplay between critical transcription factors and microRNAs in the control of normal and malignant myelopoiesis. *Cancer Letters*, 427:28–37, 2018. ISSN 18727980. doi: 10.1016/j.canlet.2018.04.010.

Stengel A., Kern W., Meggendorfer M., Nadarajah N., Perglerovà K., Haferlach T., and Haferlach C. Number of RUNX1 mutations, wild-type allele loss and additional mutations impact on prognosis in adult RUNX1-mutated AML. *Leukemia*, 32(2):295–302, 2018. ISSN 14765551. doi: 10.1038/leu.2017.239.

Sun W. and Downing J. R. Haploinsufficiency of AML1 results in a decrease in the number of LTR-HSCs while simultaneously inducing an increase in more mature progenitors. *Blood*, 104(12):3565–3572, 2004. ISSN 00064971. doi: 10.1182/blood-2003-12-4349.

Surdziel E., Cabanski M., Dallmann I., Lyszkiewicz M., Krueger A., Ganser A., Scherr M., and Eder M. Enforced expression of miR-125b affects myelopoiesis by targeting multiple signaling pathways. *Blood*, 117(16):4338–4348, 2011. ISSN 00064971. doi: 10.1182/blood-2010-06-289058.

Tahirov T. H. and Bushweller J. Structure and Biophysics of CBF$\beta$/RUNX and Its Translocation Products. In Groner Y., Liu P., Speck N. A., Ito Y., Neil J. C., and Wijnen van A., editors, *Advances in experimental medicine and biology*, volume 962, pages 21–31. Springer Nature Singapore Pte Ltd., 2017. doi: 10.1007/978-981-10-3233-2_2.

Taketani T., Taki T., Takita J., Ono R., Horikoshi Y., Kaneko Y., Sako M., Hanada R., Hongo T., and Hayashi Y. Mutation of the AML1/RUNX1 gene in a transient myeloproliferative disorder patient with Down syndrome [3]. *Leukemia*, 16(9):1866–1867, 2002. ISSN 08876924. doi: 10.1038/sj.leu.2402612.

Taketani T., Taki T., Takita J., Tsuchida M., Hanada R., Hongo T., Kaneko T., Manabe A., Ida K., and Hayashi Y. AML1/RUNX1 mutations are infrequent, but related to AML-M0, acquired trisomy 21, and leukemic transformation in pediatric hematologic malignancies. *Genes Chromosomes and Cancer*, 38(1):1–7, 2003. ISSN 10452257. doi: 10.1002/gcc.10246.

Tang J. L., Hou H. A., Chen C. Y., Liu C. Y., Chou W. C., Tseng M. H., Huang C. F., Lee F. Y., Liu M. C., Yao M., Huang S. Y., Ko B. S., Hsu S. C., Wu S. J., Tsay W., Chen Y. C., Lin L. I., and Tien H. F. AML1/RUNX1 mutations in 470 adult patients with de novo acute myeloid leukemia: Prognostic implication and interaction with other gene alterations. *Blood*, 114(26):5352–5361, 2009. ISSN 00064971. doi: 10.1182/blood-2009-05-223784.

Taylor A. M. R., Rothblum-Oviatt C., Ellis N. A., Hickson I. D., Meyer S., Crawford T. O., Smogorzewska A., Pietrucha B., Weemaes C., and Stewart G. S. Chromosome instability syndromes. *Nature Reviews Disease Primers*, 5(1), 2019. ISSN 2056676X. doi: 10.1038/s41572-019-0113-0.

Thul P. J., Akesson L., Wiking M., Mahdessian D., Geladaki A., Ait Blal H., Alm T., Asplund A., Björk L., Breckels L. M., Bäckström A., Danielsson F., Fagerberg L., Fall J., Gatto L., Gnann C., Hober S., Hjelmare M., Johansson F., Lee S., Lindskog C., Mulder J., Mulvey C. M., Nilsson P., Oksvold P., Rockberg J., Schutten R., Schwenk J. M., Sivertsson A., Sjöstedt E., Skogs M., Stadler C., Sullivan D. P., Tegel H., Winsnes C., Zhang C., Zwahlen M., Mardinoglu A., Pontén F., Von Feilitzen K., Lilley K. S., Uhlén M., and Lundberg E. A subcellular map of the human proteome. *Science*, 356(6340):eaal3321, may 2017. ISSN 10959203. doi: 10.1126/science.aal3321.

Thusberg J. and Vihinen M. Bioinformatic analysis of protein structure-function relationships: Case study of leukocyte elastase (ELA2) missense mutations. *Human Mutation*, 27(12):1230–1243, 2006. ISSN 10597794. doi: 10.1002/humu.20407.

Till J. E. and McCulloch E. A. A Direct Measurement of the Radiation Sensitivity of Normal Mouse Bone Marrow Cells. *Radiation Research*, 14(2):213, feb 1961. ISSN 00337587. doi: 10.2307/3570892.

Touw I. P. Game of clones: The genomic evolution of severe congenital neutropenia. *Hematology*, 2015(1):1–7, 2015. ISSN 15204383. doi: 10.1182/asheducation-2015.1.1.

Touw I. P., Palande K., and Beekman R. Granulocyte Colony-Stimulating Factor Receptor Signaling. Implications for G-CSF Responses and Leukemic Progression in Severe Congenital Neutropenia. *Hematology/Oncology Clinics of North America*, 27(1):61–73, feb 2013. ISSN 08898588. doi: 10.1016/j.hoc.2012.10.002.

Triot A., Järvinen P. M., Arostegui J. I., Murugan D., Kohistani N., Díaz J. L. D., Racek T., Puchałka J., Gertz E. M., Schäffer A. A., Kotlarz D., Pfeifer D., De Heredia Rubio C. D., Ozdemir M. A., Patiroglu T., Karakukcu M., De Toledo Codina J. S., Yagüe J., Touw I. P., Unal E., and Klein C. Inherited biallelic CSF3R mutations in severe congenital neutropenia. *Blood*, 123(24):3811–3817, 2014. ISSN 15280020. doi: 10.1182/blood-2013-11-535419.

Tsai F. Y. and Orkin S. H. Transcription factor GATA-2 is required for proliferation/survival of early hematopoietic cells and mast cell formation, but not for erythroid and myeloid terminal differentiation. *Blood*, 89(10):3636–3643, nov 1997. ISSN 0006-4971.

Uhlén M., Fagerberg L., Hallström B. M., Lindskog C., Oksvold P., Mardinoglu A., Sivertsson Å., Kampf C., Sjöstedt E., Asplund A., Olsson I. M., Edlund K., Lundberg E., Navani S., Szigyarto C. A. K., Odeberg J., Djureinovic D., Takanen J. O., Hober S., Alm T., Edqvist P. H., Berling H., Tegel H., Mulder J., Rockberg J., Nilsson P., Schwenk J. M., Hamsten M., Von Feilitzen K., Forsberg M., Persson L., Johansson F., Zwahlen M., Von Heijne G., Nielsen J., and Pontén F. Tissue-based map of the human proteome. *Science*, 347(6220), 2015. ISSN 10959203. doi: 10.1126/science.1260419.

Uniprot.org . UniProt:RUNX1Q01196. URL `https://www.uniprot.org/uniprot/Q`01196.

Van Der Ree M. H., Van Der Meer A. J., Van Nuenen A. C., De Bruijne J., Ottosen S., Janssen H. L., Kootstra N. A., and Reesink H. W. Miravirsen dosing in chronic hepatitis C patients results in decreased microRNA-122 levels without affecting other microRNAs in plasma. *Alimentary Pharmacology and Therapeutics*, 43(1): 102–113, 2016. ISSN 13652036. doi: 10.1111/apt.13432.

Van Wijnen A. J., Stein G. S., Gergen J. P., Groner Y., Hiebert S. W., Ito Y., Liu P., Neil J. C., Ohki M., and Speck N. Nomenclature for Runt-related (RUNX) proteins. *Oncogene*, 23(24):4209–4210, may 2004. ISSN 09509232. doi: 10.1038/sj.onc.1207758.

Velten L., Haas S. F., Raffel S., Blaszkiewicz S., Islam S., Hennig B. P., Hirche C., Lutz C., Buss E. C., Nowak D., Boch T., Hofmann W.-K., Ho A. D., Huber

W., Trumpp A., Essers M. A. G., and Steinmetz L. M. Human haematopoietic stem cell lineage commitment is a continuous process. *Nature Cell Biology*, 19 (4):271–281, 2017. ISSN 1465-7392. doi: 10.1038/ncb3493.

Wallace J. A. and O'Connell R. M. MicroRNAs and acute myeloid leukemia: Therapeutic implications and emerging concepts. *Blood*, 130(11):1290–1301, 2017. ISSN 15280020. doi: 10.1182/blood-2016-10-697698.

Wang C. Q., Mok M. M. H., Yokomizo T., Tergaonkar V., and Osato M. Runx family genes in tissue stem cell dynamics. In *Advances in Experimental Medicine and Biology*, volume 962, pages 117–138. 2017. ISBN 978-981-10-3231-8. doi: 10.1007/978-981-10-3233-2_9.

Wang P., Chen L., Zhang J., Chen H., Fan J., Wang K., Luo J., Chen Z., Meng Z., and Liu L. Methylation-mediated silencing of the miR-124 genes facilitates pancreatic cancer progression and metastasis by targeting Rac1. *Oncogene*, 33 (4):514–524, 2014. ISSN 09509232. doi: 10.1038/onc.2012.598.

Ward A. C., Van Aesch Y. M., Gits J., Schelen A. M., De Koning J. P., Van Leeuwen D., Freedman M. H., and Touw I. P. Novel point mutation in the extracellular domain of the granulocyte colony-stimulating factor (G-CSF) receptor in a case of severe congenital neutropenia hyporesponsive to G-CSF treatment. *Journal of Experimental Medicine*, 190(4):497–507, 1999. ISSN 00221007. doi: 10.1084/jem.190.4.497.

Weber S., Alpermann T., Dicker F., Jeromin S., Nadarajah N., Eder C., Fasan A., Kohlmann A., Meggendorfer M., Haferlach C., Kern W., Haferlach T., and Schnittger S. BAALC expression: A suitable marker for prognostic risk stratification and detection of residual disease in cytogenetically normal acute myeloid leukemia. *Blood Cancer Journal*, 4(1):173, 2014. ISSN 20445385. doi: 10.1038/bcj.2013.71.

Weischenfeldt J., Lykke-Andersen J., and Porse B. Messenger RNA surveillance: Neutralizing natural nonsense, jul 2005. ISSN 09609822.

Weiss C. N. and Ito K. A Macro View of MicroRNAs: The Discovery of MicroRNAs and Their Role in Hematopoiesis and Hematologic Disease. In *International Review of Cell and Molecular Biology*, volume 334, pages 99 – 175. 2018. doi: 10.1016/bs.ircmb.2017.03.007.

Welte K. and Dale D. Pathophysiology and treatment of severe chronic neutropenia. *Annals of Hematology*, 72(4):158–165, apr 1996. ISSN 09395555. doi: 10.1007/s002770050156.

Welte K. and Zeidler C. Severe Congenital Neutropenia. *Hematology/Oncology Clinics of North America*, 23(2):307–320, jul 2009. ISSN 08898588. doi: 10.1016/j.hoc.2009.01.013.

Welte K., Zeidler C., and Dale D. C. Severe Congenital Neutropenia. *Seminars in Hematology*, 43(3):189–195, 2006. ISSN 00371963. doi: 10.1053/j.seminhematol.2006.04.004.

Wilson D. B., Link D. C., Mason P. J., and Bessler M. Inherited bone marrow failure syndromes in adolescents and young adults. *Annals of Medicine*, 46(6):353–363, 2014. ISSN 13652060. doi: 10.3109/07853890.2014.915579.

Wong C. C., Wong C., Tung E. K., Au S. L., Lee J. M., Poon R. T., Man K., and Ng I. O. The MicroRNA miR-139 suppresses metastasis and progression of hepatocellular carcinoma by down-regulating rho-kinase 2. *Gastroenterology*, 140(1):322–331, jan 2011. ISSN 00165085. doi: 10.1053/j.gastro.2010.10.006.

Wünsche P., Eckert E. S., Holland-Letz T., Paruzynski A., Hotz-Wagenblatt A., Fronza R., Rath T., Gil-Farina I., Schmidt M., Kalle von C., Klein C., Ball C. R., Herbst F., and Glimm H. Mapping Active Gene-Regulatory Regions in Human Repopulating Long-Term HSCs. *Cell Stem Cell*, 23(1):132–146.e9, 2018. ISSN 18759777. doi: 10.1016/j.stem.2018.06.003.

Chen xing X., Lin J., Qian J., Qian W., Yang J., Ma chun J., Deng qun Z., Xie D., An C., Tang yan C., and Qian Z. Dysregulation of miR-124-1 predicts favorable prognosis in acute myeloid leukemia. *Clinical Biochemistry*, 47(1-2):63–66, 2014. ISSN 00099120. doi: 10.1016/j.clinbiochem.2013.09.020.

Yzaguirre A. D., Bruijn de M. F., and Speck N. A. The Role of Runx1 in Embryonic Blood Cell Formation. In Groner Y., Liu P., Speck N. A., Ito Y., Neil J. C., and Wijnen van A., editors, *RUNX Proteins in Development and Cancer*, volume 962, pages 139–147. Springer Nature Singapore Pte Ltd., 2017a. ISBN 978-981-10-3231-8. doi: 10.1007/978-981-10-3233-2_4.

Yzaguirre A. D., Bruijn de M. F., and Speck N. A. The role of Runx1 in embryonic blood cell formation. In Groner Y., Liu P., Speck N. A., Ito Y., Neil J. C., and Wijnen van A., editors, *Advances in Experimental Medicine and Biology*, volume 962, chapter 4, pages 47–64. Springer Nature Singapore Pte Ltd., 2017b. ISBN 9789811032332. doi: 10.1007/978-981-10-3233-2_4.

Zardo G., Ciolfi A., Vian L., Starnes L. M., Billi M., Racanicchi S., Maresca C., Fazi F., Travaglini L., Noguera N., Mancini M., Nanni M., Cimino G., Lo-Coco

F., Grignani F., and Nervi C. Polycombs and microRNA-223 regulate human granulopoiesis by transcriptional control of target gene expression. *Blood*, 119 (17):4034–4046, 2012. ISSN 00064971. doi: 10.1182/blood-2011-08-371344.

Zeidler C., Boxer L., Dale D. C., Freedman M. H., Kinsey S., and Welte K. Management of Kostmann syndrome in the G-CSF era. *British Journal of Haematology*, 109(3):490–495, 2000. ISSN 00071048. doi: 10.1046/j.1365-2141.2000.02064.x.

Zeidler C., Germeshausen M., Klein C., and Welte K. Clinical implications of ELA2-, HAX1-, and G-CSF-receptor (CSF3R) mutations in severe congenital neutropenia. *British Journal of Haematology*, 144(4):459–467, 2009. ISSN 00071048. doi: 10.1111/j.1365-2141.2008.07425.x.

Zeidler C., Nickel A., Sykora K.-W., and Welte K. Improved Outcome Of Stem Cell Transplantation for Severe Chronic Neutropenia With Or without Secondary Leukemia: A Long-Term Analysis of European Data For More Than 25 Years By the SCNIR. *Blood*, 122(21):3347–3347, nov 2013. ISSN 0006-4971. doi: 10.1182/blood.v122.21.3347.3347.

Zhang H., Coblentz C., Watanabe-Smith K., Means S., Means J., Maxson J. E., and Tyner J. W. Gain-of-function mutations in granulocyte colony–stimulating factor receptor (CSF3R) reveal distinct mechanisms of CSF3R activation. *Journal of Biological Chemistry*, 293(19):7387–7396, 2018. ISSN 1083351X. doi: 10.1074/jbc.RA118.002417.

Zhao L. J., Wang Y. Y., Li G., Ma L. Y., Xiong S. M., Weng X. Q., Zhang W. N., Wu B., Chen Z., and Chen S. J. Functional features of RUNX1 mutants in acute transformation of chronic myeloid leukemia and their contribution to inducing murine full-blown leukemia. *Blood*, 119(12):2873–2882, 2012. ISSN 00064971. doi: 10.1182/blood-2011-08-370981.

Zhuang D., Qiu Y., Haque S. J., and Dong F. Tyrosine 729 of the G-CSF receptor controls the duration of receptor signaling: involvement of SOCS3 and SOCS1. *Journal of Leukocyte Biology*, 78(4):1008–1015, 2005. ISSN 0741-5400. doi: 10.1189/jlb.0105032.

Ziegler S. F., Bird T. A., Morella K. K., Mosley B., Gearing D. P., and Baumann H. Distinct regions of the human granulocyte-colony-stimulating factor receptor cytoplasmic domain are required for proliferation and gene induction. *Molecular and Cellular Biology*, 13(4):2384–2390, 1993. ISSN 0270-7306. doi: 10.1128/mcb.13.4.2384.

# 9 Erklärung zum Eigenanteil

Die Arbeit wurde in der Medizinischen Klinik Abteilung IM II des Universitäts Klinikums Tübingen unter Betreuung von Prof. Dr. Julia Skokowa (Ph.D) durchgeführt.

Die Konzeption der Studie erfolgte in Zusammenarbeit mit Prof. Dr. Julia Skokowa (Ph.D, habilitierte Betreuerin), Maksim Klimiankou (Ph.D) und Frederic Stein (medizinischer Doktorrand).

Sämtliche Versuche wurden (nach Einarbeitung durch die Labormitglieder Ingeborg Steiert (MTA), Karin Hähnel (MTA), Regine Berhard (MTA), Ursula Hermanutz-Klein (MTA), Perihan Mir (Ph.D), Benjamin Dannenmann (Ph.D) und Maksim Klimiankou (Ph.D)) von Frederic Stein durchgeführt. Die Methoden hiPS und Differenzierung wurden von Benjamin Dannenmann durchgeführt. Die Methode CFU wurde von Benjamin Dannenmann, Anna Solovyeva (PhD Student) und Maksim Klimiankou durchgeführt. Die Sanger-Sequenzierung und Analyse wurden von Maksim Klimiankou durchgeführt. Die der Studie zugrundeliegenden Patientendaten aus Tabelle 3.1 wurden von Skokowa et al. [2014] erhoben und von Frederic Stein adaptiert. Die MACS Isolation von $CD33^+$ und $CD34^+$ Spenderzellen wurde von Ingeborg Steiert (MTA), Karin Hähnel (MTA), Regine Berhard (MTA), Ursula Hermanutz-Klein (MTA), Perihan Mir (Ph.D), Benjamin Dannenmann (Ph.D) und Malte Ritter (PhD Student) durchgeführt. Die ‘Big Wig’ files wurden von Siarhei

Kandabarau zur Verfügung gestellt. Die statistische Auswertung erfolgte eigenständig und nach Anleitung durch Maksim Klimiankou und Siarhei Kandabarau. Ich versichere, das Manuskript selbständig und nach Anleitung und Korrektur durch Prof. Dr. Julia Skokowa (Ph.D) verfasst zu haben und keine weiteren, als die von mir angegebenen Quellen verwendet zu haben.

Tübingen, den 18.11.2020

Frederic Stein

# 10 Publication

Parts of this thesis have already been published in:

Dannenmann B., Klimiankou M., Oswald B., Solovyeva A., Mardan J., Nasri M., Ritter M., Zahabi A., Arreba-Tutusaus P., Mir P., Stein F., Kandabarau S., Lachmann N., Moritz T., Morishima T., Konantz M., Lengerke C., Ripperger T., Steinemann D., Erlacher M., Niemeyer C. M., Zeidler C., Welte K., and Skokowa J. iPSC modeling of stage-specific leukemogenesis reveals BAALC as a key oncogene in severe congenital neutropenia. Cell Stem Cell, 28(5):906-922.e6, 2021. ISSN 18759777. doi: 10.1016/j.stem.2021.03.023.

# Acknowledgements

**Without the following people, this work would not have been possible.**

I would like to thank Professor Dr. med. Julia Skokowa (Ph.D) for accepting me as a Doctoral student in her group and supporting me through the years and pushing me to achieve the results presented in this work - thank you!

The same goes for Maksim Klimiankou (Ph.D), who always had time for advice and help, thank you very much.

Another important person for the completion of this thesis was Professor Dr. med. Karl Welte, who kindly offered his knowledge, time and advice for scientific and career-oriented questions.

I would also like to thank Ingeborg Steiert, Ursula Hermanutz-Klein, Regine Bernhard and Karin Hähnel for their great every day work, support and advice in technical matters. Without them this work would have been much more difficult or nearly impossible. This also applies for for Benjamin Dannenmann, Perihan Mir, Malte Ritter, Masoud Nasri and Diana Amend who all contributed to this work in word and deed, but above all through their contribution to the good atmosphere in the laboratory.

A big thank you goes to AG Wehkamp and their members, who provided me with their LightCycler - I would especially like to thank Jutta Bader for the great breakfast, lunch and coffee breaks.

I would like to thank all those of you who have become friends over the years and are an important part of my life.

A big thank you to everyone who may not be listed here but contributed to this work in one way or another - thank you, I will always appreciate your support!